

Table of Contents

Table of Contents.....	1
5.2 Material properties	3
Results	7
Discussion.....	15
Conclusions and recommendations	16
5.3 Adhesive tests	21
Theory & Introduction.....	21
Method	23
Results	27
Discussion, Conclusions and recommendations	33
5.4 Glass pull-out tests	35
Test sequence 1.....	35
Test sequence 2.....	51
Test sequence 3.....	71
5.5 Preliminary beam tests.....	101
Introduction & Method.....	101
Results	106
6. Beam tests.....	117
Determination relevant moments & stresses.....	117
Hypothesis for additional tests.....	123

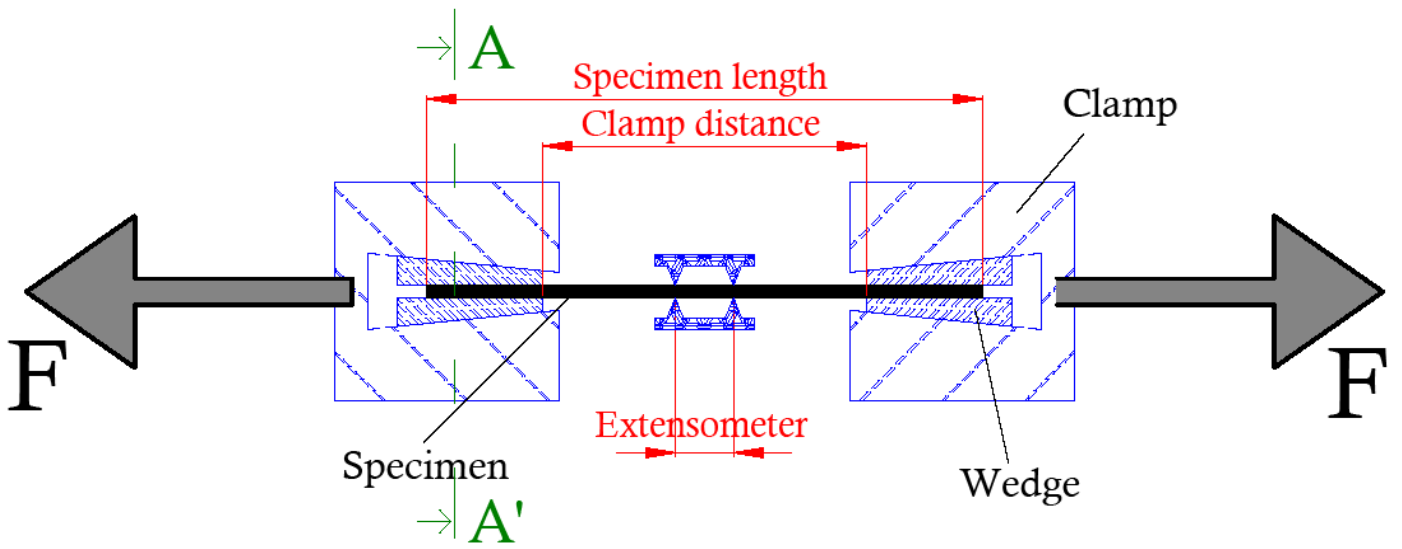


Figure 2, Test set-up schematic representation (not to scale)

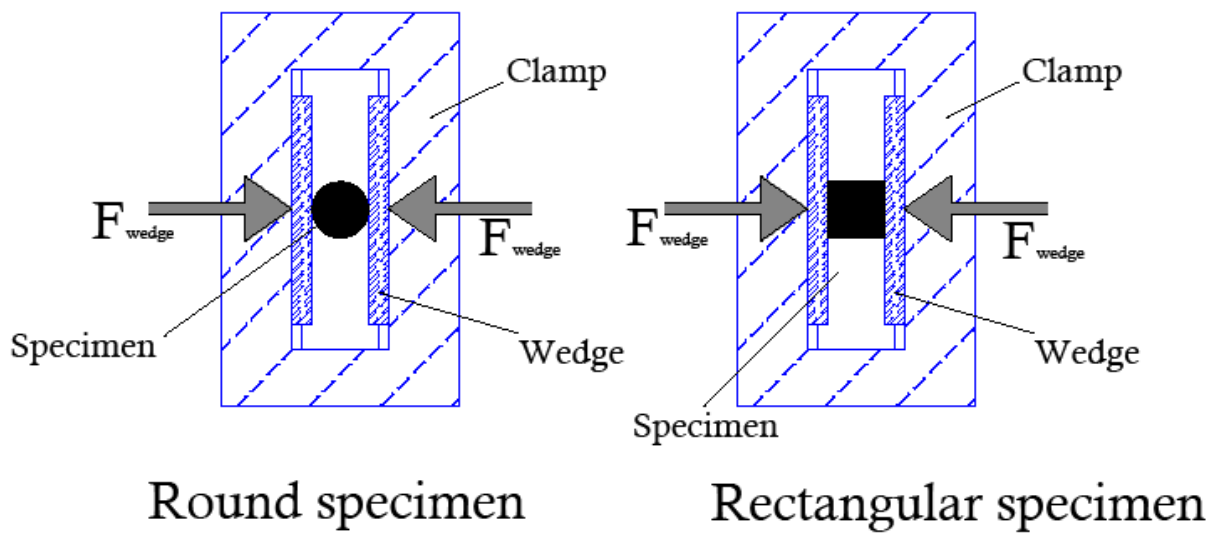


Figure 1, Cross section AA' for a round and a rectangular specimen (not to scale)

5.2 Material properties

Method

See *Figure 2*, *Figure 1* and **Error! Reference source not found..**

The specimens are tested in a displacement controlled tensile test. The set-up is presented schematically in *Figure 2*. The specimens are fixed by wedges that are able to slide in the clamps as the force increases.

Note that with a round profile, the compressive stress in the specimen due to the wedge clamps become very high. With a rectangular profile the gripping area is larger and therefore the local stress lower.

The specimen is mounted by a Zwick Extensometer. This device measures the extension of the specimen over a length of 20,31 mm.

Known properties of the specimens are:

1. Material
2. Height and width or diameter
3. Clamp to clamp distance

The variables which are measured in this test are:

1. Clamp displacement
2. Clamp force
3. Extension of Zwick extensometer

From these data the Young's modulus, ultimate tensile stress, elongation at break, etc. can be derived.



Figure 3, Photo of test set-up with round carbon fiber specimen. The device in the middle of the picture (circled in red) is the Zwick extensometer

Clamping principles

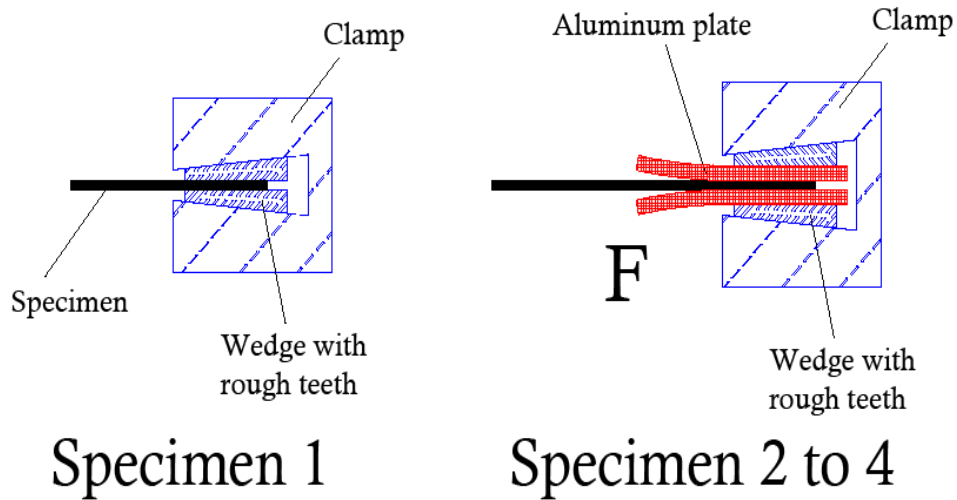


Figure 4, Specimen clamping with- and without aluminum plates.



Figure 5, Flat specimens 1 to 4. Specimen 1 failed due to clamping force. The tests of specimens 2 to 4 resulted in higher ultimate tensile stresses

Fixation is the biggest problem in testing high strength materials on ultimate tensile strength.

With Stainless steel the standard set-up works fine: the specimen does not slip in the wedges, nor does it fail due to the compressive forces of the wedge-clamp.

With carbon- and glass fiber this is different. Because of the pultrusion principle the strength and stiffness perpendicular to the fibers is much lower than that in the direction of the fibers. The specimen is crushed due to the compressive force of the wedge-clamp, long before the tensile stress in het fibers reaches its maximum. Measures have to be taken to prevent this.

The first tests on carbon fiber were done with a round specimen with a diameter of 2mm similar to the stainless steel described on page 7.

The specimen failed due to the compressive force of the wedge clamp. It crushed and started slipping.

Next attempt was with two flat wedges, this gave even poorer results.

The first flat specimen that is tested is a strip of 0,6x8mm. First attempt was done with two rough wedges. The strip failed at the wedge clamp due to a combination of tensile stress and clamping force

The second run was conducted with two aluminum plates between the wedge and the specimen. The aluminum deformed slightly and the tensile force at break was considerably higher. This test was repeated twice and the results were comparable in ultimate tensile stress and modulus of elasticity.

This clamping principle still did not suffice for the round specimens. For the next try the aluminum plates were replaced by sand paper from an industrial belt sander.

There are several different grades on the market, varying from 'grain 20' (20 big grains per square inch) to 'grain 1200' (1200 little grains). Using a low number results in a very firm gripping of the specimen, but it causes damage to the specimen. A high number does not grip the specimen enough and it will slip in the wedge clamps. Several tests were done with grains 40 to 180. Grain 80 seemed to be the best: it does not damage the specimen and is rough enough to prevent slipping.



Figure 6, Picture take before testing of specimen 2

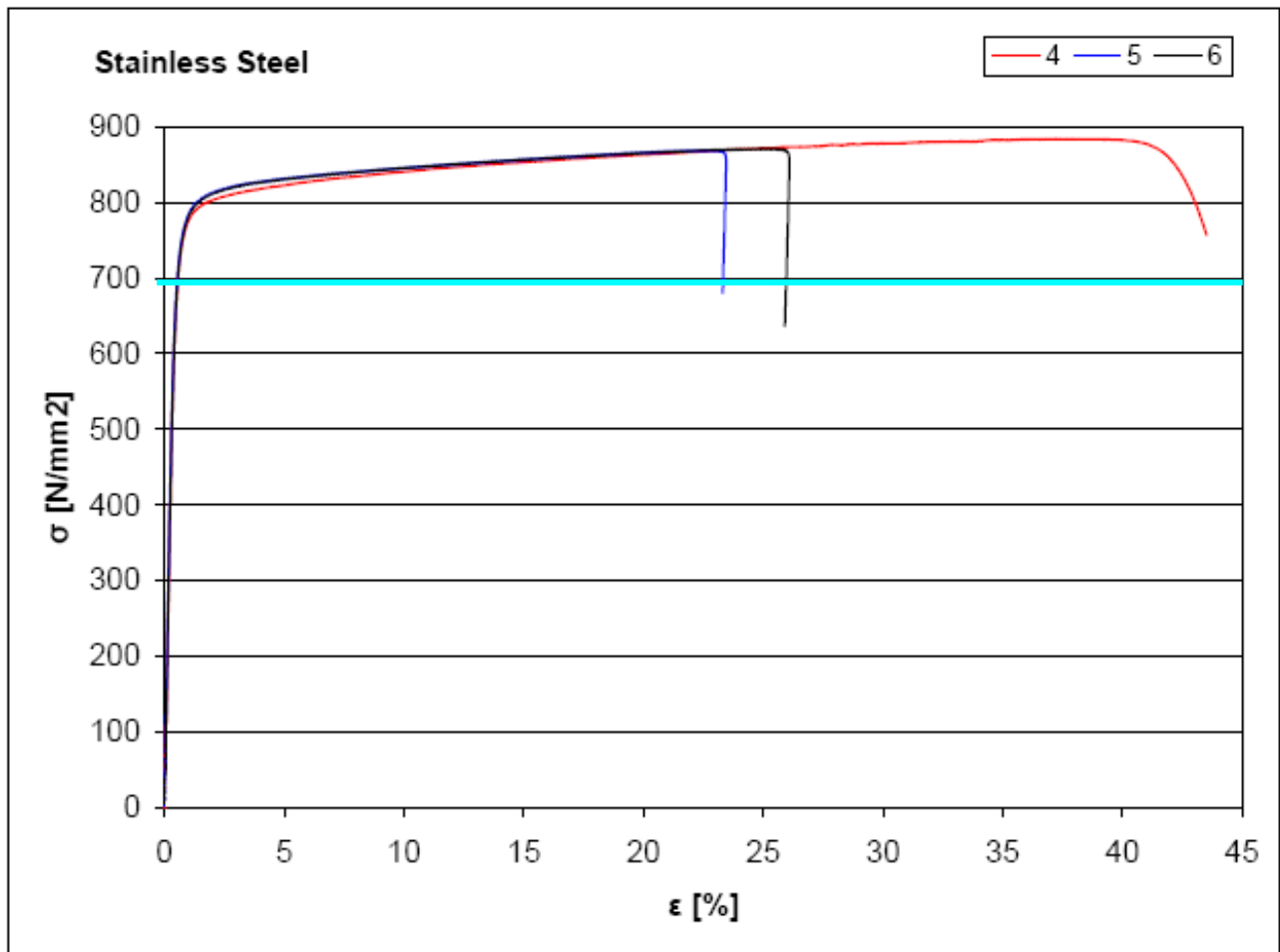


Figure 7, Stress-strain diagram of stainless steel specimens. The presumed yield strength is presented by the light blue line

Table 2, Mechanical properties of 316 stainless steel [18]

Grade	Tensile Strength [N/mm^2]min	Yield Strength 0.2% Proof [N/mm^2]min	Elongation (% in 50mm) min	Modulus of elasticity [N/mm^2]
316	515	205	40	193.000

Table 1, Summary of test results

Specimen #	Shape	Cross-section [mm^2]	Clamp to clamp distance [mm]	Strain at break [%]	Tensile strength [N/mm^2]
4	$\text{Ø}2\text{mm}$	3,14	91,0	44	884
5	$\text{Ø}2\text{mm}$	3,14	90,5	23	869
6	$\text{Ø}2\text{mm}$	3,14	90,5	30	871
Average				32	875

Results

Stainless steel

See literature study, page 34/35.

Hypothesis

The used material is Stainless steel 316.

Results

Three specimens were tested. The results are presented in *Table 1*.

The round specimens are clamped by different wedges: 1 flat wedge and 1 wedge with a groove with a depth of 1 mm. This way the specimen is fixated better than between two flat wedges.

The average ultimate tensile strength is 875 N/mm^2 . This value is however not acceptable for permanent loading. This material should not be loaded beyond the yield strength, which is assumed 700 N/mm^2 (see horizontal line in *Figure 7*).

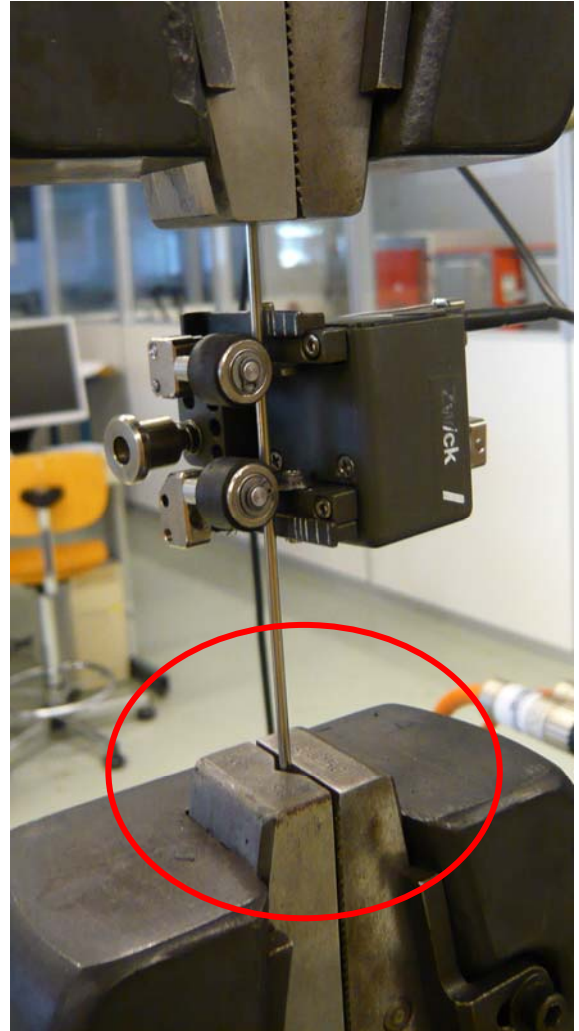


Figure 8, Stainless steel specimen in tensile test set-up prior to testing. Notice the two different wedges denoted by the red circle.

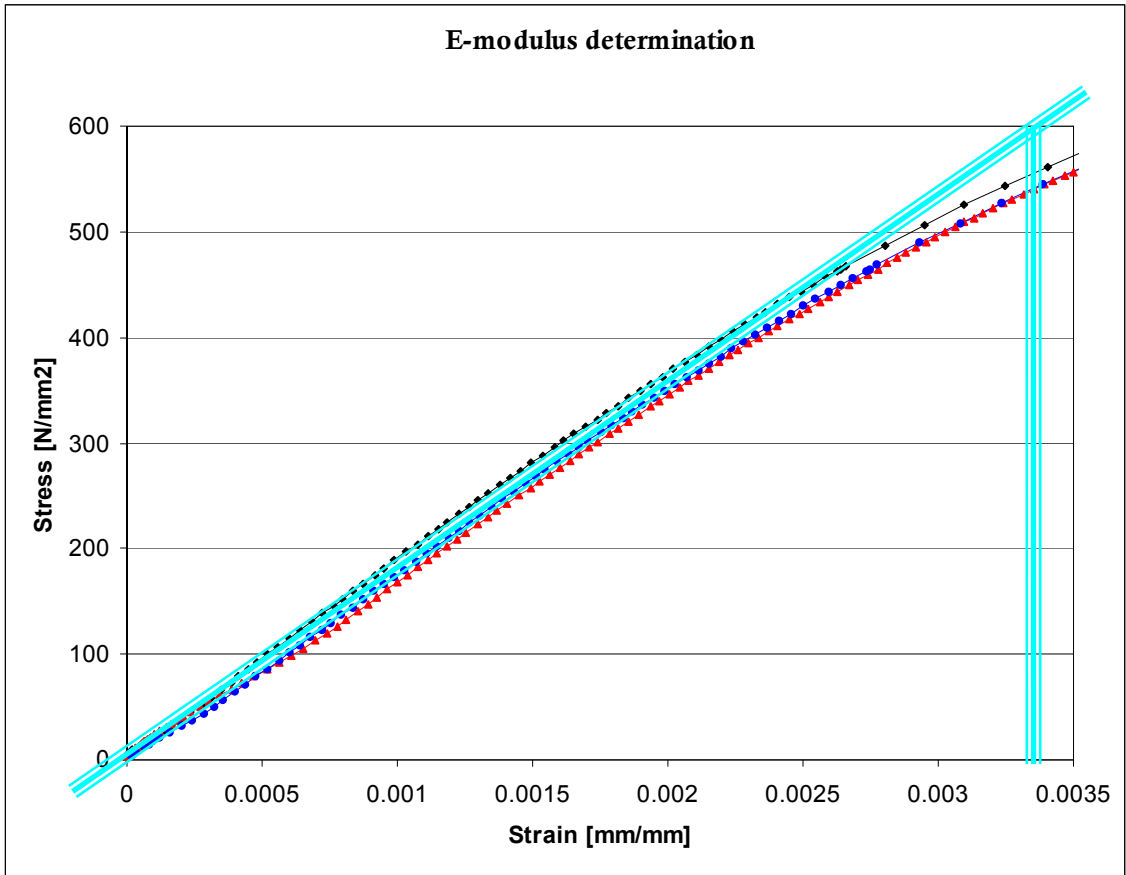


Figure 10, E-modulus determination

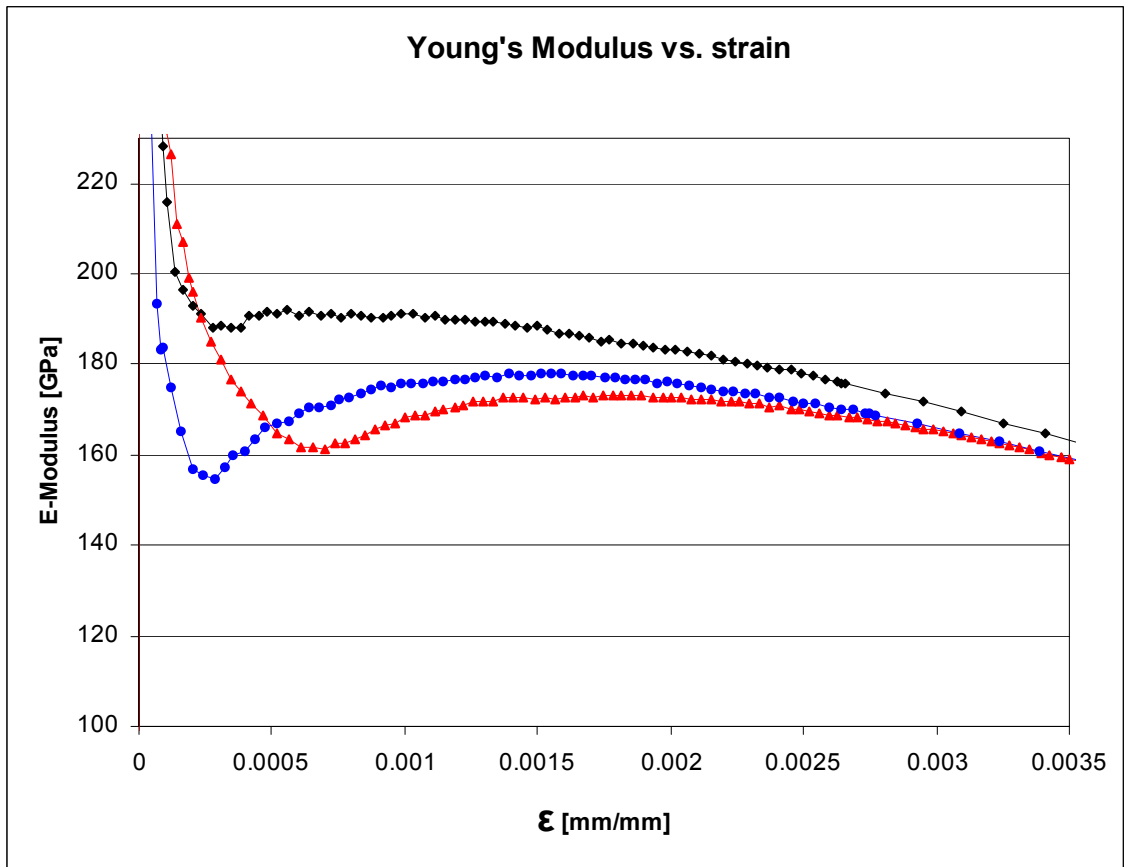


Figure 10, Young's modulus vs. strain

The Young's modulus can be derived from the results with help of the σ - ε diagram. The steel is most stiff at low strain.

The E-modulus is measured between 200 and 400 N/mm², indicated by the blue line in *Figure* . Above 400 N/mm² the E modulus drops which is also presented by *Figure 10*.

$$E = \frac{\Delta\sigma}{\Delta\varepsilon} \hat{=} \frac{600\text{N/mm}^2}{0.00335} = 179.104\text{N/mm}^2$$

$$E = 180\text{GPa}$$

Note that this is lower than the 193 GPa that is presented in *Table 2*.

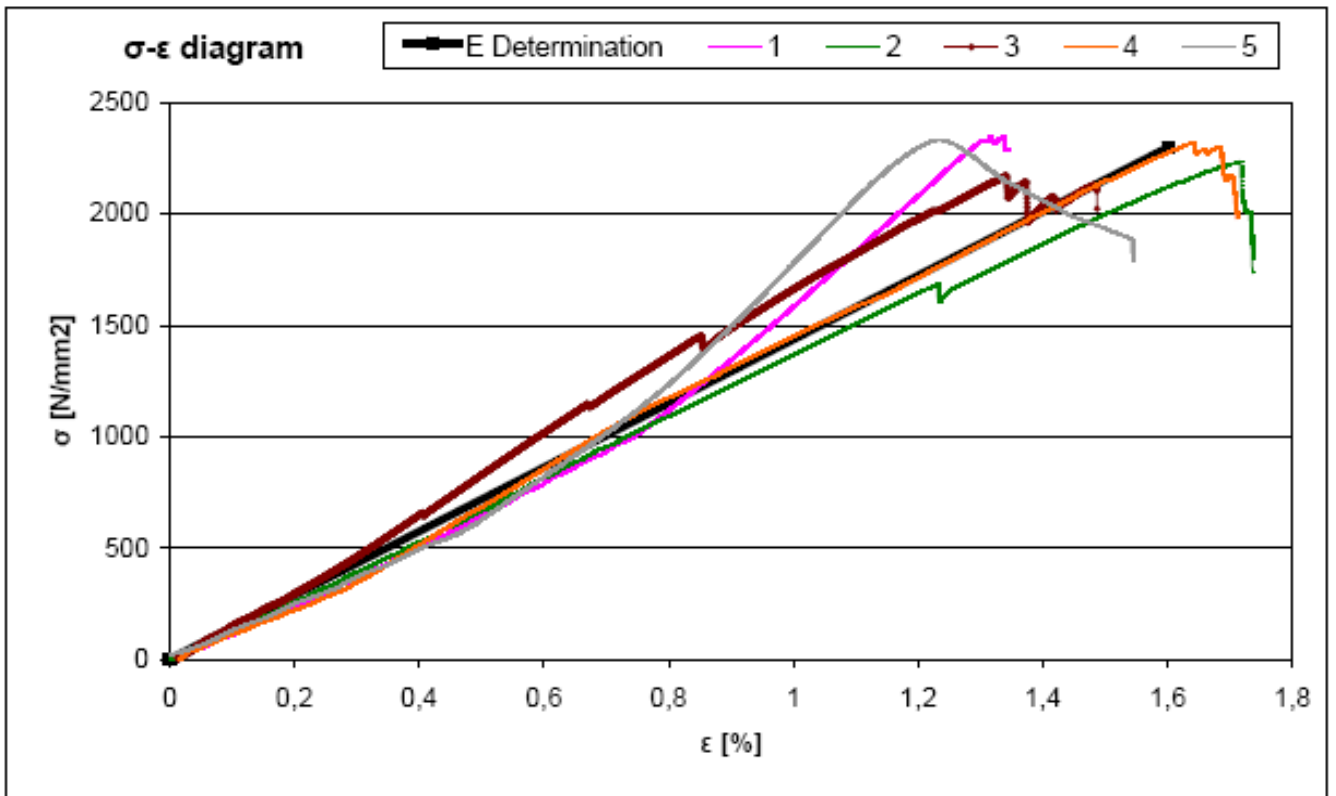


Figure 13, Stress-strain diagram of carbon fiber specimens with E-modulus determination

Table 4, Summary carbon fiber specimens

Specimen #	Dimension [mm ²]	Cross-section [mm ²]	σ -max [N/mm ²]
1	1,6 x 8 mm	12,80	2347
2	2,4 x 8 mm	14,40	2237
3	1 x Ø2mm	3,14	2172
4	2 x Ø2mm	6,28	2322
5	3 x Ø2mm	9,42	2332
Average			2282

Table 3, Mechanical properties of used carbon fiber rovings

Tenax [®] Fibers	HTA 5131
σ_{\max} [MPa]	3950
E [GPa]	238
ϵ_{\max} [%]	1,5
ρ [g/cm ³]	1,77

Carbon fiber

Hypothesis

Normal pultruded carbon fiber strips consist of 40-50% carbon filled with epoxy resin. The structural properties (for example strength and stiffness) of the resin are negligible to that of the carbon fiber and it serves merely to assure the shape of the profile. The used carbon fiber rods consist of 63% carbon, which is extraordinary high. The producer expects that evolutions in technology will enable this number to rise in the near future, granting an even higher ultimate tensile stress of the profile. Apart from this the technology in carbon roving production evolves. The used carbon rovings have an ultimate tensile strength of 4000 N/mm². Theoretically this value can increase a great deal as well.

The specimens are tested for ultimate tensile strength and E-modulus.

The theoretical value of these properties can be calculated to anticipate on the test. The E-modulus and ultimate tensile strength of the rovings (*Table 3*) are multiplied by a factor for the claimed amount of resin, which is 0,63.

$$\sigma_{u,roving} = 3950 \text{ N / mm}^2$$

$$\gamma_{resin} = 0,63$$

$$\sigma_{u,profile} = 3950 * 0,63 = 2488,5 \text{ N / mm}^2$$

$$E_{roving} = 238 \text{ GPa} = 238.000 \text{ N / mm}^2$$

$$E_{profile} = 238 * 0,63 = 149,94 \text{ GPa} \approx 150.000 \text{ N / mm}^2$$

$$\varepsilon_u = \frac{\sigma_u}{E} = \frac{2488 \text{ N / mm}^2}{150000 \text{ N / mm}^2} = 0,0165$$

$$\varepsilon_u = 0,016 * 100\% = 1,6\%$$

Results

The summary of used specimens can be found in *Table 4*.

The Modulus of elasticity is presented by the slope of the σ - ε diagram. This is comparable for all specimens. Although specimens 1 and 5 become stiffer at a stress of 1000 N/mm², it is fair to say that for E-modulus determination the slope of the σ - ε curve of specimen 4 is representative for all specimens.

$$E = \frac{\Delta\sigma}{\Delta\varepsilon} = \frac{2300 - 0 \text{ N / mm}^2}{0 - 1,6\%} = 143.750 \text{ N / mm}^2$$

$$E = 144 \text{ GPa}$$

The average ultimate tensile strength of the specimens is 2282 N/mm².

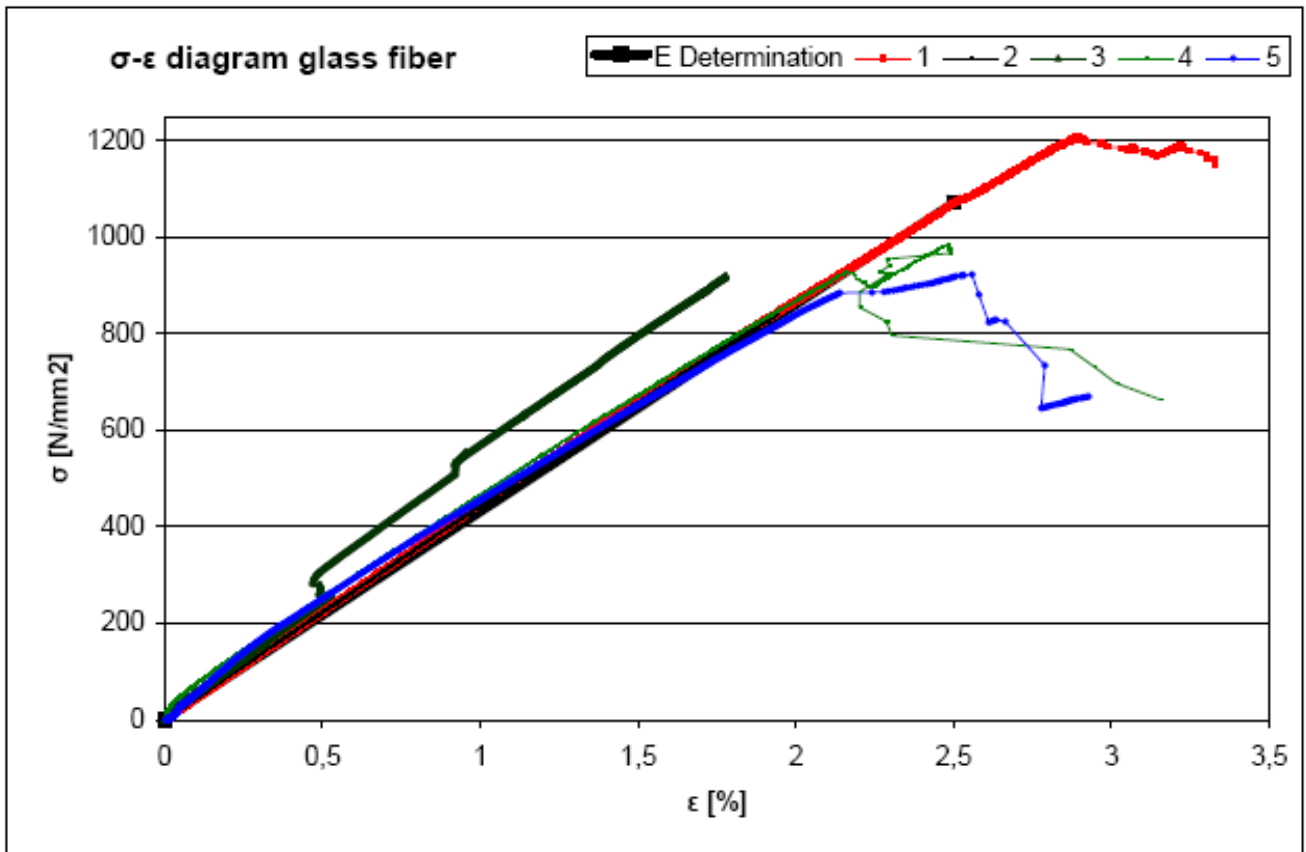


Figure 14, Stress strain diagram of glass fiber specimens

Table 5, Summary glass fiber specimens

Specimen #	Dimension [mm]	Cross-section [mm ²]	Total failure?	σ_{\max} [N/mm ²]
1	1 x Ø2mm	3,14	Yes	1208
2	1 x Ø2mm	3,14	No	841
3	1 x Ø2mm	3,14	No	919
4	3 x Ø2mm	9,42	Yes	984
5	3 x Ø2mm	9,42	Yes	923
Average 1,4 & 5				1038

Glass fiber

Initially the same fixating problems occurred as with the round carbon fiber specimens. Glass fiber is even more fragile than carbon fiber herein. The slipping nor crushing problems occurred when the 'grain 80' sand paper was used in the wedge clamps

The only pultruded glass fiber profiles available are round staffs. Chosen is for similar dimensions as tested in stainless steel and carbon fiber: Ø2mm.

Hypothesis

The same theoretical expectations for the tests can be made as for the carbon fiber specimens.

The rovings consist of R-glass fiber with a theoretical tensile strength of 3600 N/mm² and an E-modulus of 85 GPa.

$$\sigma_{u,roving} = 3600 \text{ N/mm}^2$$

$$\gamma_{resin} = 0,63$$

$$\sigma_{u,profile} = 3600 * 0,63 = 2268 \text{ N/mm}^2 \approx 2300 \text{ N/mm}^2$$

$$E_{roving} = 85 \text{ GPa} = 85.000 \text{ N/mm}^2$$

$$E_{profile} = 85 * 0,63 = 53,55 \text{ GPa} = 53.500 \text{ N/mm}^2$$

$$\varepsilon_u = \frac{\sigma_u}{E_u} = \frac{2268 \text{ N/mm}^2}{53500 \text{ N/mm}^2} = 0,0424$$

$$\varepsilon_u = 0,0424 * 100\% = 4,24\%$$

Results

The summary of used specimens can be found in *Table 5*.

The only odd curve is that of specimen 3. The two sudden fallbacks in strain are explained by slipping of the Zwick extensometer. This is proven by the fact that the force-displacement diagram did not show a fallback at those points.

$$E = \frac{\Delta\sigma}{\Delta\varepsilon} = \frac{1073 - 0 \text{ N/mm}^2}{0,025 - 0} = 42.920 \text{ N/mm}^2$$

$$E = 43 \text{ GPa}$$

The average maximum tensile stress is 1038 N/mm².

Table 6, Summary of test deviations

Material			Hypothesis	Measured	Deviation
Steel	σ_{\max}	[N/mm ²]	515	875	+70%
	E	[GPa]	193	180	-7%
Carbon fiber	σ_{\max}	[N/mm ²]	2488	2282	-8%
	E	[GPa]	150	144	-4%
Glass Fiber	σ_{\max}	[N/mm ²]	2300	1038	-55%
	E	[GPa]	53	43	-19%

Discussion

The expected ultimate tensile strength for both carbon fiber and glass fiber were not reached, as can be seen in *Table 6*.

This could be a consequence of the test set-up. For instance, the way of gripping is not ideal: the specimens are slightly damaged with the sand paper or hardened steel wedge clamps. This results in lower ultimate tensile strengths.

However, this should not have an effect on the measured Modulus of Elasticity. The expected values were not reached for all three materials.

The ultimate tensile strength of stainless steel that was given in *Table 2* is a minimum value for the strength up to yielding (0.2% yielding strength). It can be seen in *Figure 10* and *Figure 10* that the stiffness starts to degrade above 515 MPa.

The measured structural properties of the carbon fiber are for the E-modulus and for the ultimate tensile strength a bit lower than expected. This could be caused by the fact that not the proclaimed 63% of the surface consists of carbon roving, but a slightly lower amount.

$$\sigma_{\max, profile} = \sigma_{\max, roving} * \gamma_{resin}$$

$$\sigma_{\max, profile} = 3950 N / mm^2 * 0,58 = 2291 N / mm^2$$

$$E_{profile} = E_{roving} * \gamma_{resin}$$

$$E_{profile} = 238 GPa * 0,58 = 138 GPa$$

Remarkable is that the Glass fiber specimens did not by far reach the expected maximum tensile strength. This can be explained by the fact that the rovings did not consist of R-glass fiber, as was promised by the producer, but by an inferior roving.

The rovings probably consisted of the much more common E-glass fiber, which has a theoretical maximum tensile strength of 2100 N/mm².

If the amount of resin is also not 37%, but 50%, this would give the following theoretical tensile strength of the profile:

$$\sigma_{\max, profile} = \sigma_{\max, roving} * \gamma_{resin}$$

$$\sigma_{\max, profile} = 2100 N / mm^2 * 0,5 = 1050 N / mm^2$$

$$E_{profile} = E_{roving} * \gamma_{resin}$$

$$E_{profile} = 85 GPa * 0.5 = 42,5 GPa$$

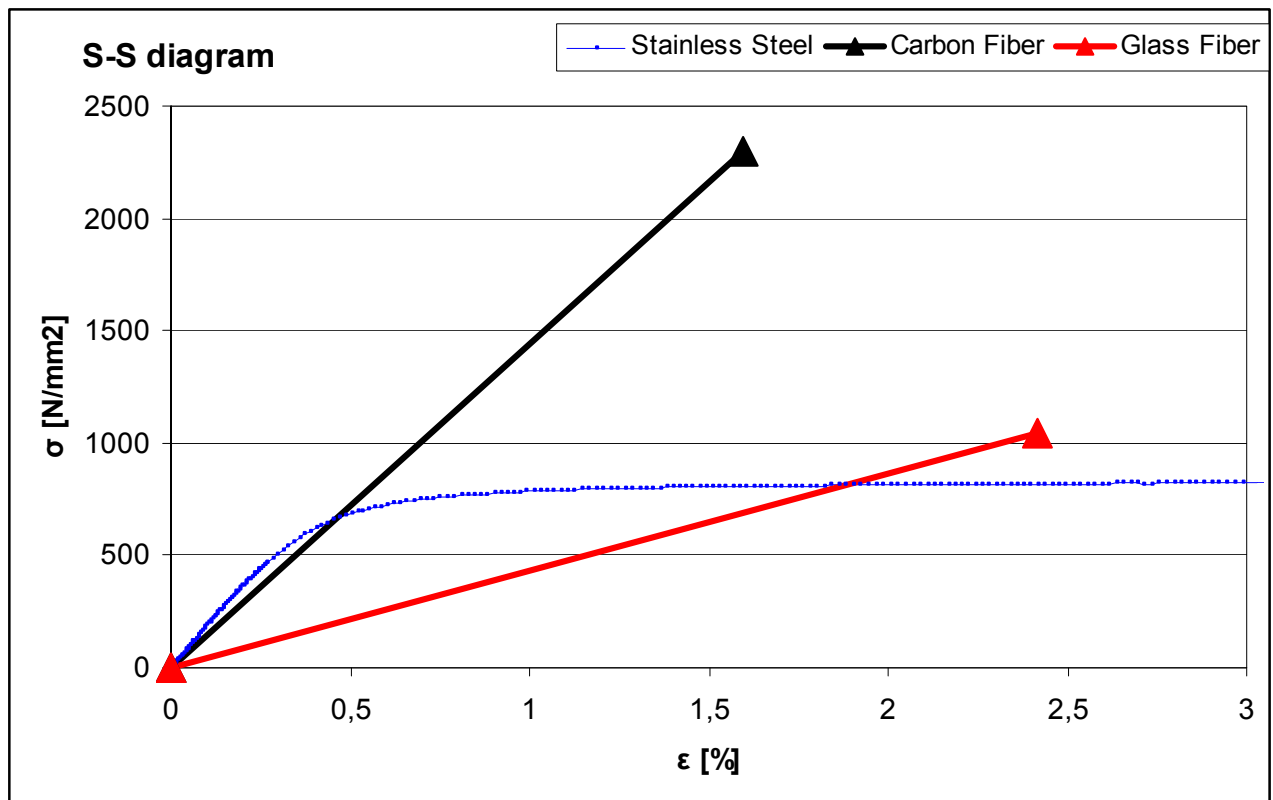


Figure 15, σ - ϵ curves of stainless steel, carbon fiber and glass fiber

Table 7, Concluded structural properties of tested materials

Carbon fiber	σ_{\max}	2300	[N/mm ²]
	E	145	[GPa]
Glass Fiber	σ_{\max}	1050	[N/mm ²]
	E	45	[GPa]
Steel	σ_{\max}	700	[N/mm ²]
	E	180	[GPa]

Concluded structural properties can be found in *Figure 15* and *Table 7*.

Other conclusions that are drawn from these tests are:

1. From the three tested materials, carbon fiber is the most suitable for the intended use in this thesis. It has the highest tensile strength and is relatively stiff. Carbon fiber has an elastic behavior up to total failure. Negative property is its lack of transparency.
2. Glass fiber also has an elastic behavior up to total failure. This type of glass fiber is not suitable for use as reinforcement in a structural glass girder. It is not transparent, less stiff than carbon fiber and less strong. The used glass fiber did not meet the expectations. Although the producer proclaimed to have delivered an R-glass fiber staff, it is more plausible that this profile consisted of E-glass fiber rovings. Further search for a transparent, strong and stiff glass fiber profile is recommended.
3. The used stainless steel specimens are not suitable for use in the intended glass girder. The tensile stress to which it can be loaded is low compared to carbon fiber and glass fiber. The modulus of elasticity is not much higher than carbon fiber.

Table 9, Used material at test 1, 2 and 3

Test #	Adhesive	Reinforcement				
		Measurement			Area [mm ²]	Material
1	DELO Rapid 03 Thix	2 Ø 2,0 mm			6,283185307	Carbon Fiber
2	DELO Rapid 03 Thix	2x 3x0,8 + 1x 6x0,8 mm			9,6	Carbon Fiber
3	Araldite 2013	2x 3x0,8 + 2x 3x0,13 mm			5,58	Carbon Fiber
	Girder	l	b	h		
	Float glass	1500	12	115	[mm]	

Table 8, Data of used adhesives

Adhesive Data	DELO Rapid 03 Thix	Araldite 2013
Color	Yellowish Transparent	Grey paste
Mixing Ratio	A:B = 1:1	A:B=1:1
Density [g/cm ³]	1,17	ca. 1,2
Viscosity (mixture) [mPas]	38000	Thixotropic
Pot lif in 3 g preparation [min]	4	50-80
Processing time in 3 g preparation [min]	3	ca. 30
Curing time untill firmness to touch [min]	13	240
Curing time until functional strength [h]	2	10
Cruing time untill final strength [h]	24	48
Tensile shear strength AI/AI [Mpa]	13	18
Compression shear strength AI/AI [Mpa]	14	N/A
Tensile strength [Mpa]	35	N/A
Elongation at tear [%]	20	
Young's modulus [Mpa]	2000	2500
Temperature resistance [C]	280	
Creep resistance CTI	525 M	

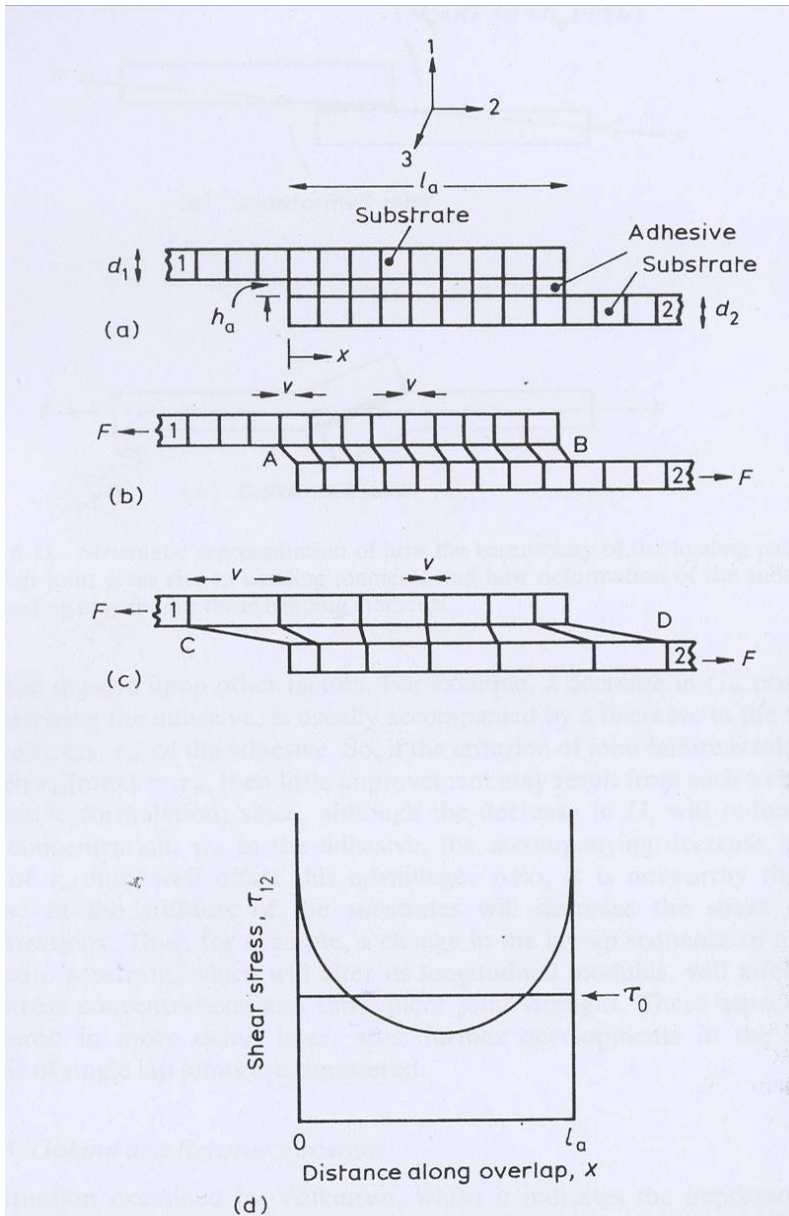


Figure 16 a-d. Schematic representation of single overlap joint: a) unloaded, b) loaded in tension with inextensible substrates, c) - with extensible substrates and d) shear stress distribution along overlap for (c)

5.3 Adhesive tests

Theory & Introduction

The tensile force in the reinforcement is transferred to the glass by an adhesive. This adhesive is therefore loaded primarily by shear stress.

In a typical 'single lap joint' this is not constant over the length of the connection because the substrates (glass and reinforcement) are not infinitely stiff.

Figure 16-d shows the shear stress distribution over a single lap joint. The joint in the tests is comparable to a double lap joint, but the principles are similar: a stress peak will arise in the beginning of the joint, decreasing fast along the joint.

In case of a completely elastic adhesive:

If this stress peak exceeds the maximum shear stress capacity of the adhesive, the adhesive connection will fail locally, resulting in a shift of the peak along the length of the connection, resulting in total failure of the joint.

If the adhesive has a perfect elastic-plastic behavior, the adhesive will start to creep where the stress peak exceeds the strength. The peak will widen as shear force on the joint increases until the maximum shear capacity of the joint is reached and the adhesive fails.

The strength of each adhesive is different. This depends (amongst other things) on the type of adhesive, thickness of the adhesive layer, substrate materials, roughness of the surface and stiffness of the substrates.

The exploring tests described in this chapter are done to gain a rough insight in the behavior of selected adhesive systems to differences in the thickness of the layer and stiffness of the used substrates.

Goal is to find out if there is a great difference in shear stress capacity between the used adhesives and if the variables have a great influence on the strength of the connection. A secondary goal is to develop routine in

applying the adhesive systems and experiencing if they are useful in practice.

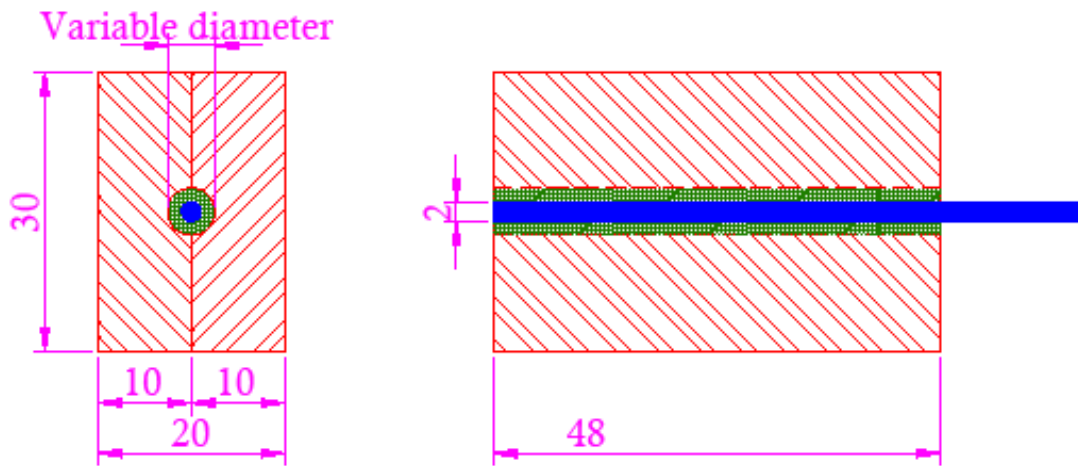
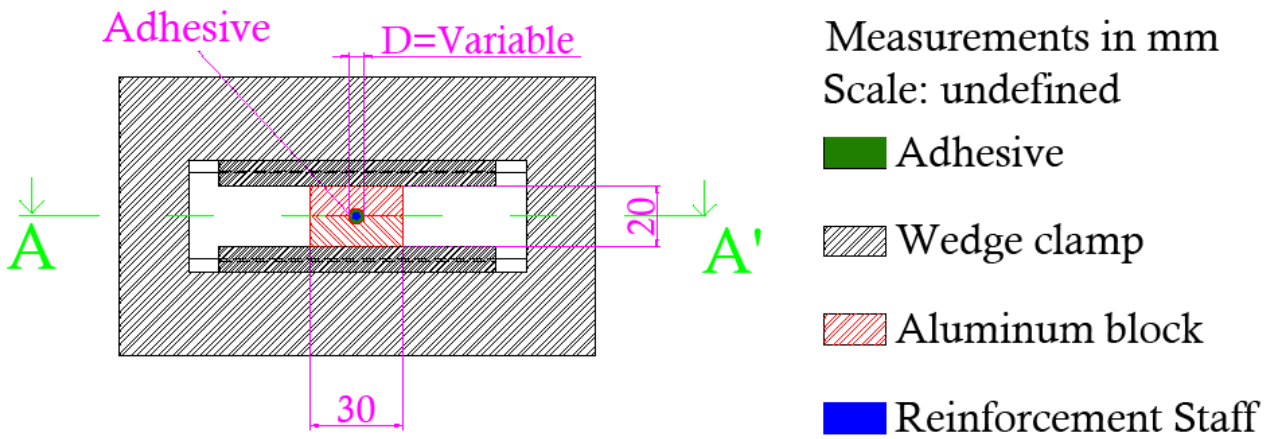
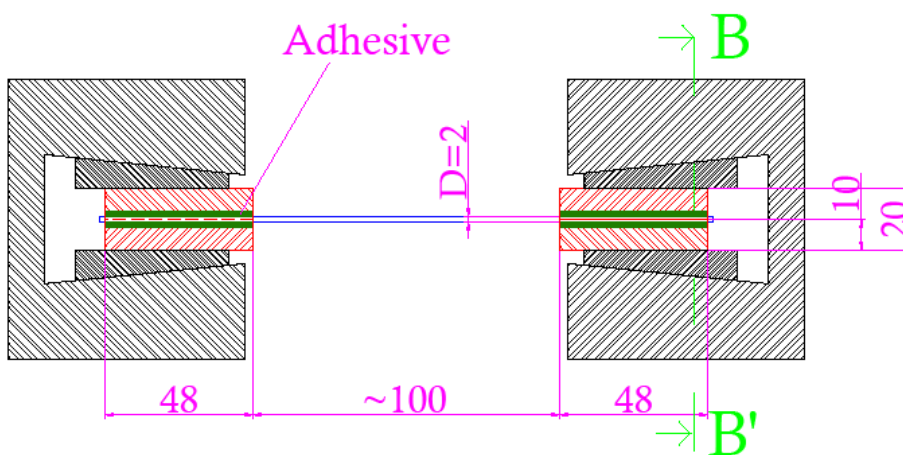


Figure 18, Close-up of specimen in cross-section BB' (left) and AA' (right) Legend of Error!
Reference source not found. applies



Crosssection BB'



Crosssection AA'

Figure 17, Test set-up

Method

It is expected that the tensile force on the aluminum blocks will be transferred to the reinforcement staff in the first approximately 5mm of the connection. A factor 10 (~50mm) seems reasonable for an exploring test.

First idea was to create a round hole in an aluminum block, place a circular staff in the centre and fill it up with adhesive. However, drilling a hole with a diameter of 2mm and a depth of 50 mm in an aluminum block seemed very hard. The drill became unstable after approximately 5 mm and broke off.

Decided was to create an identical specimen as follows:

The surface of two aluminum blocks with dimensions 48*30*10mm is mounted with a half-round groove of constant diameter thru the centre line. The blocks are placed together so that the two grooves form a circular shaped hole. In the centre of this hole a round staff with a diameter of 2 mm is placed. The hole is filled up with adhesive. The thickness of the adhesive layer is varied by varying the size of the groove and therefore the diameter of the hole.

Three adhesive systems are tested:

- Huntsman Araldite 2013
- DELO Rapid 03 Thix
- Huntsman Araldite 2020

The specimens are tested in a displacement controlled tensile test setup similarly to the one described in the former paragraph.

The aluminum blocks are clamped in the wedge clamps, the Zwick extensometer is attached to the middle of the staff. The clamp displacement, tensile force and strain of the staff are measured.

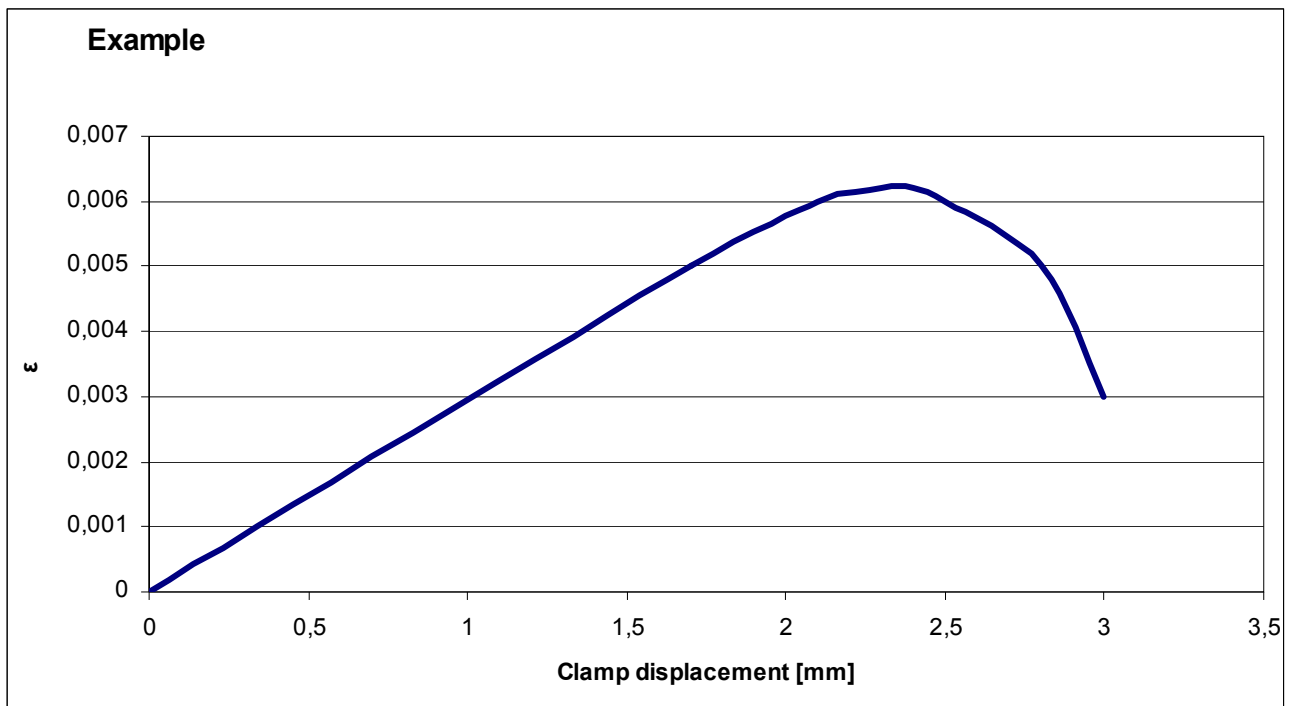


Figure 19, Example of stress-strain diagram

Table 10, Tested specimens

#	Staff material	Adhesive	Diameter hole [mm]		Adhesive thickness [mm]	
1	Carbon fiber	R 03 Th	2,0	[mm]	< 0,1	[mm]
2	Carbon fiber	R 03 Th	3,0	[mm]	0,5	[mm]
3	Carbon fiber	R 03 Th	5,0	[mm]	1,5	[mm]
4	Glass fiber	R 03 Th	2,0	[mm]	< 0,1	[mm]
5	Glass fiber	R 03 Th	3,0	[mm]	0,5	[mm]
6	Glass fiber	R 03 Th	5,0	[mm]	1,5	[mm]
7	Glass fiber	2013	2,0	[mm]	< 0,1	[mm]
8	Glass fiber	2013	3,0	[mm]	0,5	[mm]
9	Glass fiber	2013	5,0	[mm]	1,5	[mm]
10	Glass fiber	2020	2,0	[mm]	< 0,1	[mm]
11	Glass fiber	2020	5,0	[mm]	1,5	[mm]

The theoretical extension of the staff can be calculated from the E-modulus of the staff material (gained in the previous tests) and the initial distance between the aluminum blocks. The difference between this and the clamp displacement is caused by deformation (failure) of the adhesive connection between aluminum and staff.

If the strain-clamp displacement diagram is presented (see example *Figure 19*), it should give a linear curve up to the point where the adhesive reaches its maximum shear stress. At that point the curve should bend off to level and eventually drop down when the adhesive totally fails.

With a stiff adhesive the curve will bend off sharp and drop down abruptly when the maximum shear stress is reached. With a ductile adhesive the curve will bend off more gradually.

An overview of the specimen geometries can be found in *Table 10*.

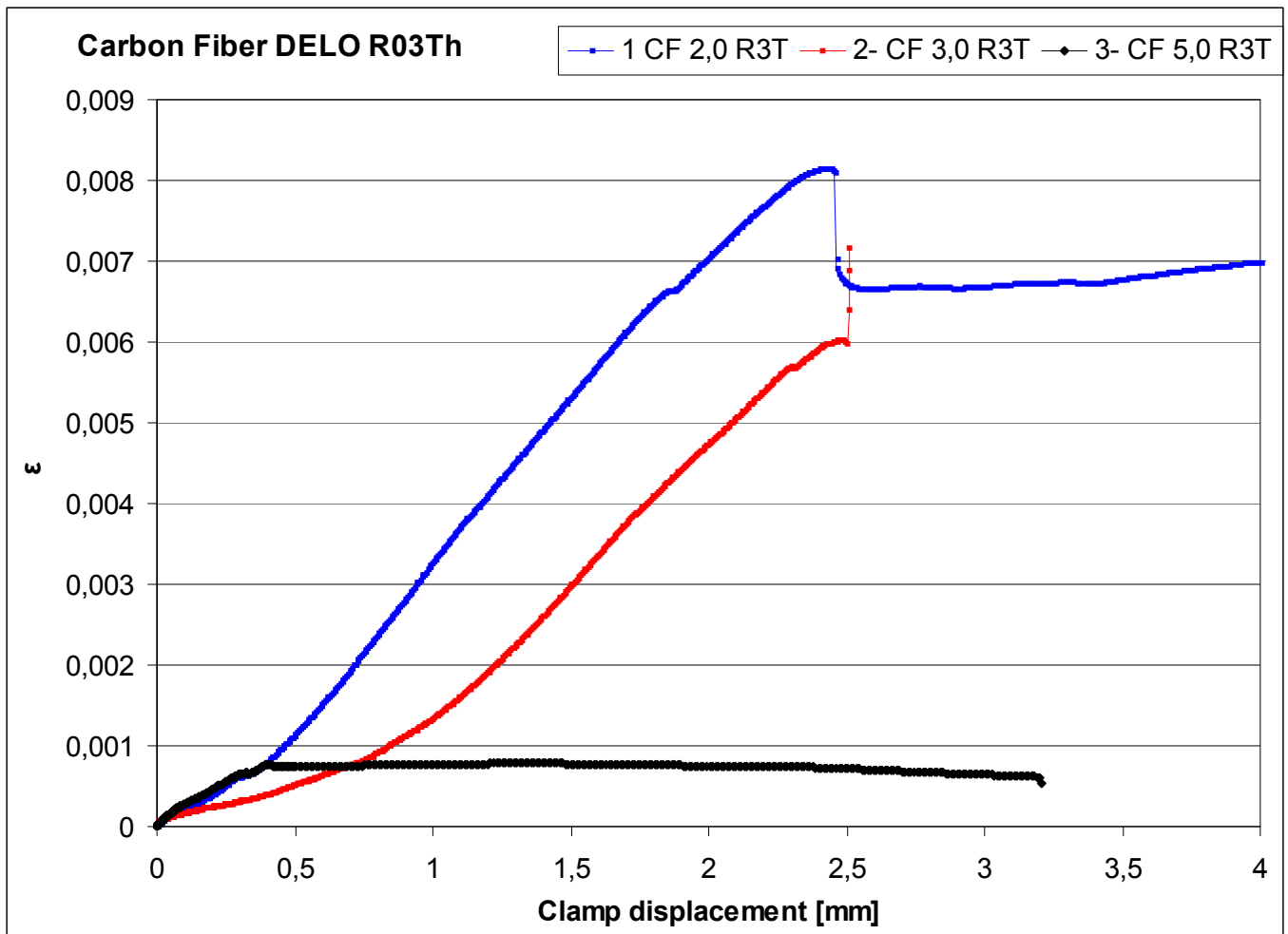


Figure 20, Strain-displacement curve of carbon fiber staff in combination with DELO Rapid 03 Thix

Table 11, Results specimens 1 to 3

#	Staff material	Adhesive	Diameter hole [mm]		Adhesive thickness [mm]		F _{max} [F]		Failure mode	
									Adhesive	Staff
1	Carbon fiber	R 03 Th	2,0	[mm]	< 0,1	[mm]	3395	[N]	X	
2	Carbon fiber	R 03 Th	3,0	[mm]	0,5	[mm]	2496	[N]	X	
3	Carbon fiber	R 03 Th	5,0	[mm]	1,5	[mm]	333	[N]	X	

Results

Carbon fiber

Hypothesis

Hypothesis is that the maximum tensile strength of the carbon fiber will not be reached.

The carbon fiber staff will break at a tensile force of:

$$F_{\max} = \sigma_{\max} * \pi r^2$$

$$F_{\max} = 2300 * \pi \approx 7200\text{N}$$

Results

The results are presented in *Figure 20* and *Table 11*.

None of the specimens failed due to breaking of the carbon fiber strip

The highest force was gained with the thinnest adhesive layer.

Specimen 3 failed at a tensile force of 333N. This is much less than expected.

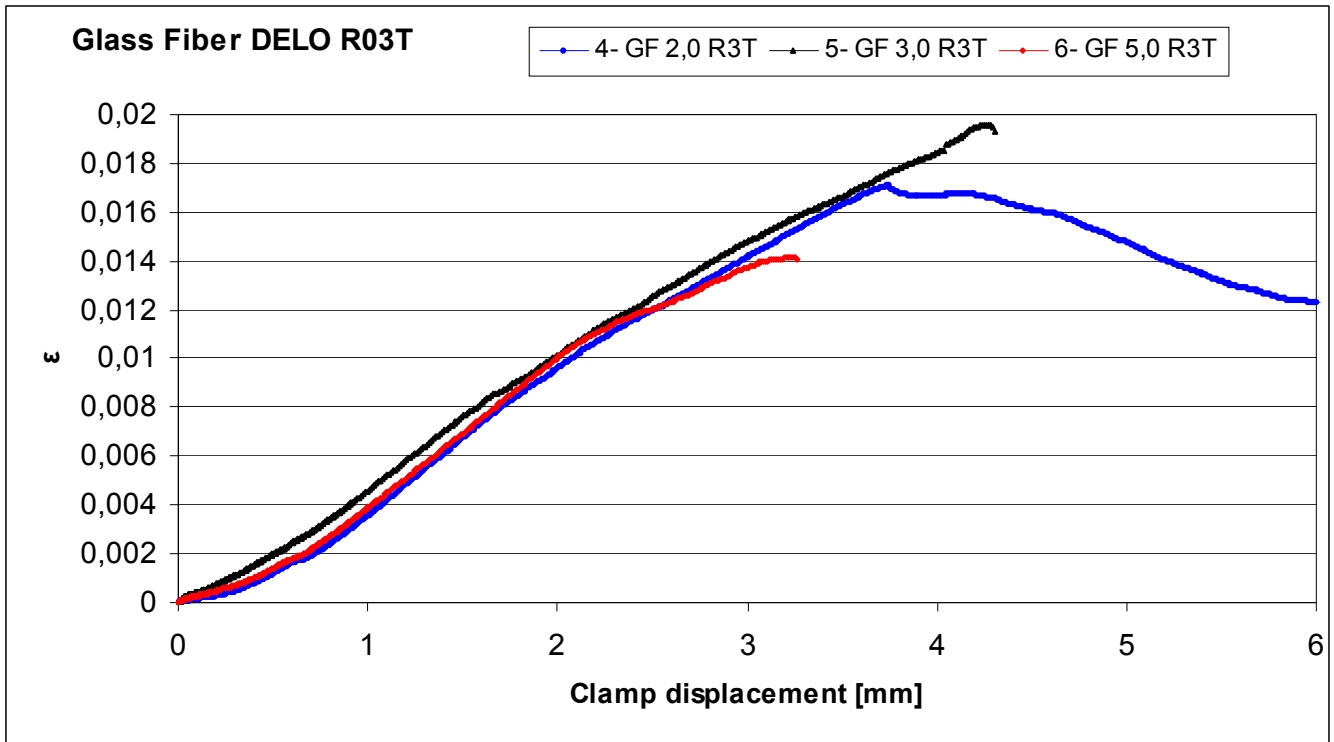


Figure 21, Strain-displacement diagram for specimens 4 to 6

Table 12, Results specimens 4 to 6

#	Staff material	Adhesive	Diameter hole		Adhesive thickness		F _{max}		Failure mode	
									[mm]	[mm]
4	Glass fiber	R 03 Th	2,0	[mm]	< 0,1	[mm]	2336	[N]	X	
5	Glass fiber	R 03 Th	3,0	[mm]	0,5	[mm]	2668	[N]	X	
6	Glass fiber	R 03 Th	5,0	[mm]	1,5	[mm]	2035	[N]	X	

Glass fiber

Hypothesis

Hypothesis is that the maximum tensile strength of the glass fiber might be reached and the glass fiber could break before the adhesive fails.

The glass fiber staff will break at a tensile force of approximately:

$$F_{\max} = \sigma_{\max} * \pi r^2$$

$$F_{\max} = 1050 * \pi \approx 3300\text{N}$$

Results

The glass fiber staff has not broken for specimens 4 to 6.

The highest tensile force was reached with a adhesive thickness of 0,5 mm.

Specimen 4 started slipping in the aluminum block after the maximum tensile force was reached.

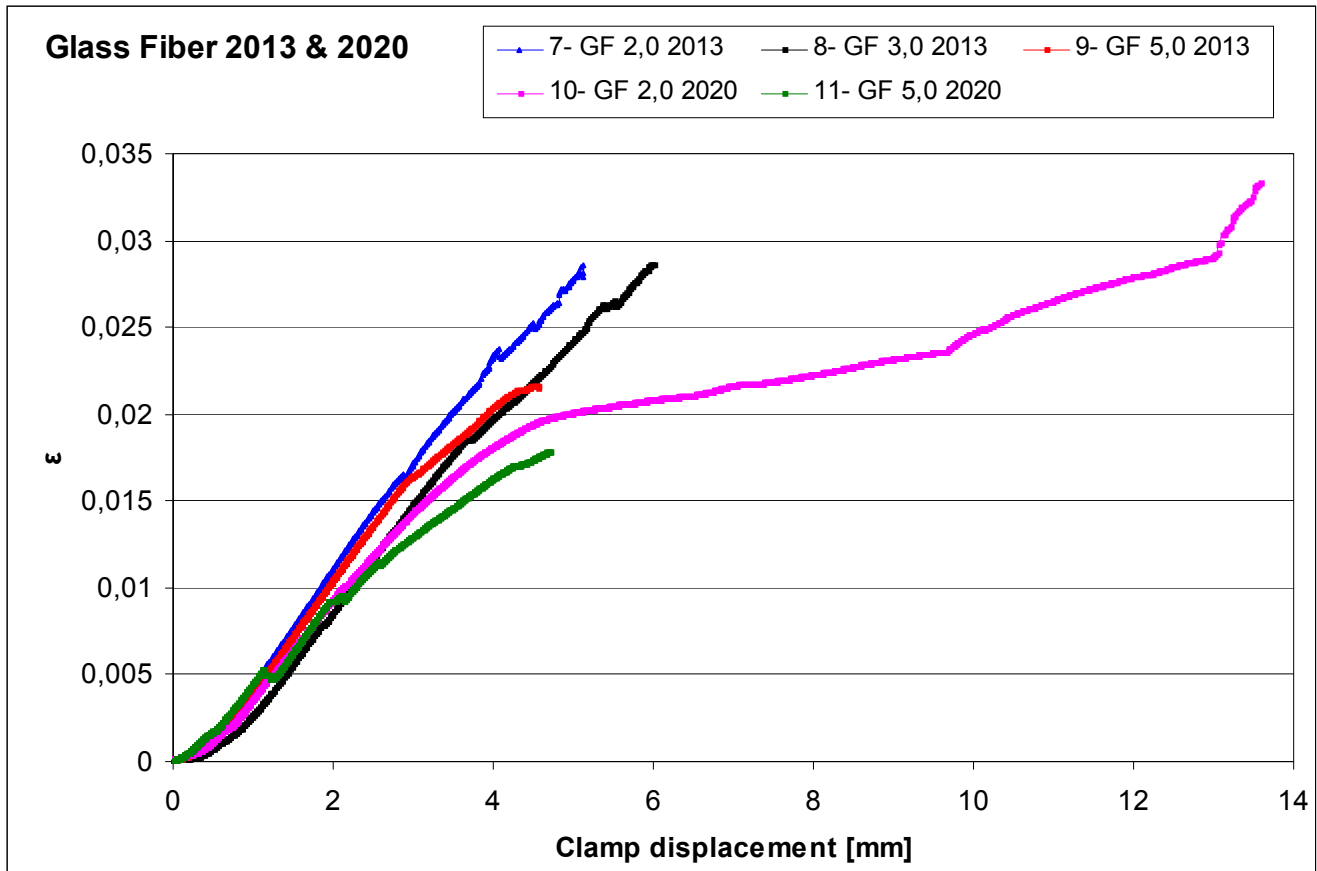


Figure 22, strain-displacement diagram for specimens 7 to 11

Table 13, Test results for specimens 7 to 11

#	Staff material	Adhesive	Diameter hole [mm]	[mm]	Adhesive thickness [mm]	[mm]	Fmax [F]	[N]	Failure mode	
									Adhesive	Staff
7	Glass fiber	2013	2,0	[mm]	< 0,1	[mm]	3073	[N]		X
8	Glass fiber	2013	3,0	[mm]	0,5	[mm]	3474	[N]	X	X
9	Glass fiber	2013	5,0	[mm]	1,5	[mm]	3012	[N]	X	
10	Glass fiber	2020	2,0	[mm]	< 0,1	[mm]	3796	[N]	X	X
11	Glass fiber	2020	5,0	[mm]	1,5	[mm]	2887	[N]	X	

Specimen 10 failed at a force of approximately 2700 N. The rest of the curve is caused by slipping in the block. This continued for about 10mm. Eventually the force increased again because the specimen was thicker at the end and the friction increased.

The highest tensile force was reached with a layer thickness of 0,5 mm.

The curves of specimens 9, 10 and 11 bend off, unlike specimens 7 and 8.

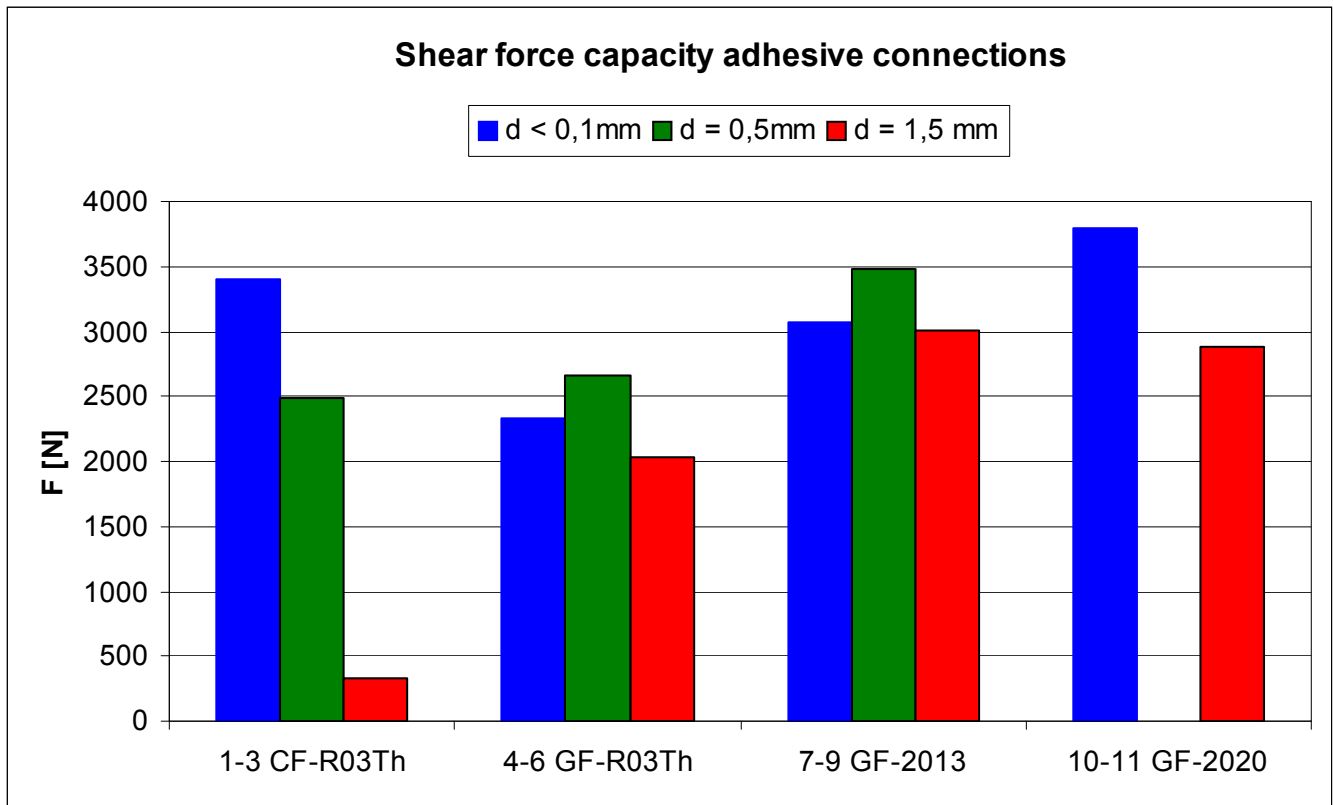


Figure 23, Maximum tensile forces for specimens 1 to 11, from left to right. The colors mark the adhesive layer thicknesses.

Table 14, Test results for specimens 1 to 11

#	Staff material	Adhesive	D-hole [mm]		Adhesive thickness [mm]		Fmax [F]		Failure mode	
									Adhesive	Staff
1	Carbon fiber	R 03 Th	2,0	[mm]	< 0,1	[mm]	3395	[kN]	X	
2	Carbon fiber	R 03 Th	3,0	[mm]	0,5	[mm]	2496	[kN]	X	
3	Carbon fiber	R 03 Th	5,0	[mm]	1,5	[mm]	333	[kN]	X	
4	Glass fiber	R 03 Th	2,0	[mm]	< 0,1	[mm]	2336	[kN]	X	
5	Glass fiber	R 03 Th	3,0	[mm]	0,5	[mm]	2668	[kN]	X	
6	Glass fiber	R 03 Th	5,0	[mm]	1,5	[mm]	2035	[kN]	X	
7	Glass fiber	2013	2,0	[mm]	< 0,1	[mm]	3073	[kN]		X
8	Glass fiber	2013	3,0	[mm]	0,5	[mm]	3474	[kN]	X	X
9	Glass fiber	2013	5,0	[mm]	1,5	[mm]	3012	[kN]	X	
10	Glass fiber	2020	2,0	[mm]	< 0,1	[mm]	3796	[kN]	X	X
11	Glass fiber	2020	5,0	[mm]	1,5	[mm]	2887	[kN]	X	

Discussion, Conclusions and recommendations

Discussion

General remark that has to be made is that the amount of tested specimens is not enough to draw solid conclusions. The tests are done for roughly exploring these adhesive systems and to interpret a trend in the results. Further research has to be conducted after these tests.

The results for specimen 3 are remarkably bad. Half of the length of the adhesive connection failed due to adhesive failure to the carbon, the other half due to adhesive failure to the aluminum.

The outcome of this test will not be taken seriously into consideration.

Comparing specimens 4 to 6 with 7 to 9, one could get the impression that Araldite 2013 is stronger than DELO Rapid 03 thix. Araldite 2020 also delivered better results than DELO Rapid 03 Thix.

Comparing specimens 1 and 4 implies that a stiffer staff (carbon fiber) has better results with a thin adhesive layer. This endorses the hypothesis that the shear stress peak in the adhesive layer spreads out as the substrate becomes stiffer.

Comparing specimens 4 to 6 and 7 to 9 implies that a less stiff staff (glass fiber) has better results with a slightly thicker adhesive layer. This implies that the optimum adhesive layer thickness for these specimens lies somewhere between 0,1 and 1,5mm.

Conclusions and recommendations

Araldite 2020 reached the highest shear strength with a thin adhesive layer.

Araldite 2013 reached the highest shear strength with a thick adhesive layer.

Delo Rapid 03 Thix is a very fast curing adhesive. For the intended use in a girder the processing time is too short. Apart from that it seems that the structural properties are not as good as those of for instance the Araldite 2020, which is also a transparent adhesive.

The best overall results with Glass fiber in combination with Rapid 03 Thix were gained with an adhesive layer thickness of 0,5mm. This gives the idea that there is an optimum in the thickness of the adhesive layer which is somewhere between 1,5mm and 0,1mm.

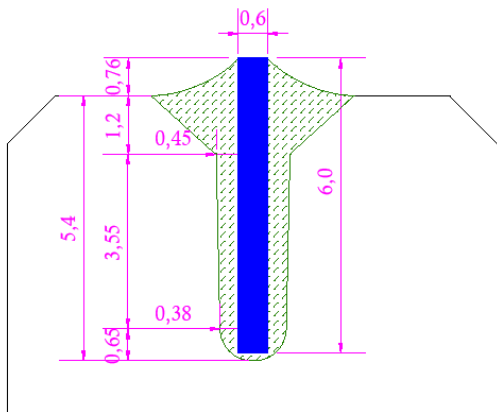


Figure 24, configuration of carbon strip in groove

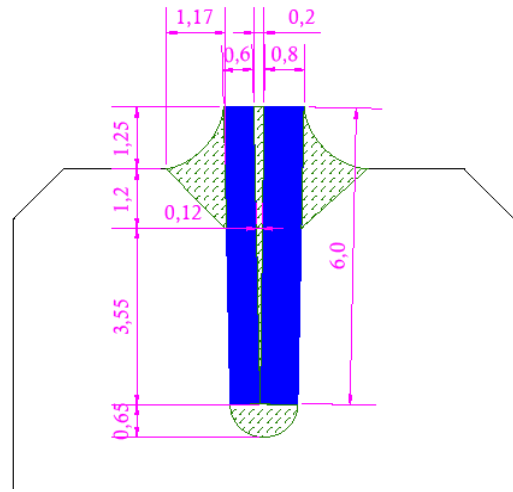

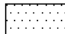

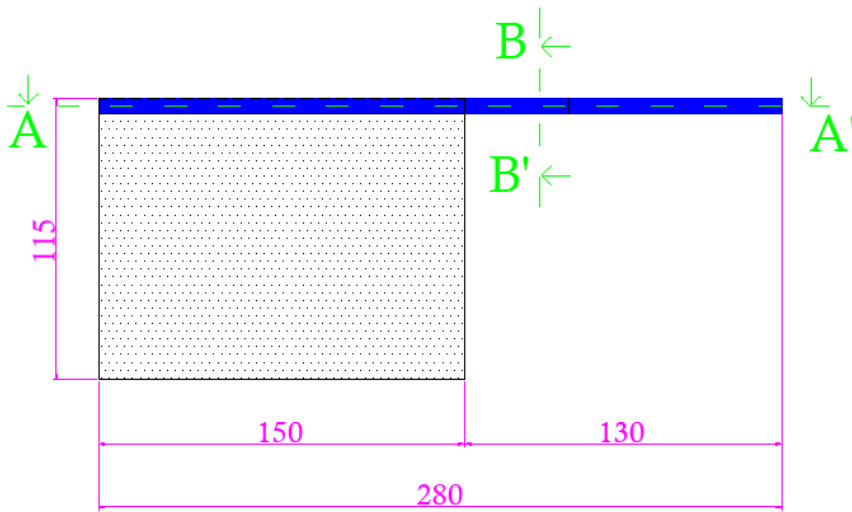


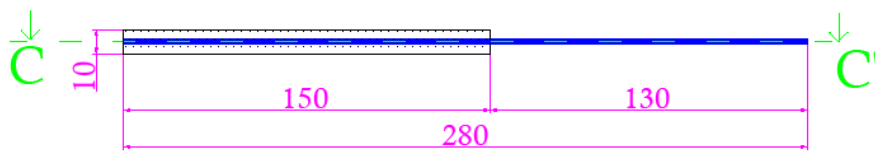
Figure 26, Close-up of Plug-in groove in cross-section BB'

Measurements in mm
Scale: undefined

-  Adhesive
-  Glass
-  Reinforcement



Cross section CC'



Cross section AA'

Figure 25, Specimen dimensions

5.4 Glass pull-out tests

Test sequence 1

Introduction

The goal is to find the maximum tensile force that can be applied to the reinforcing element.

This is done by testing samples of the glass pane in a tensile test setup: The glass pane is fixed and the reinforcement is pulled out.

Three adhesive systems are tested in the same configuration and compared for strength and failure behavior.

Method

Specimens

The specimens consist of glass panes measuring 150x115x10 mm (*Figure 25*). The long edge of 150 mm is finished with the Plug-in groove. In this groove two carbon fiber strips are bonded to the glass by an adhesive (*Figure 26*).

The materials are thoroughly cleaned with acetone and cloth.

9 specimens are prepared (*Table 15*); 3 with Araldite 2011, 3 with 2013 and 3 with 2020. The configuration is constant: two carbon fiber strips of 0,6x6mm and 0,8x6mm.

Because the Araldite 2020 has a long curing time of >7 days at 23°C, all specimens are cured for 24 hours at 23°C and 3 days at 55°C. The glass panes of all 2020 specimens fractured at the groove due to thermal expansion and were discarded.

The specimens rested for 2 hours at room temperature before testing commenced.

Table 15, Remaining specimens, test sequence 1

Specimen #	Adhesive	Configuration	Adhesion length
2011_01	Araldite 2011	0,6x6 + 0,8x6 mm	150 mm
2011_02	Araldite 2011	0,6x6 + 0,8x6 mm	150 mm
2011_03	Araldite 2011	0,6x6 + 0,8x6 mm	150 mm
2013_01	Araldite 2013	0,6x6 + 0,8x6 mm	150 mm
2013_02	Araldite 2013	0,6x6 + 0,8x6 mm	150 mm
2013_03	Araldite 2013	0,6x6 + 0,8x6 mm	150 mm

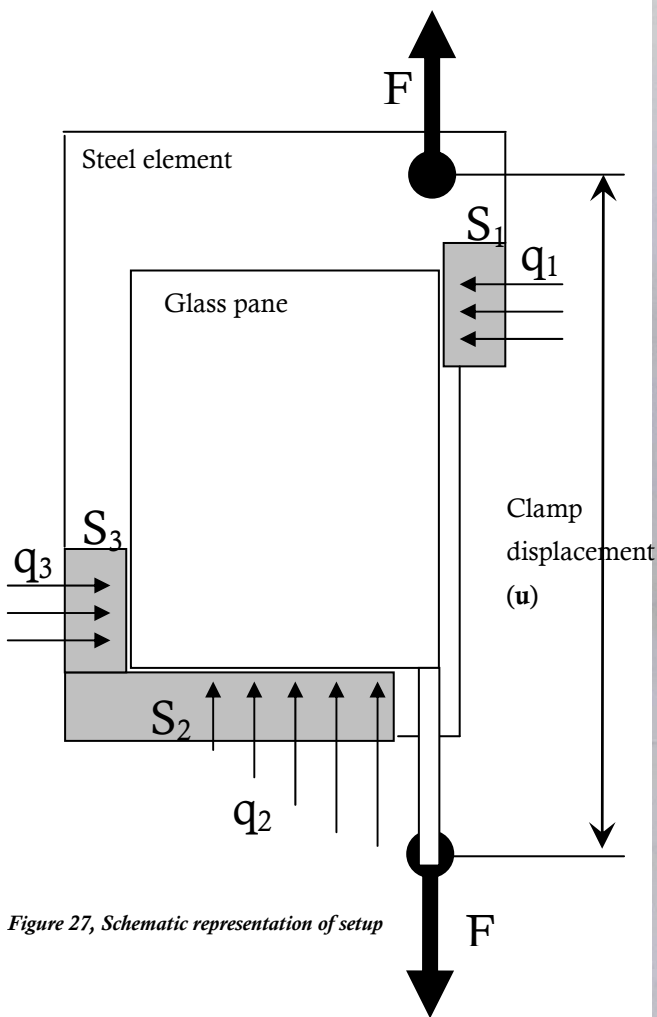


Figure 27, Schematic representation of setup

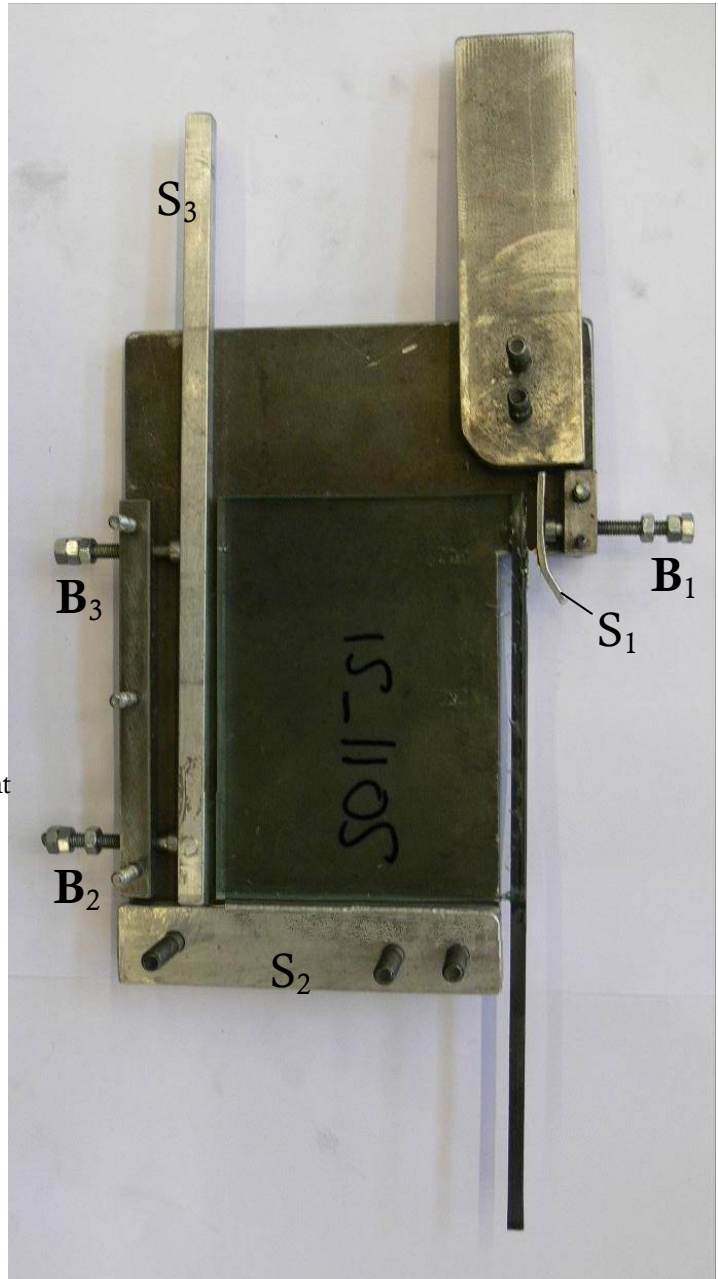


Figure 28, Steel supporting element (opened out) with specimen.

Setup

Schematic representation is given in *Figure 27*, photograph of opened out element in *Figure 28*. In short: the glass pane is fixed and the reinforcement is pulled out of the glass pane by a bank draft.

Fixing the glass pane is done by a stiff element consisting of two steel plates with a thickness of 12mm and aluminum support blocks. The centre line of the reinforcement of the specimen coincides with the centre line of the steel gripping handle that will be clamped in the upper wedge clamp.

Dimensional inaccuracy of the glass panes demanded fine-tuning options for positioning each specimen. Horizontal position and rotation of the specimen can be altered by adjusting the bolts B_1 , B_2 and B_3 .

The top of S_2 is filed off a bit round so that the concentration of q_2 is minimized.

After each test the specimen has to be replaced. This is possible without removing it from the bank draft or opening the whole element. Specimen can be taken out by removing one bolt from the handle and then turning the rest of the element (*Figure 29*).

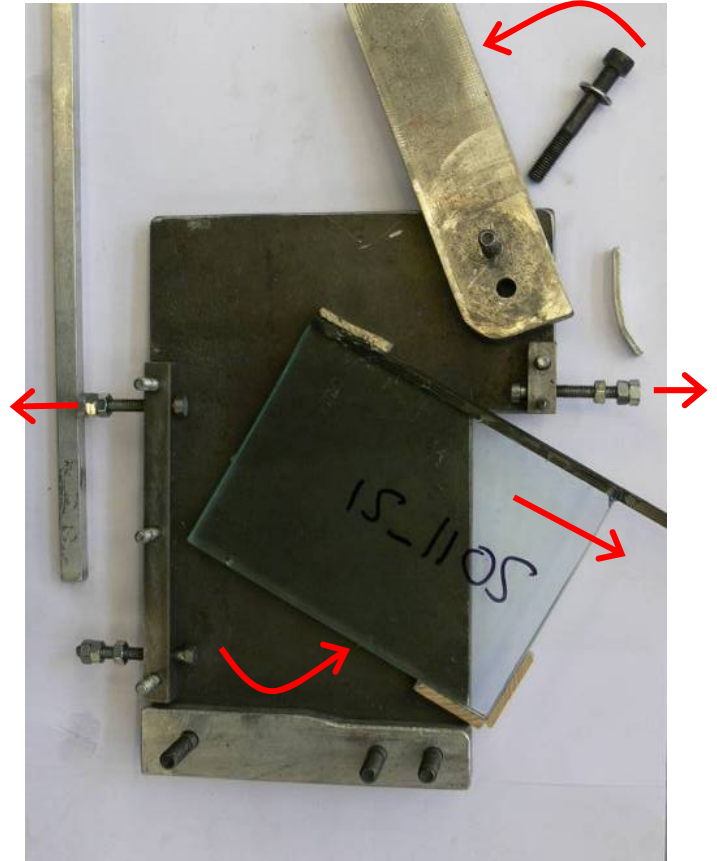


Figure 29, Replacing specimens; 1 bolt and 2 supports are removed to allow turning.



Figure 30, Overview of test setup with camera position

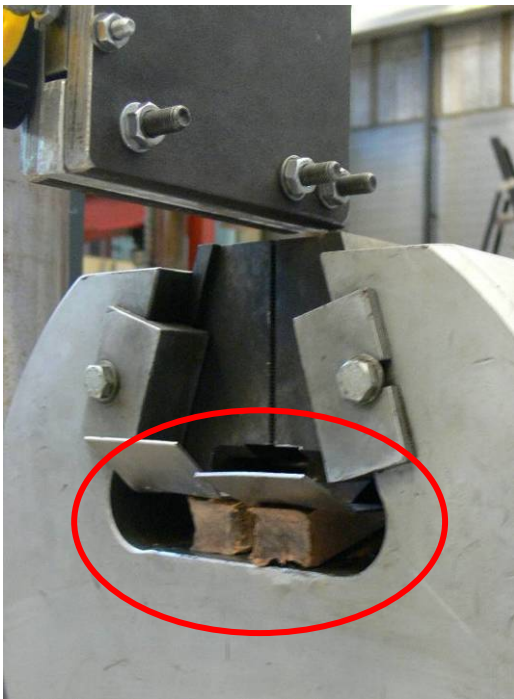


Figure 32, Lower wedge clamp with wooden wedges encircled in red

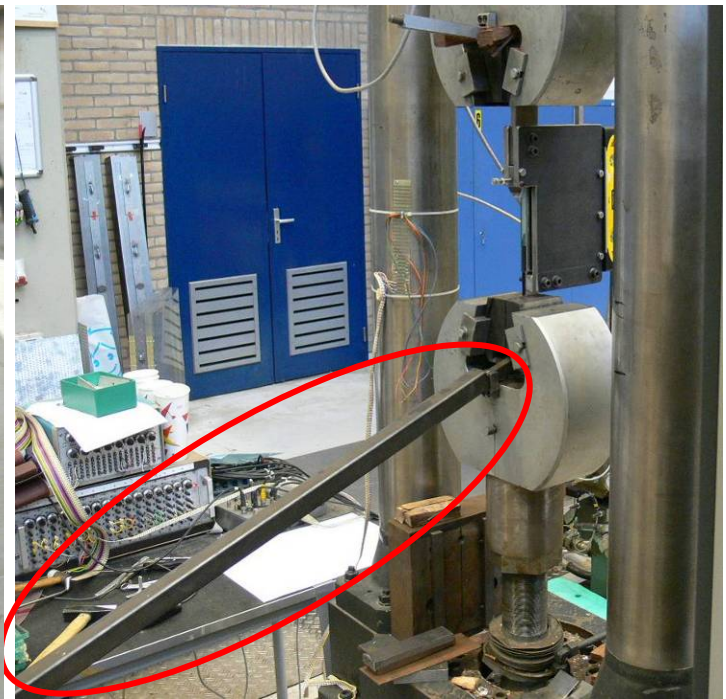


Figure 31, Test setup with steel bar encircled in red

The supporting element is placed in the upper wedge clamp. The reinforcement is clamped in the lower wedge clamp with sand paper grain 80. To prevent slipping, the clamping force is increased by lifting the wedges. This is done by pressing down on the steel bar that is visible in *Figure 31*. The specimen starts slipping if the pressing force on the bar is released during the test.

After a few runs the steel bar was replaced by wooden wedges that were hammered under the steel wedges (see *Figure 32*). Slipping still occurred occasionally.

After several tests new, bigger wedges were made, with these slipping did not occur.

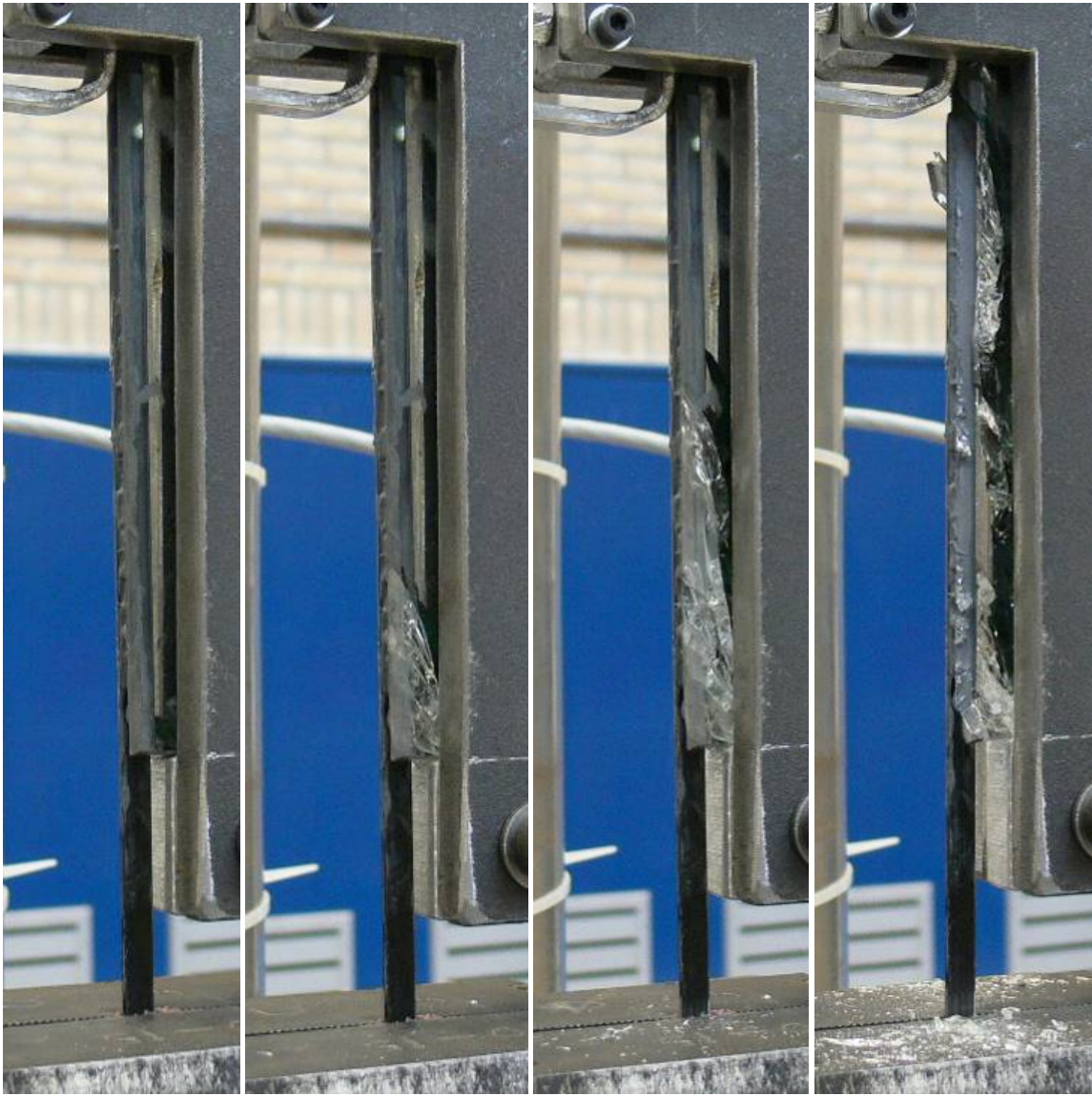


Figure 34, Specimen 2013_01 at different moments during the test.



Figure 33, Specimens 2013_01, 2013_02 and 2013_03 after the test

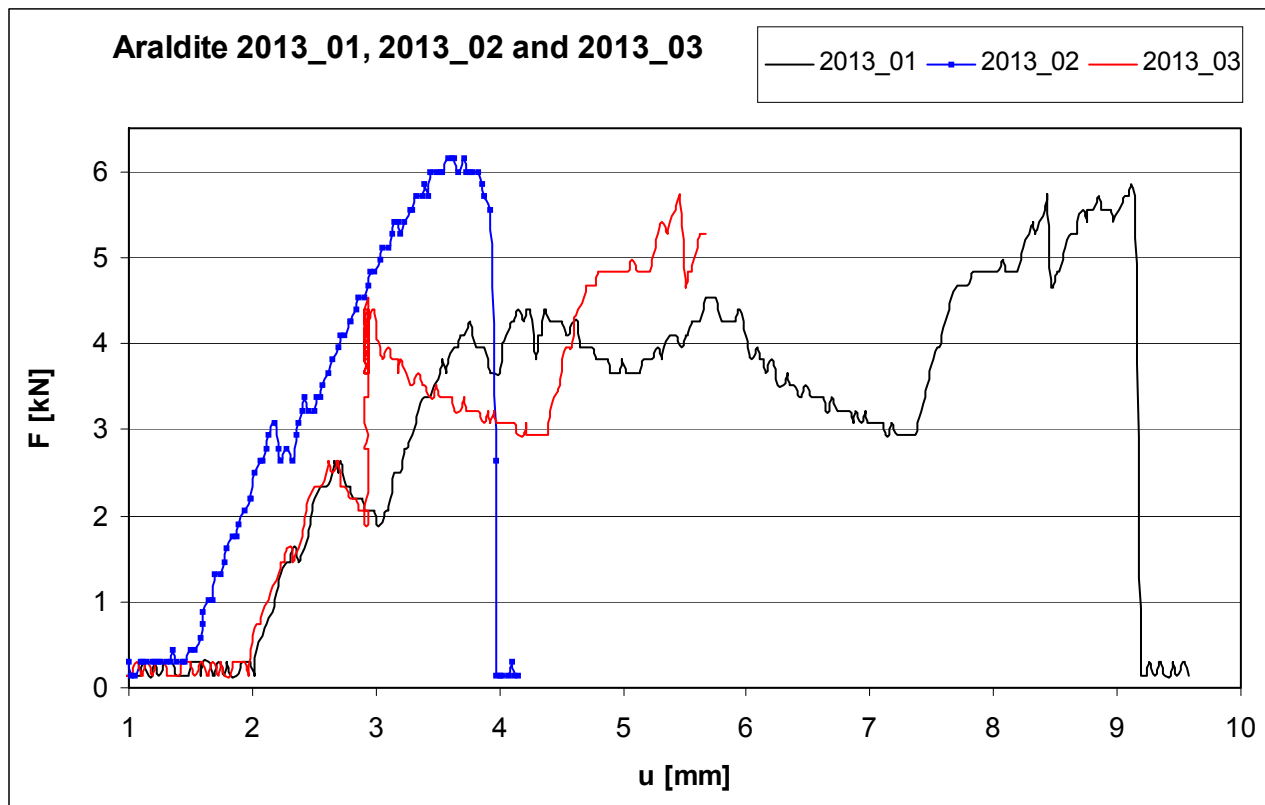


Figure 35, Force displacement diagram of specimens 2013_01 to 2013_03

Specimens 2013_01 to 2013_03

The carbon fiber rod is clamped in the support with sand paper, grain 100. To prevent slipping, the clamp is pressed shut by a bar during the test. When this pressing is released, the carbon rod starts slipping in the clamp. This is observable in the diagrams: the fallbacks in the force-displacement curve are mostly clarified by this.

The first observable failure of the specimen was the failure of the glass pane. After the first crack in the glass pane, more cracks occurred. Failure of the adhesive layer is not noticed before the glass fractured and the

force dropped back to 0. The adhesive eventually failed on 100% adhesive failure with the glass pane; the whole adhesive layer is stuck to the carbon fiber, not to the glass fractures.

Table 16, Summary of tests specimens 2013_01, 2013_02 and 2013_03

Specimen	2013_01		2013_02		2013_03	
Configuration	6x0,6 6x0,8	[mm]	6x0,6 6x0,8	[mm]	6x0,6 6x0,8	[mm]
Anchorage length	150	[mm]	150	[mm]	150	[mm]
Ultimate strength	5,9	[kN]	6,1	[kN]	6,4	[kN]

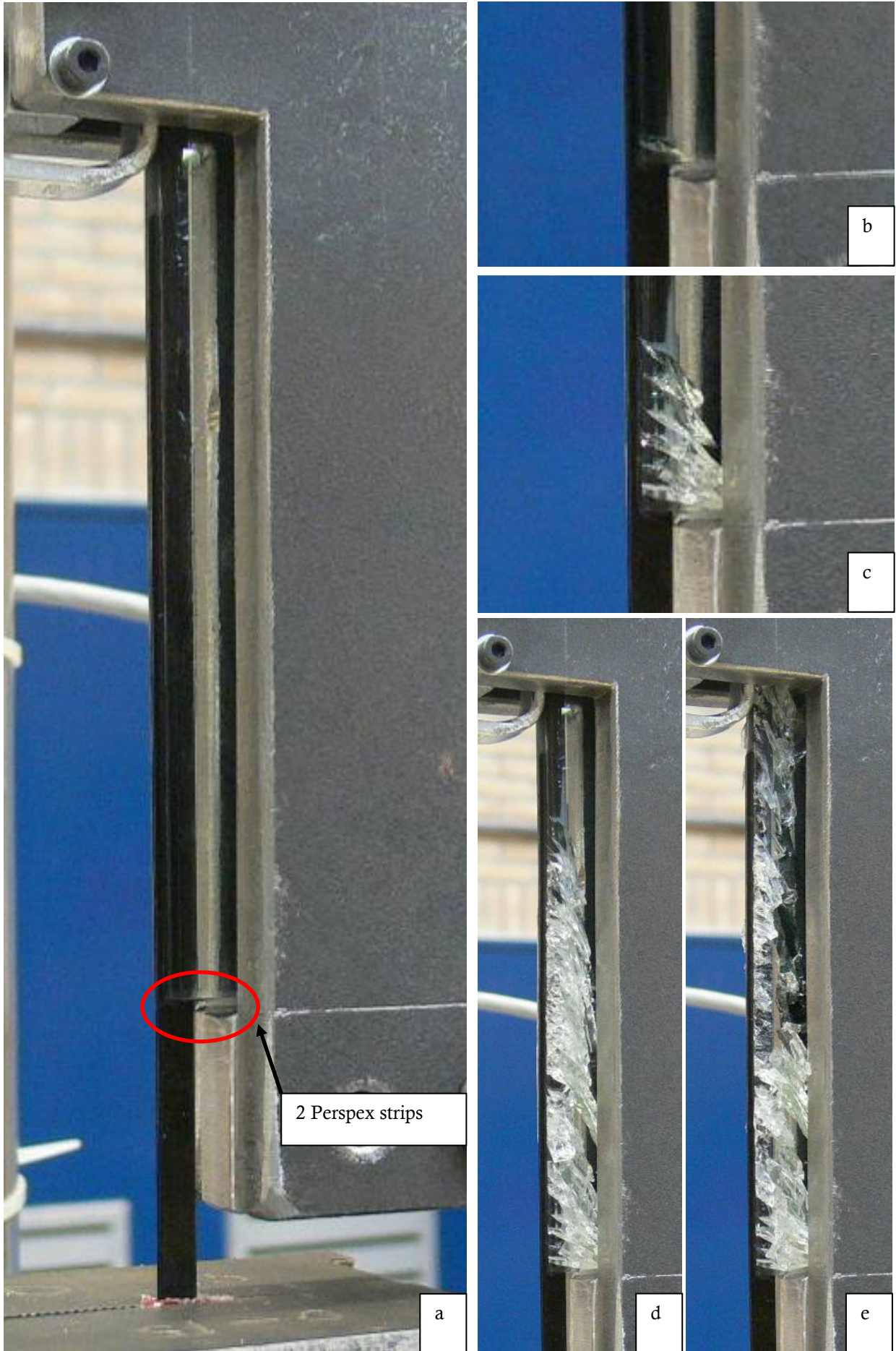


Figure 36 (a-e), specimen 2011_01 during different moments of the test

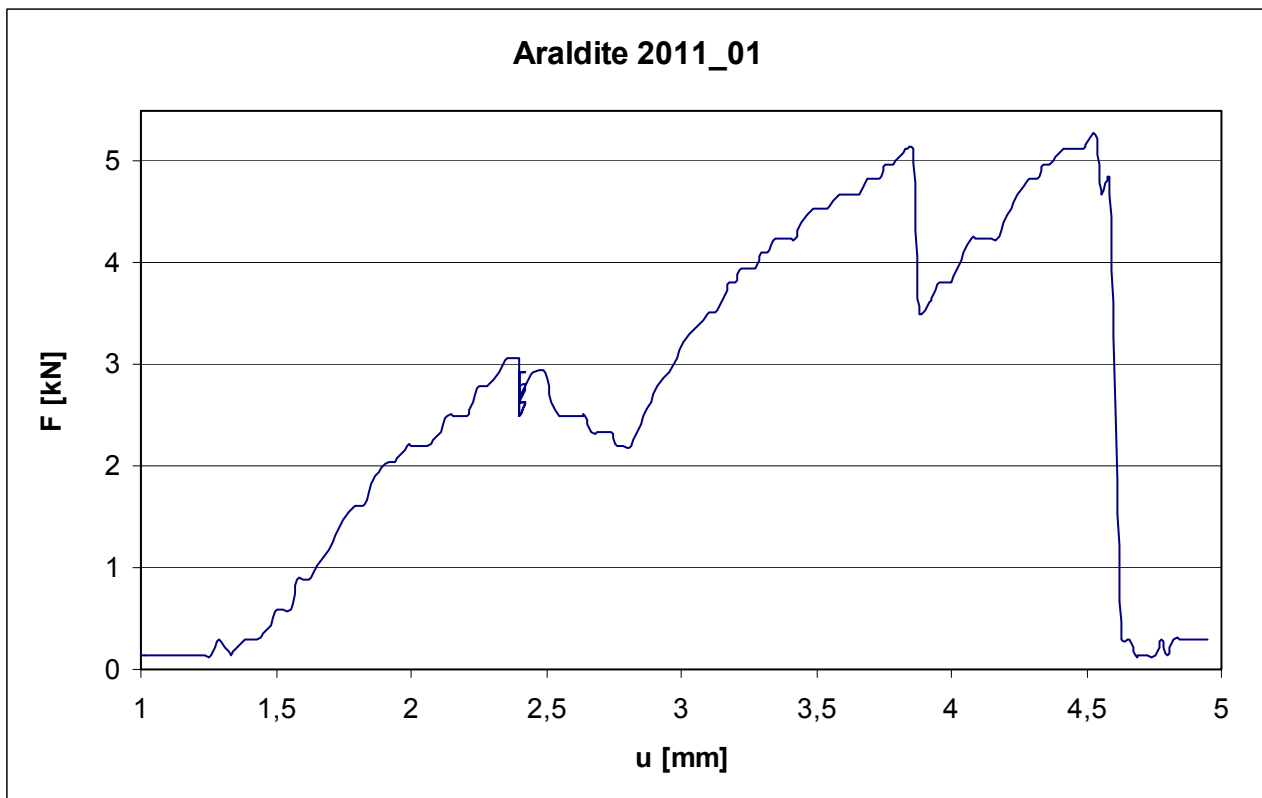


Figure 37, Force-displacement curve of specimen 2011_01

Specimen 2011_01

To prevent the glass pane from breaking because of the introduction of the compressive stress, Perspex strips with a thickness of 1 mm are placed between the glass and the aluminum support.

The first test (2011_01) is done with two strips.

The first observed failure is adhesive failure at the glass pane. The adhesive layer at one side of the carbon fiber strip detached for over 6 cm. This is not observable on the photos since it occurred on the other side of the carbon strip. Then glass failure occurred: small cracks arised at the other side of the carbon fiber strip approximately 5mm from the edge of the glass (see Figure 36b). Then more cracks and eventually the carbon strip detached from the glass pane.

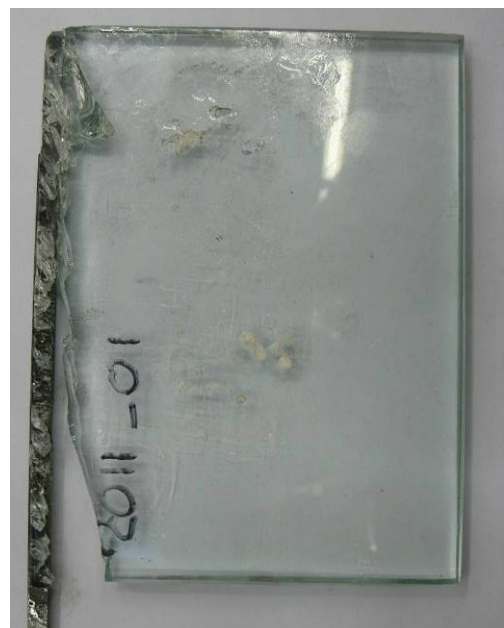


Figure 38, 2011_01 after the test

Table 17, summary of specimen 2011_01

Specimen	2011_01	
Configuration	6x0,6 6x0,8	[mm]
Anchorage length	150	[mm]
Ultimate strength	5,3	[kN]

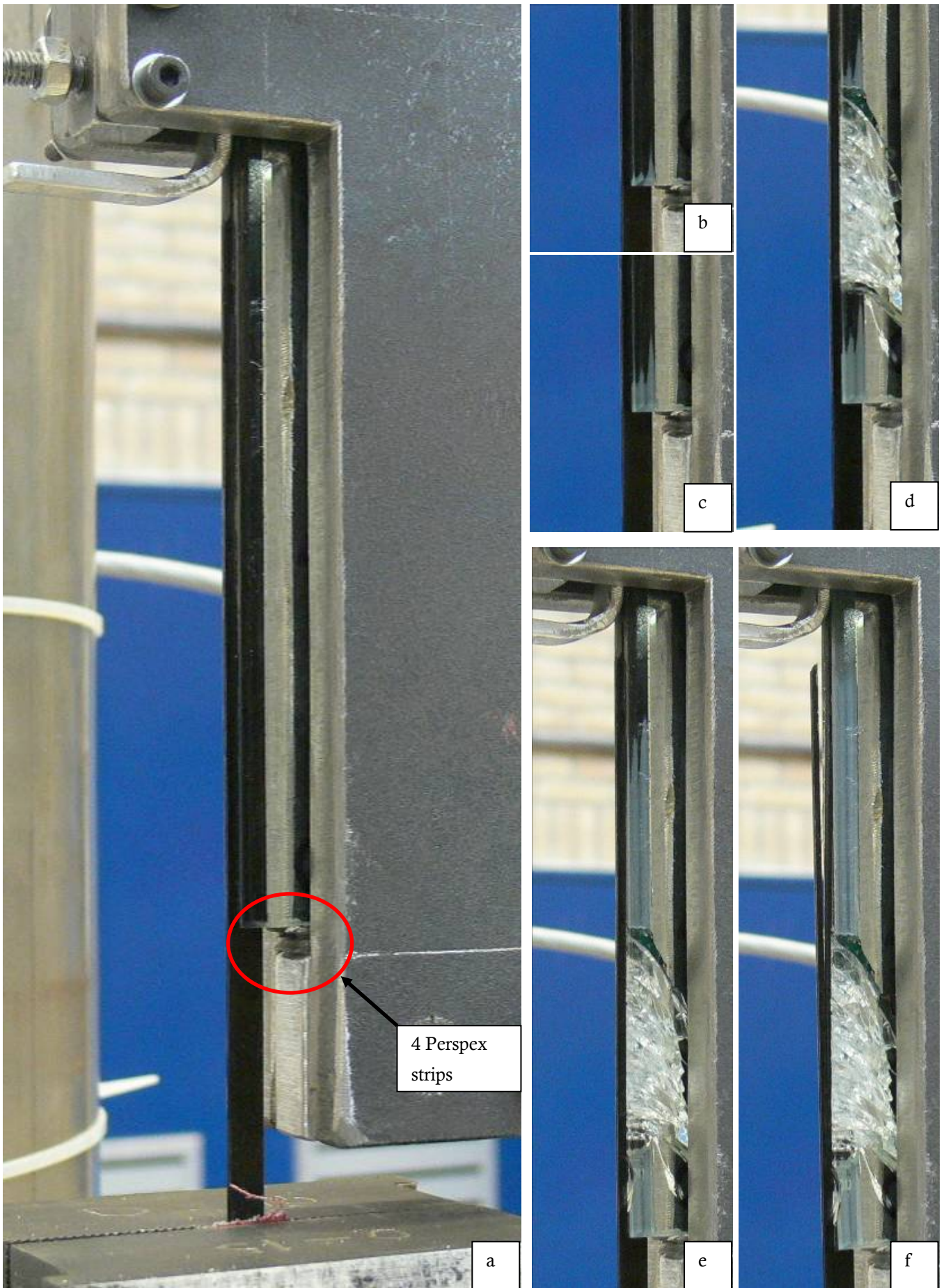


Figure 39 a-f, Test 2011_02 in chronological order from a (begin) to f (total failure)

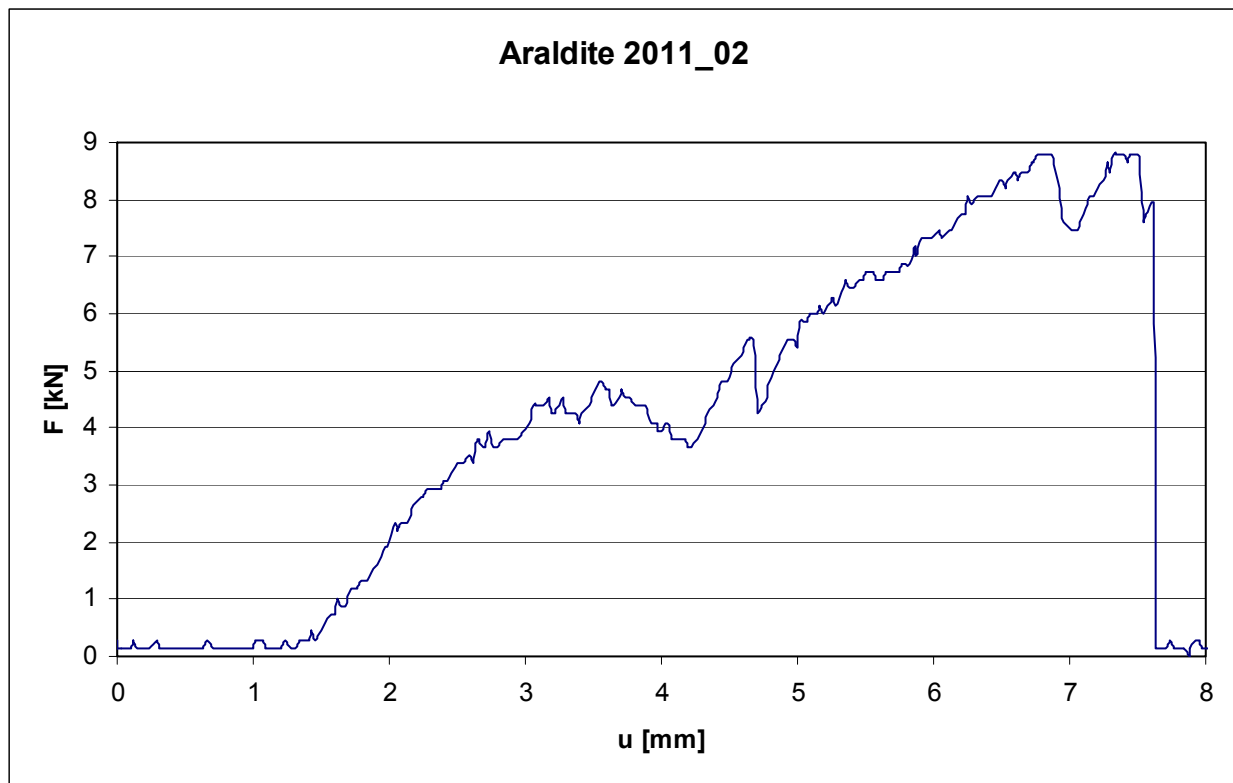


Figure 40, Force-displacement diagram of specimen 2011_02

Specimen 2011_02

Four Perspex strips are placed between the glass and the aluminum (Figure 39a).

The first failure occurred by adhesive failure at the glass (Figure 39b+c). Then the glass failed (Figure 39d) probably from the heart of the compressive zone to the carbon fiber strip (see crack Figure 41). Then the adhesive progressed again (Figure 39d-f).

Figure 41 shows the specimen after the test.



Figure 41, 2011_02 after the test

Table 18, summary of specimen 2011_02

Specimen	2011_02	
Configuration	6x0,6 6x0,8	[mm]
Anchorage length	150	[mm]
Ultimate strength	8,7	[kN]

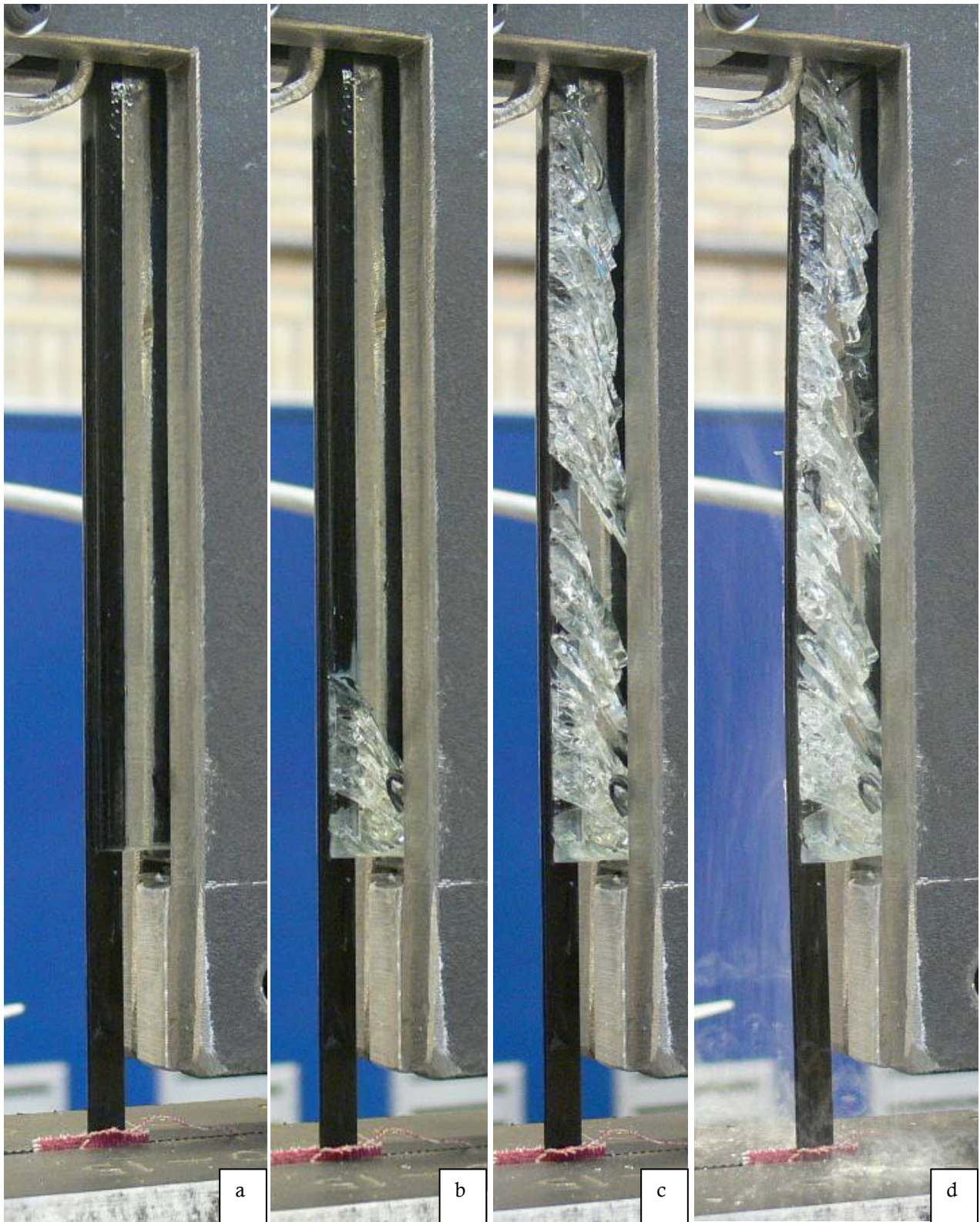


Figure 42 a-d, Specimen 2011_03 before, during and after the test

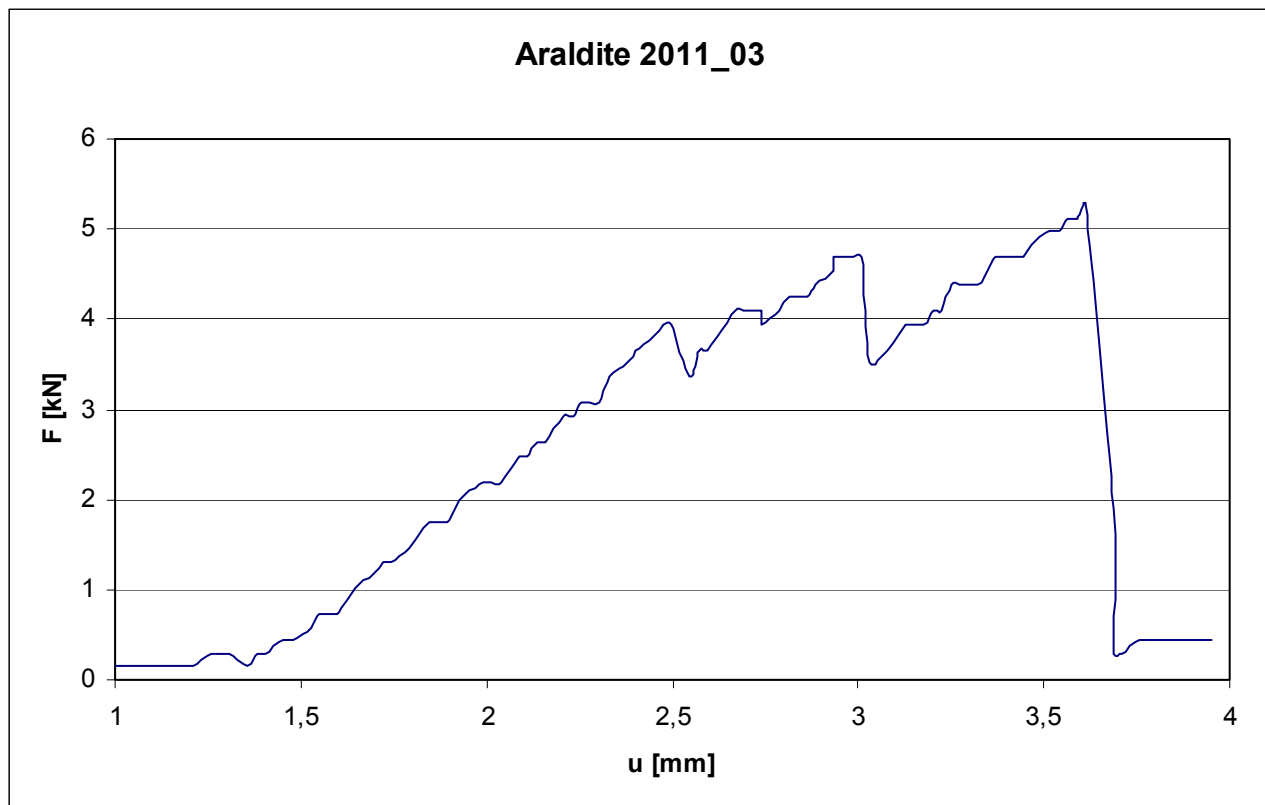


Figure 43, Force displacement diagram of specimen 2011_03

Specimen 2011_03

The failure behavior is comparable to that of 2011_01; progressive glass fracturing, no adhesive failure was observed.



Figure 44, Specimen 2011_03 after the test

Table 19, summary of specimen 2011_03

Specimen	2011_03	
Configuration	6x0,6 6x0,8	[mm]
Anchorage length	150	[mm]
Ultimate strength	5,3	[kN]

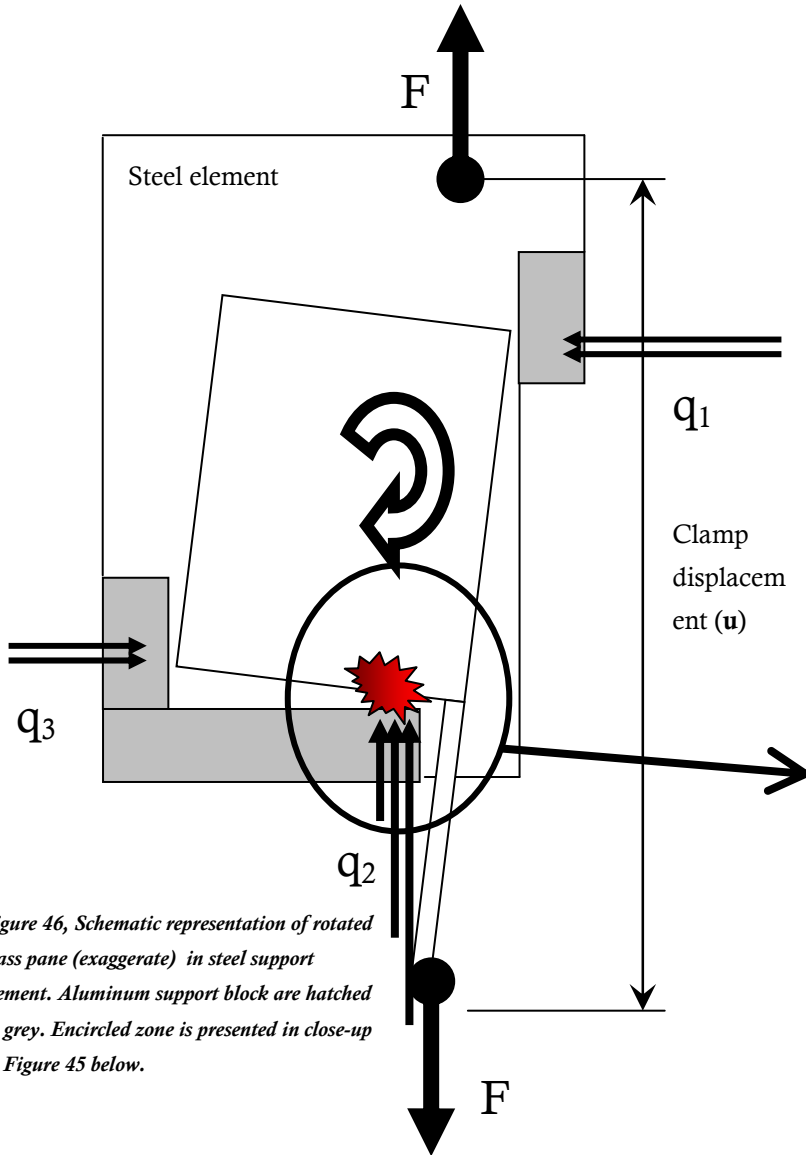


Figure 46, Schematic representation of rotated glass pane (exaggerate) in steel support element. Aluminum support block are hatched in grey. Encircled zone is presented in close-up in Figure 45 below.

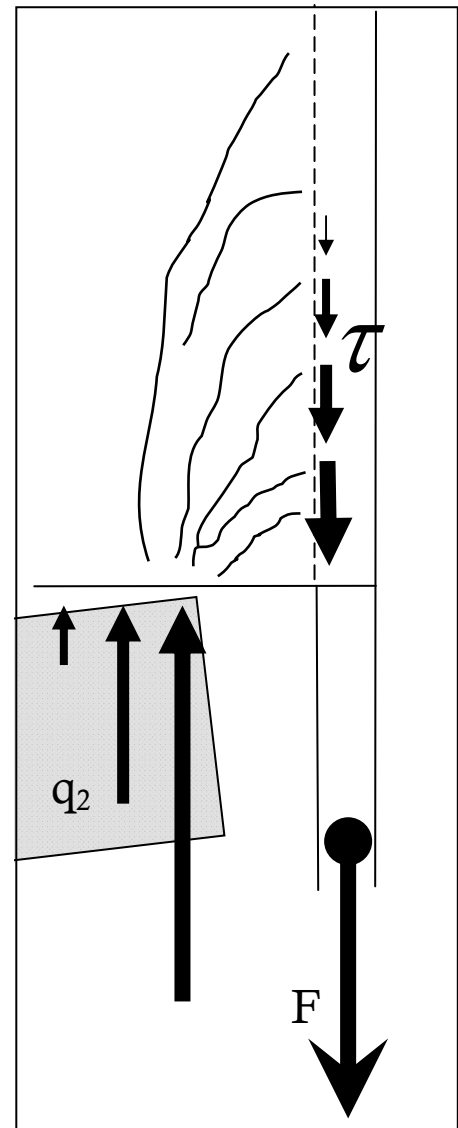


Figure 45, Close-up of fractured glass pane with stress introduction.

Table 20, proposal for specimen configuration for test sequence 3

Specimen type number	Adhesive system	Configuration	Approximate adhesive layer thickness	Anchorage length	amount
			[mm]	[mm]	
1	2013	6x0,6+6x0,8mm	<0,05	150	3
2	2011	6x0,6 mm	0,45	150	3
3	2020	6x0,6+6x0,8mm	<0,05	150	3
4	2011	6x0,6+6x0,8mm	<0,05	75	3
5	2011	6x0,6+6x0,8mm	<0,05	40	3
6	2011	6x0,6+6x0,8mm	<0,05	20	3
7	2011	6x0,6+6x0,8mm	<0,05	150	3
Total					21

Discussion

The force applied by the bank draft is equal to the divided load q_2 ($\Sigma F_x=0$). When force is applied to the carbon strip, the glass pane tends to rotate a little bit due to the moment that is generated by the lever between F and q_2 (Figure 46). This will cause q_2 to concentrate at the tip of the aluminum block, near the reinforcement, introducing the supporting force more or less as point load into the glass. The shear stress introduced into the glass by the carbon fiber (τ in Figure 45) has a peak in the beginning of the joint. These two are near to each other.

In the first 3 tests the glass pane fractured due to the combination of these. As the fracturing of the glass progresses, τ and q_2 progress as well respectively to the left and bottom (in Figure 45), creating more and longer fractures.

To reduce the stress peak, perspex strips were placed between the glass and the aluminum block for the last 3 tests.

The fractures are caused indirectly by compressive stress. Tensile stress in the glass arises square to the compressive stress from q_2 to τ , this is what causes the cracks.

The introduction of perspex strips for specimens 2011_01 to 2011_03 spread out q_2 , reducing the stress peak and moving the hart of the compressive zone slightly away from the carbon fiber. This had good results for specimen 2011_02, but was not satisfactory for 2011_01 and 2011_03.

It is recommended to disperse the stress concentration discussed above. This can be done by moving away the

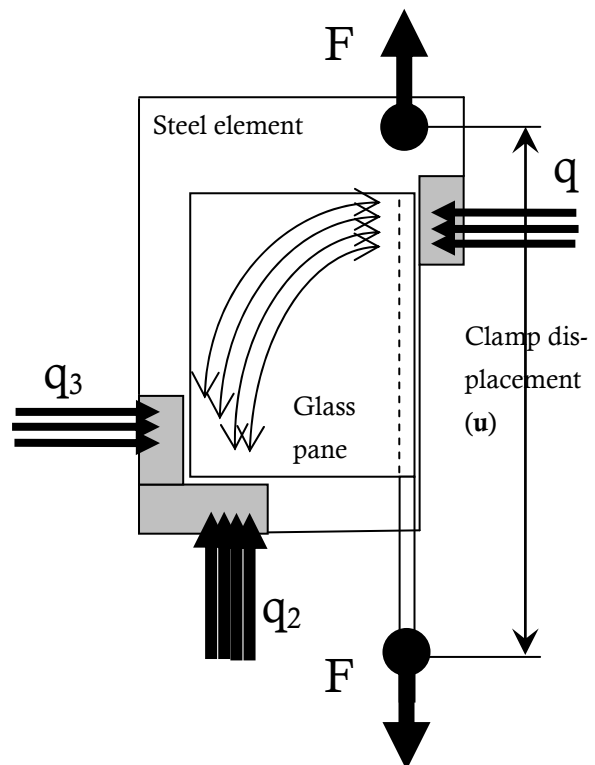


Figure 47, Schematic representation of recommended setup. Notice the change of the aluminum support, shifting of q_2 and increase of q_1 and q_3 . The new compressive zone is denoted by the bent arrows.

support from the top-right corner of the glass pane (as in Figure 46) to the middle- or bottom-right corner of the glass pane. This will increase the lever between q_2 and F severely, creating a large moment that has to be absorbed by q_1 and q_3 . This will create a new compressive stress zone as denoted in Figure 47. This compressive zone will not interfere with the shear stress zone due to the carbon fiber until failure of the adhesive connection has progressed a great deal.

Recommendations

Alterations to setup as discussed.

Anew testing of similar specimens for more reliable results.

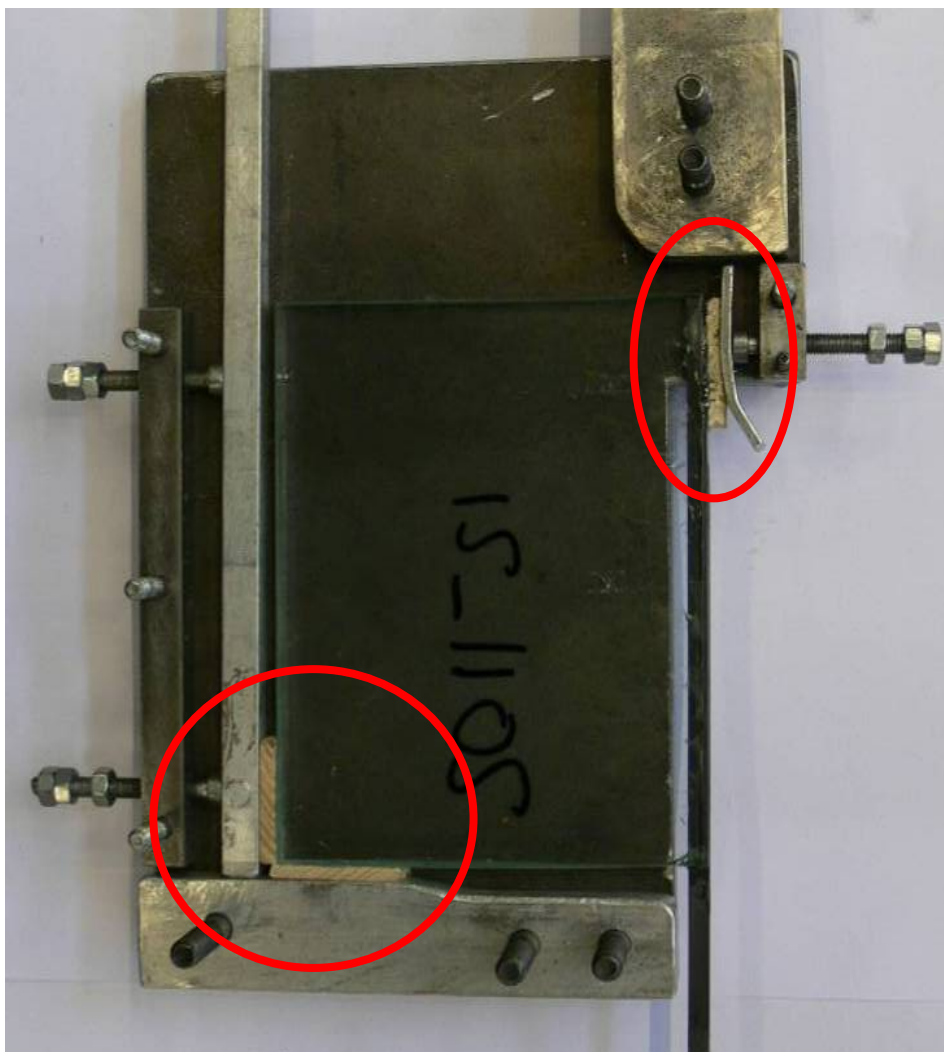
Recommended proposal for new specimens in found in Table 20.



Figure 48

Above: Specimen mounted with wooden blocks.

Below: Adjusted setup with specimen. Notice the wooden blocks denoted by the red circles.



Test sequence 2

Method

The test setup is slightly adjusted as discussed on page 49.

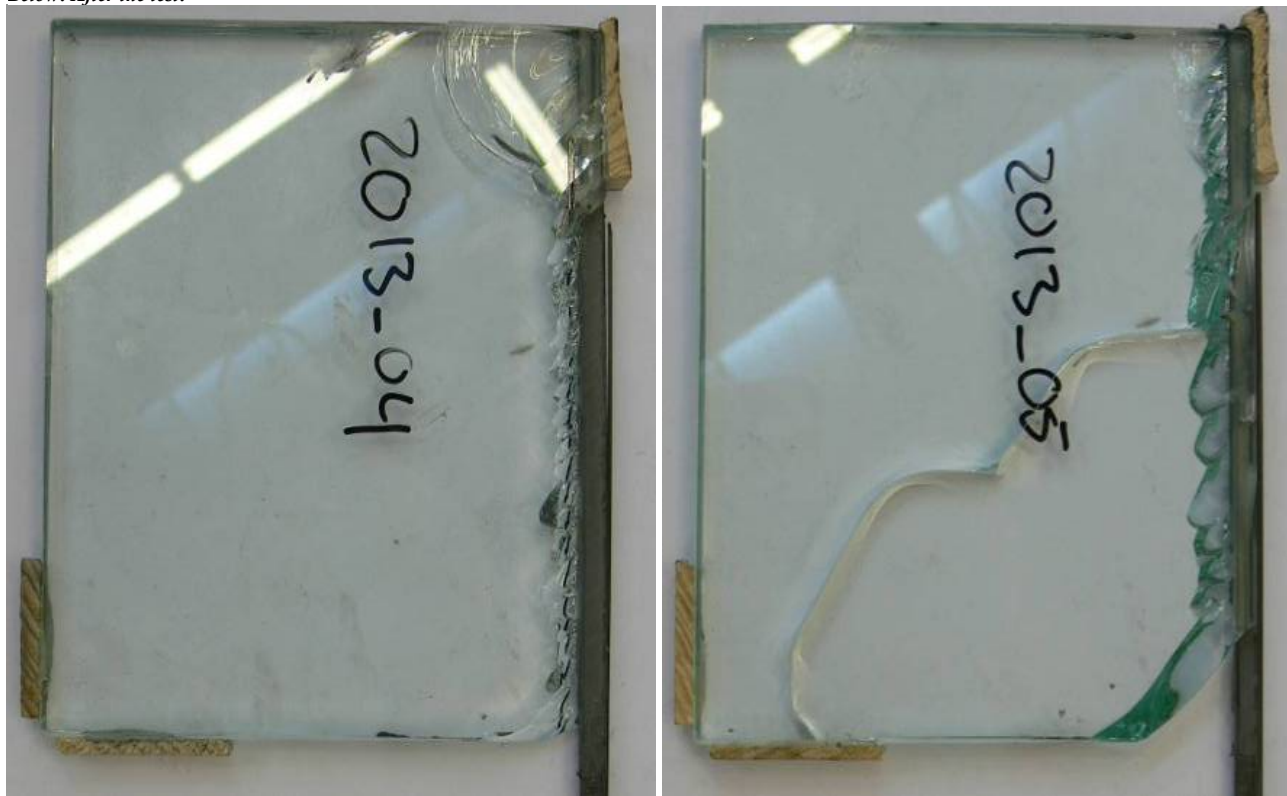
The specimens in sequence 2 are mounted by small wooden blocks with a thickness of 5 mm, in the corners of the glass (see *Figure 48*).



Figure 49

Above: Specimen 2013_05 at different moments during the test. The letters correspond with the letters in the curve.

Below: After the test.



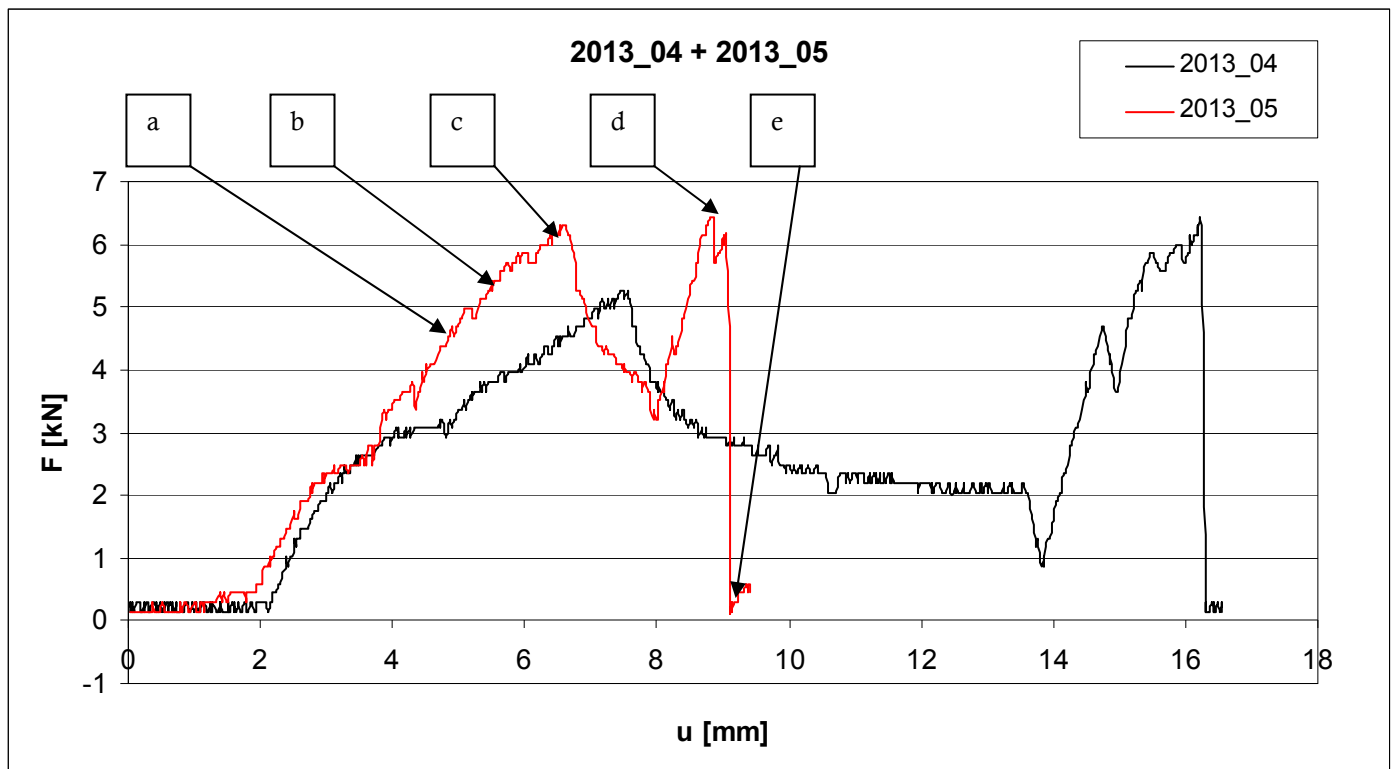


Figure 50, Force-displacement diagram of specimens 2013_04 and 2013_05

Specimen 2013_04

After the first peak in the force-displacement diagram ($u=7,5$ mm), the carbon started slipping in the wedge-clap. At $u=14$ mm the carbon is fixed by hammering the wooden wedges more firmly. This explains the dip in the curve to 1 kN and the sudden rise after that.

The wooden blocks are impressed.

The glass failed before the adhesive failed. According to the failure pattern near the carbon strip it is clear that the glass did not fail due to compressive stress, but solely to shear stress. The fracture in the top-right corner is due to q_1 (see Figure 47).

Specimen 2013_05

The same slipping as with 2013_04 occurred. At $u=8$ mm the wooden wedges were fixed better.

The glass failed before the adhesive failed. It failed primarily due to shear stress. One crack occurred from the compressive zone to the shear stress zone in the middle of the adhesive joint.

Table 21 summary of 2013_04 and 2013_05

Specimen	2013_04		2013_05	
Configuration	6x0,6 6x0,8	[mm]	6x0,6 6x0,8	[mm]
Anchorage length	150	[mm]	150	[mm]
First adhesive failure	-	[kN]	-	[kN]
First glass failure	3,5	[kN]	3,3	[kN]
Ultimate strength	6,4	[kN]	6,4	[kN]

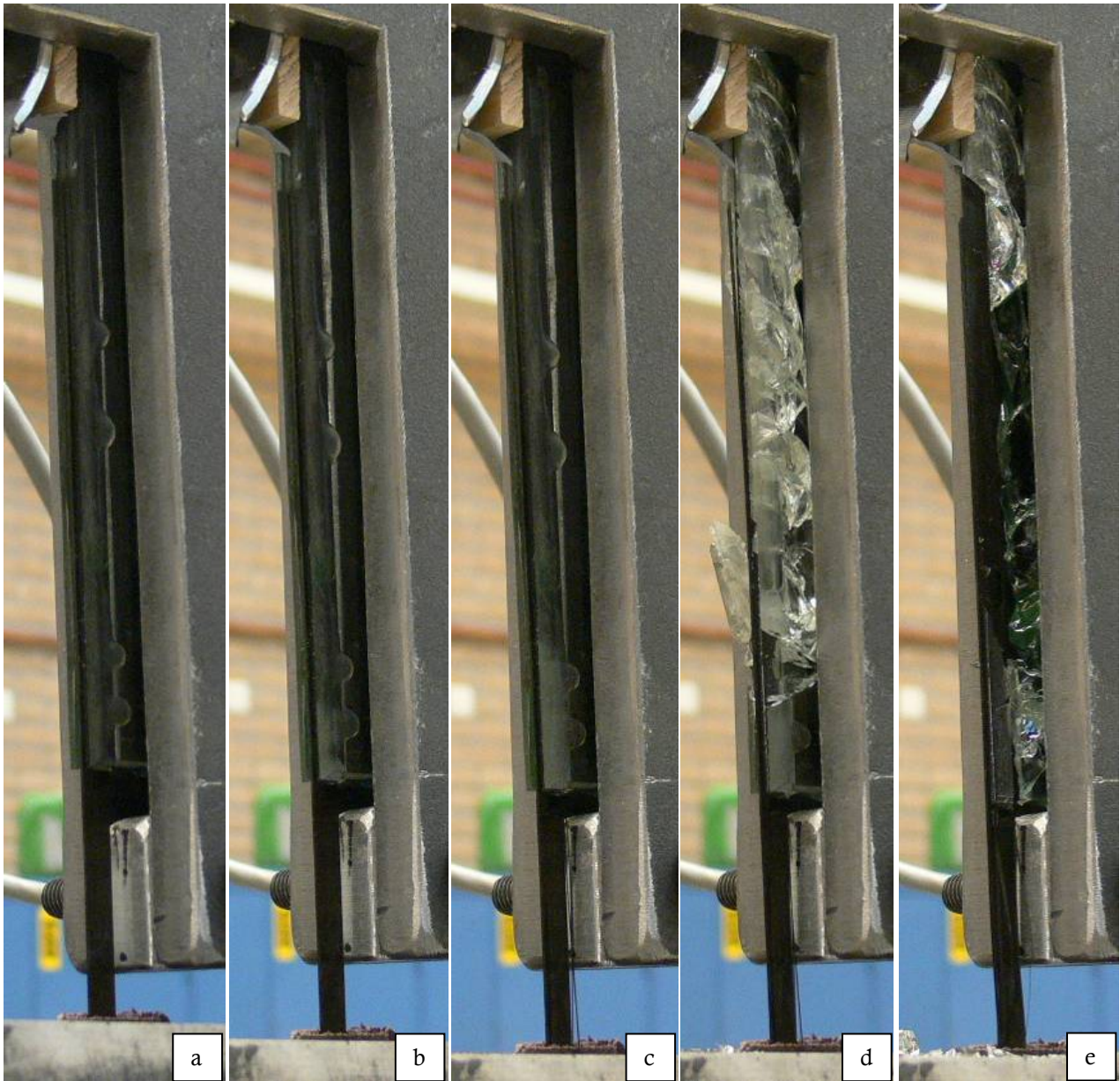


Figure 51, Above: 2011_09 at different moments during the test. Below: Specimens after the test.



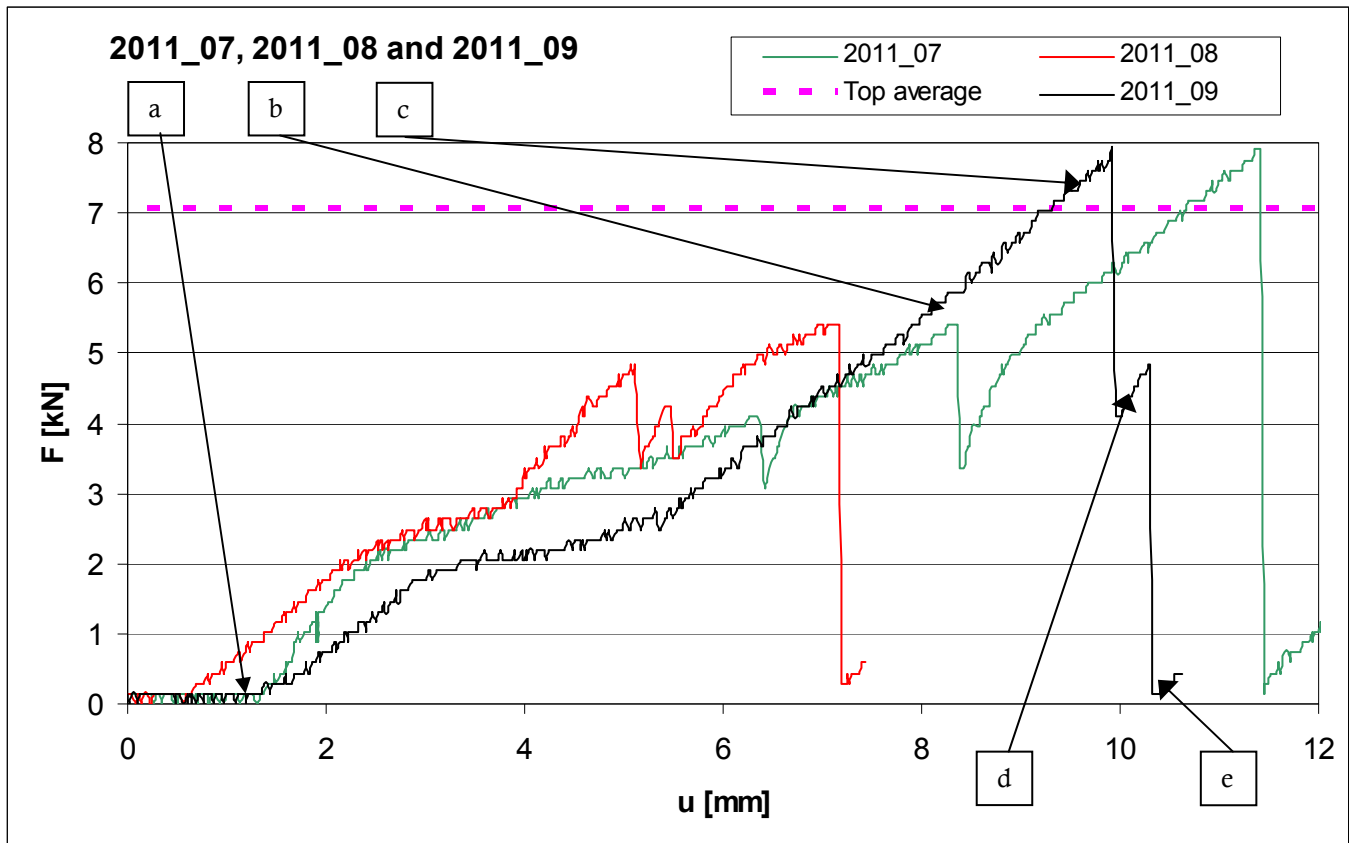


Figure 52, Force-displacement curve of specimens 2011_07 to 2011_09. The letters refer to Figure 51.

Specimens 2011_07 to 2011_09

2011-07 to 2011-09 are specimens with a thin carbon profile and a thicker adhesive layer.

Specimen 2011_07 shows a small glass fracture at $u=6,5\text{mm}$. Then no adhesive failure, nor glass failure is observed until $u=8,3\text{mm}$; a large fracture over half the specimen (red arrow in Figure 51). Again no glass or adhesive failure until $u=11,5\text{mm}$.

Specimen 2011_08 failed at much lower force as 07 and 09. The failure mechanism was due to progressive glass fracturing; no adhesive failure was observed (like

specimen 2013_05 in Figure 49.

The adhesive of 2011_09 on the left side of the carbon fiber strip started progressive failure at 2,4 kN, this is not visible on the photo. At the right side the adhesive started failing at 6,0 kN. This is visible on Figure 51 (b) which was taken slightly after that at 7,4 kN. The maximum difference in adhesive failure progression is approximately 40 mm.

Table 22, summary of specimens 2011_07 to 2011_09

Specimen	2011_07		2011_08		2011_09	
Configuration	6x0,6	[mm]	6x0,6	[mm]	6x0,6	[mm]
Anchorage length	150	[mm]	150	[mm]	150	[mm]
First adhesive failure	2	[kN]	2,4	[kN]	2,6	[kN]
First glass failure	2,9/5,5	[kN]	2,6	[kN]	-	[kN]
Ultimate strength	7,9	[kN]	5,5	[kN]	8	[kN]

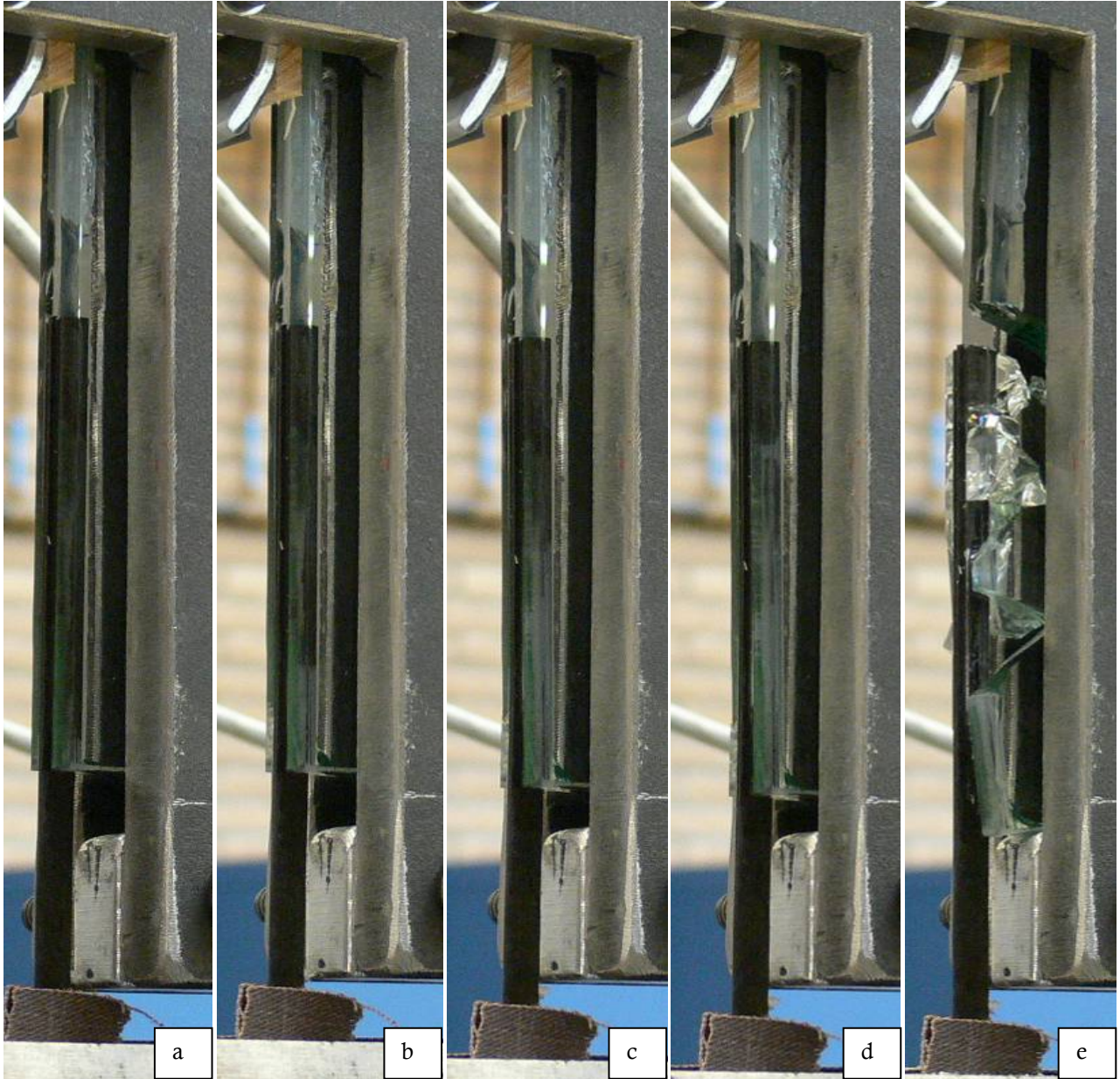
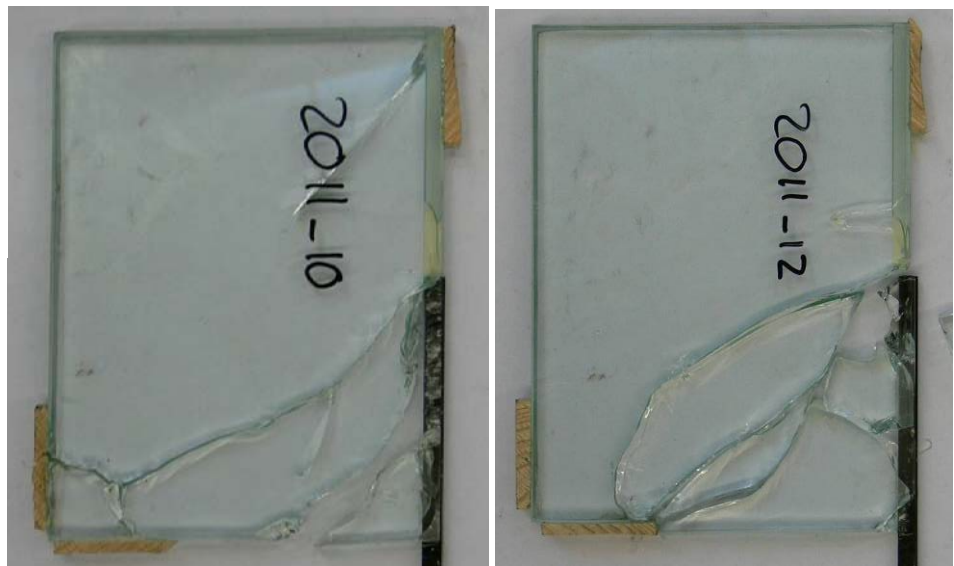


Figure 53

Above: specimen 2011_12 at different moments during the test.

Right: specimens 2011_10 and 2011_12 after the test.



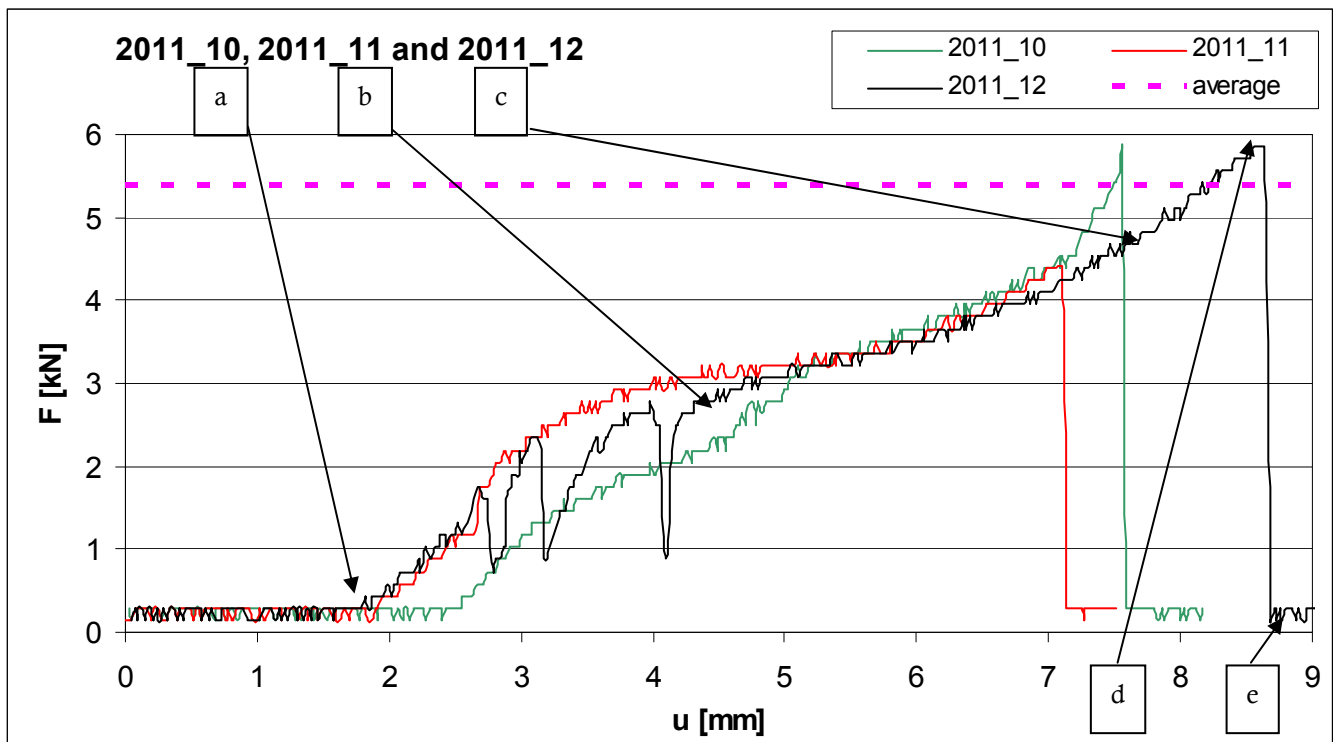


Figure 54, force-displacement diagram of specimens 2011_10 to 2011_12

Specimens 2011_10 to 2011_12

The configuration consists of two carbon profiles. The length of the joint is 75 mm.

Table 23, summary of specimens 2011_10 to 2011_12

Specimen	2011_10		2011_11		2011_12	
Configuration	6x0,6 6x0,8	[mm]	6x0,6 6x0,8	[mm]	6x0,6 6x0,8	[mm]
Anchorage length	75	[mm]	75	[mm]	75	[mm]
First adhesive failure	2,9	[kN]	2,5	[kN]	2,5	[kN]
First glass failure	5,85	[kN]	4,4	[kN]	5,85	[kN]
Ultimate strength	5,585	[kN]	4,4	[kN]	5,585	[kN]

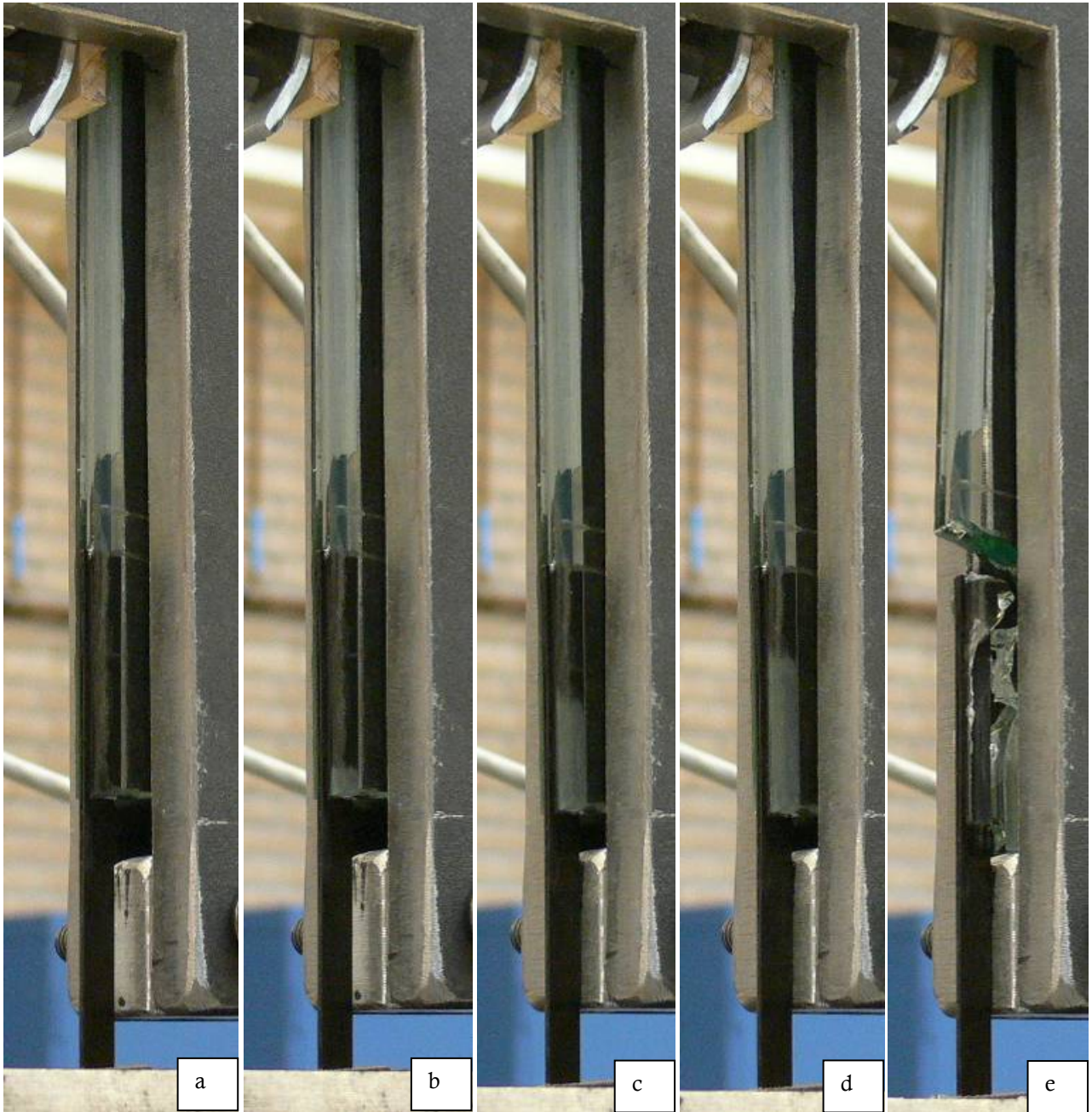
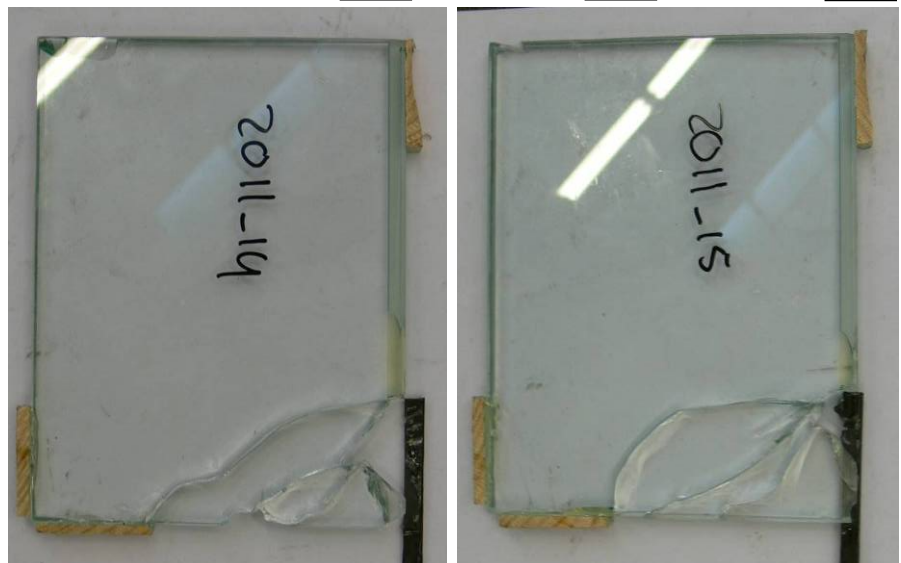


Figure 55

Above: specimen 2011_15 at different moments during the test.

Right: specimens 2011_14 and 2011_15 after the test.



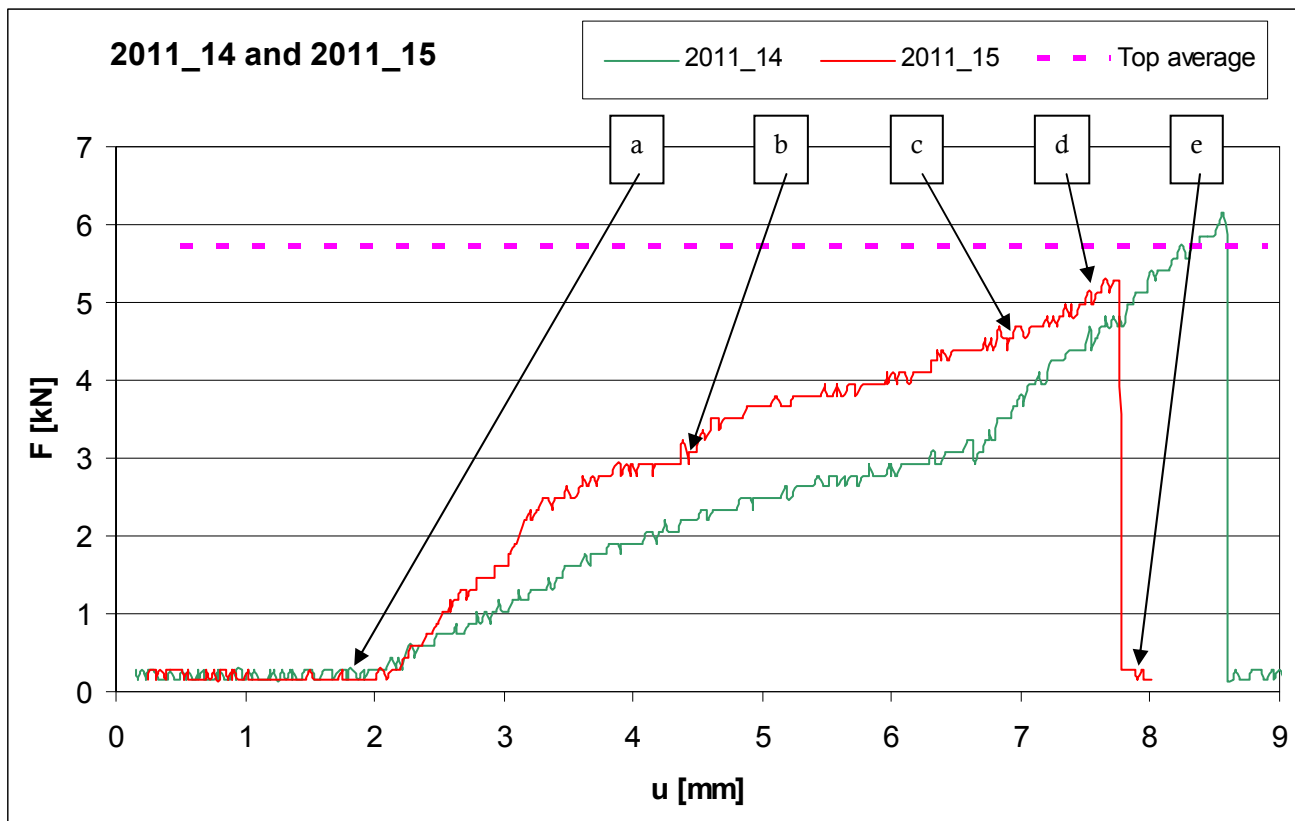


Figure 56, Force-displacement diagram of specimens 2011_14 and 2011_15

Specimens 2011_14 and 2011_15

The configuration of the specimens is 2 carbon profiles and thin adhesive. The anchorage length is 40 mm.

For 2011_14: The adhesive started progressive failure first at the left side at 2,5 kN.

For 2011_15: The adhesive started progressive failure a bit faster for the right side than for the left side.

Fracture pattern is comparable for both specimens.

Table 24, summary of specimens 2011_14 and 2011_15.

Specimen	2011_14		2011_15	
Configuration	6x0,6 6x0,8	[mm]	6x0,6 6x0,8	[mm]
Anchorage length	40	[mm]	40	[mm]
First adhesive failure	2,5	[kN]	2,5	[kN]
First glass failure	3,0	[kN]	--	[kN]
Ultimate strength	6,14	[kN]	5,27	[kN]

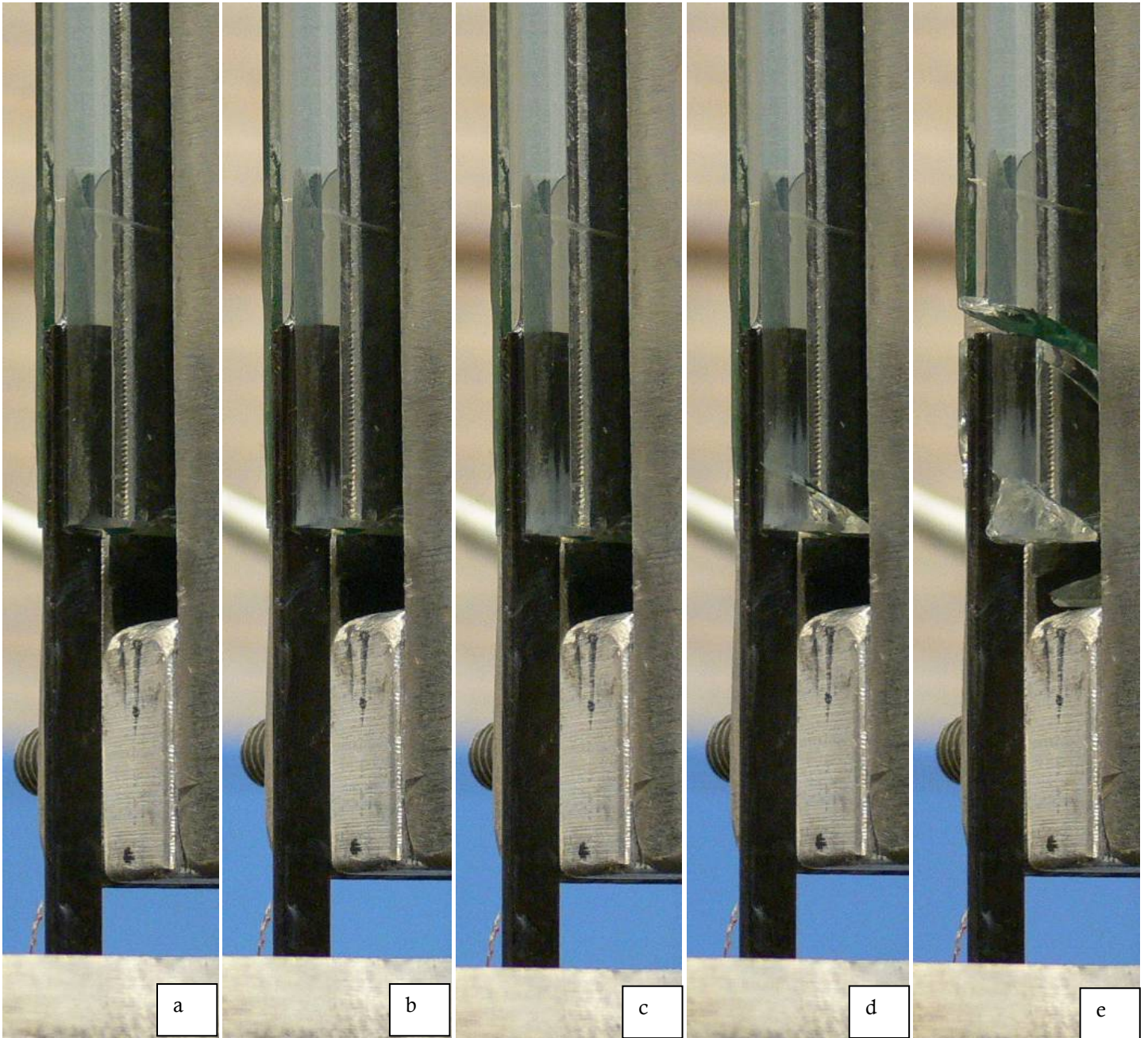


Figure 57,

Above: specimen 2011_18 at different moments during the test.

Right: specimen 2011_18 after the test. Fracture pattern is comparable for all three specimens. The small missing piece at the top left corner was already broken of when testing started.



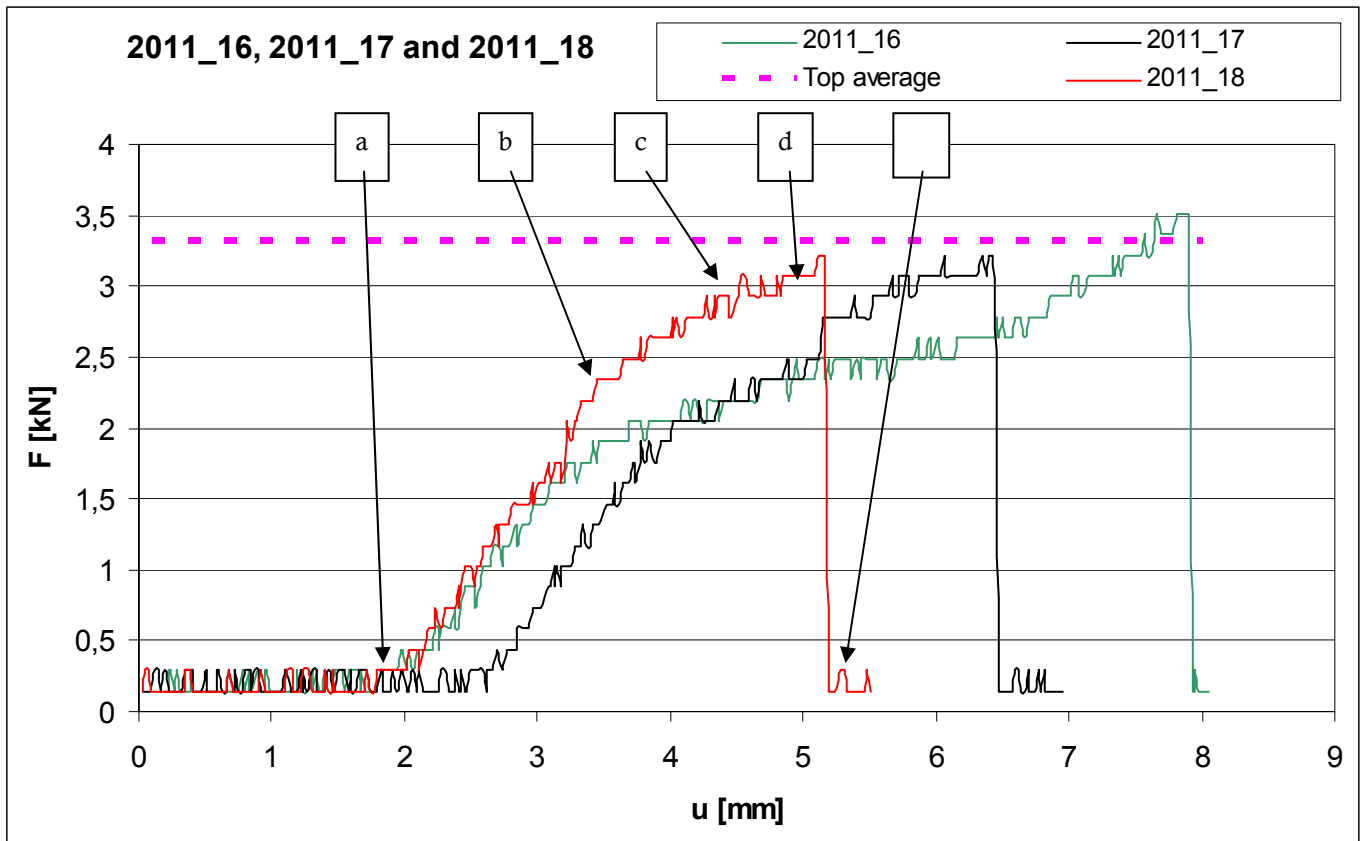


Figure 58, force-displacement diagram of specimens 2011_16 to 2011_18

Specimens 2011_16 to 2011_18

The configuration is two carbon profiles with thin adhesive layer, geometry 2. The anchorage length is 20 mm.

Table 25, summary of specimens 2011_16 to 2011_18

Specimen	2011_16		2011_17		2011_18	
Configuration	6x0,6 6x0,8	[mm]	6x0,6 6x0,8	[mm]	6x0,6 6x0,8	[mm]
Anchorage length	20	[mm]	20	[mm]	20	[mm]
First adhesive failure	2,2	[kN]	2,8	[kN]	2	[kN]
First glass failure	2	[kN]	3	[kN]	2,7	[kN]
Ultimate strength	3,5	[kN]	3,2	[kN]	3,2	[kN]

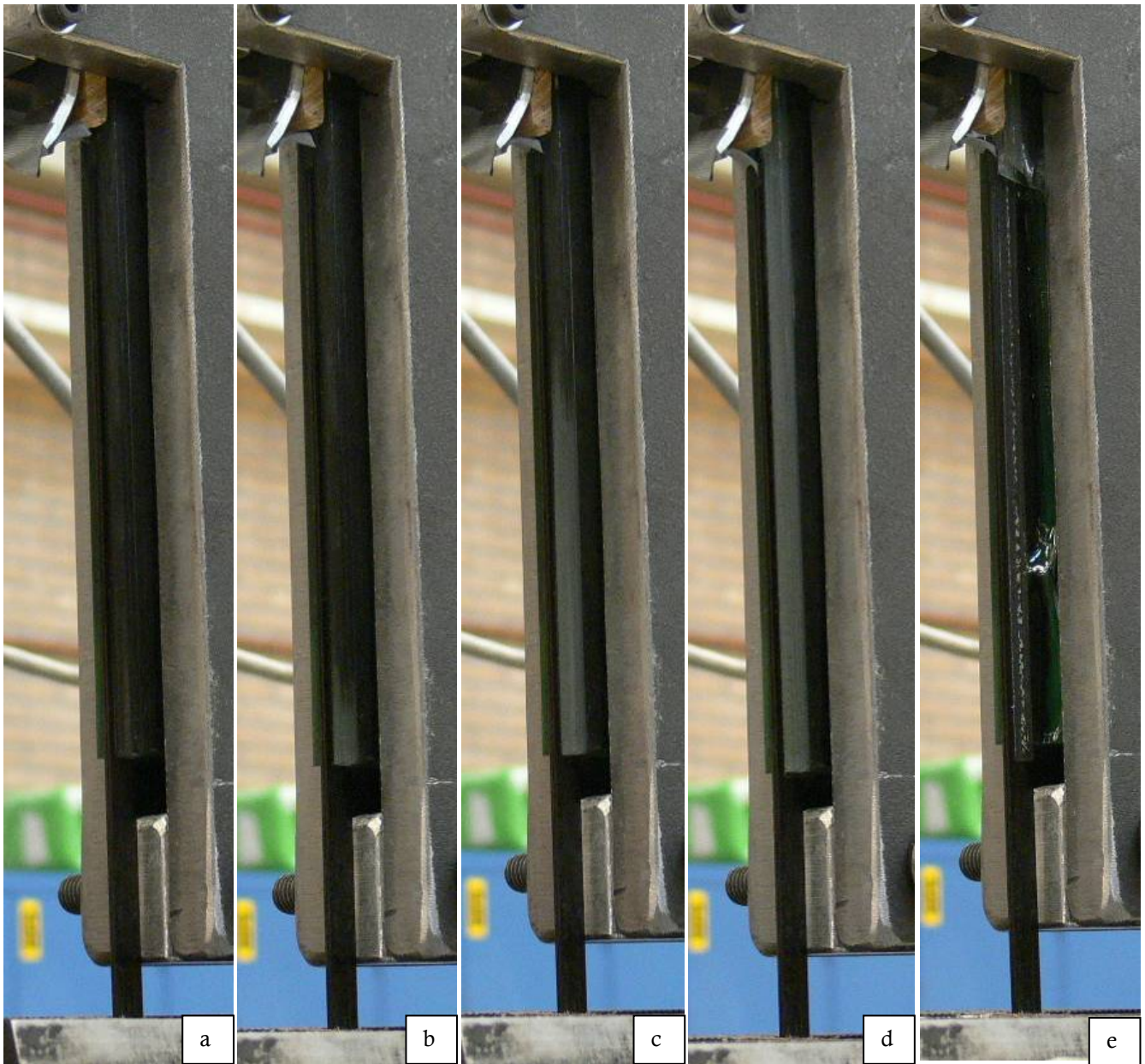


Figure 59

Above: Specimen 2020_03 at different moments during the test.

Right: Specimen 2020_01 and 2020_03 after the test. Fracturing of 2020_02 is comparable to 2020_03



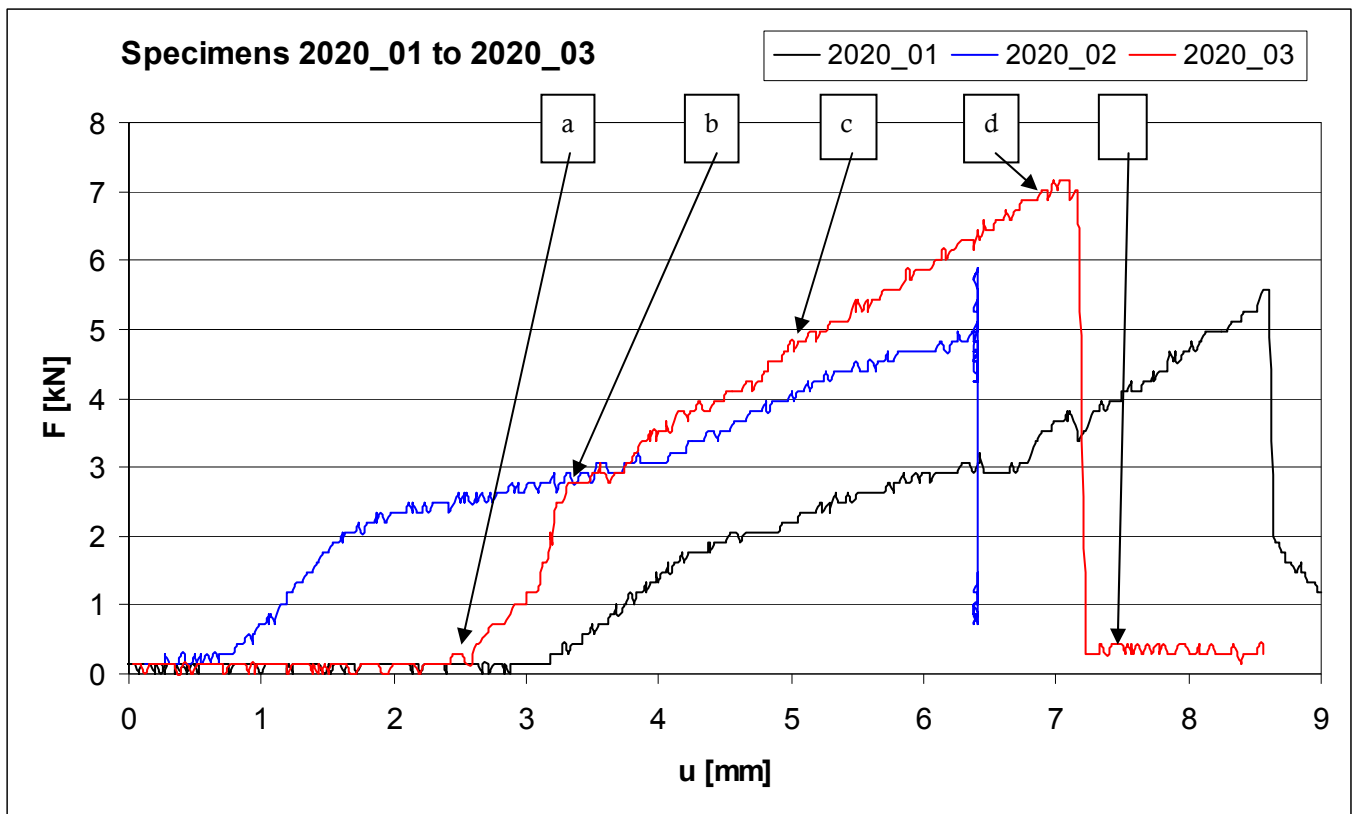


Figure 60, Force-displacement curve of specimens 2020_01, 2020_02 and 2020_03.

Specimen 2020_01 to 2020_03

The specimens are reinforced with geometry 2.

The adhesive fails before the glass does. The failure mechanism is cohesive failure, which is visible in Figure 61.

Notice the sudden steep rise of the 2020_03 curve between 'a' and 'b' (Figure 60). Because the wooden support blocks impress during the test, the specimen tends to rotate in the supporting element. This can be compensated by twisting the bolts B_1 and B_2 (Figure 28). The specimen is relocated in the supporting element causing the force to rise suddenly. This also explains

the sudden rise from 5,0 to 5,8 kN at the end of test 2020_02.

Figure 61, Close-up of specimen 2020_03 after the test. The carbon strip is dislocated (marked by red lines) and the adhesive is visible in white.



Table 26, summary of specimens 2020_01 to 2020_03

Specimen	2020_01		2020_02		2020_03	
Configuration	6x0,6 6x0,8	[mm]	6x0,6 6x0,8	[mm]	6x0,6 6x0,8	[mm]
Anchorage length	150	[mm]	150	[mm]	150	[mm]
First adhesive failure	1,6	[kN]	2,0	[kN]	2,6	[kN]
First glass failure	5,5	[kN]	-	[kN]	7	[kN]
Ultimate strength	5,6	[kN]	5,8	[kN]	7,1	[kN]

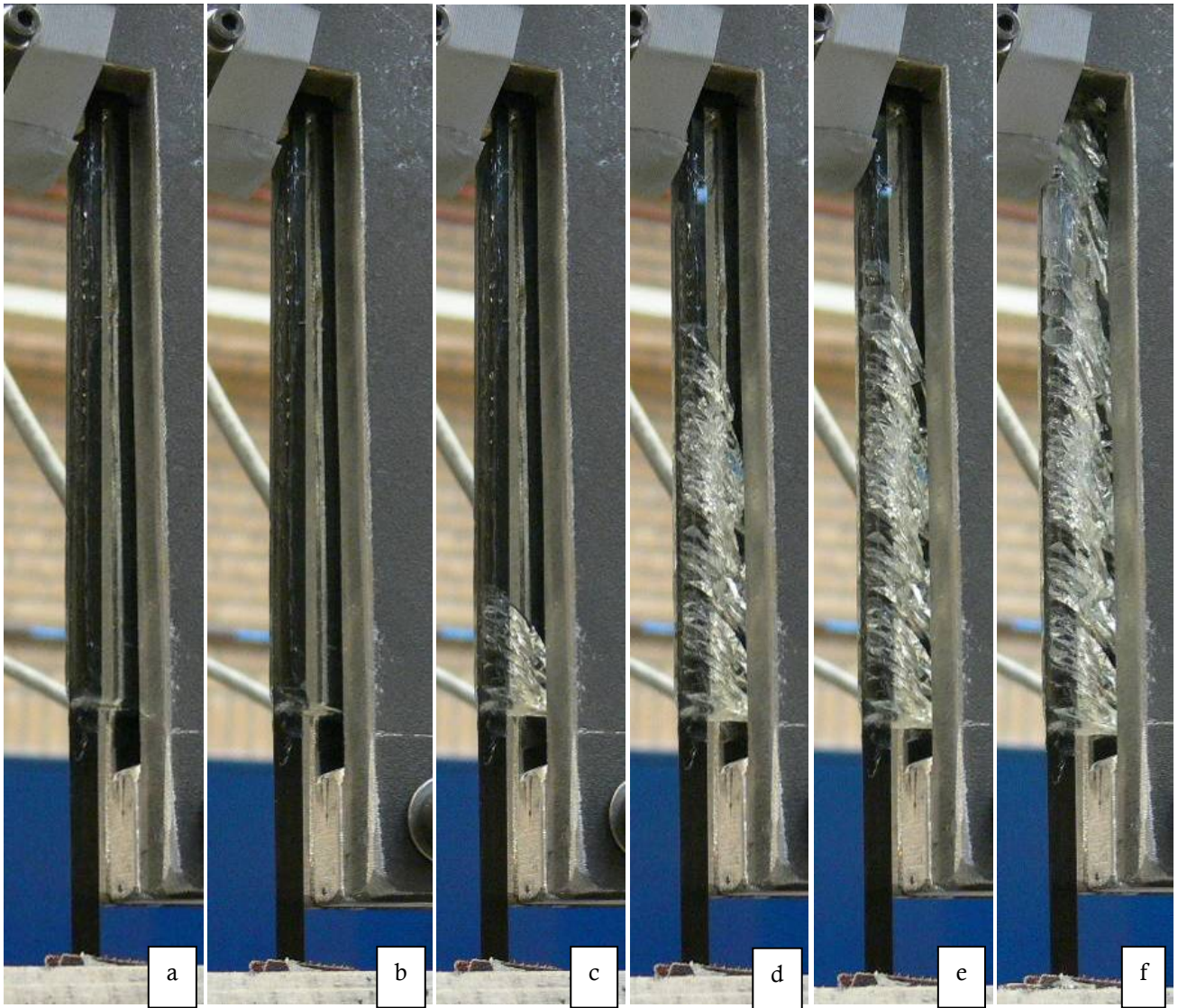


Figure 62

Above: specimen 2020_10 at different moments during the test.

Right: 2020_10 after the test.



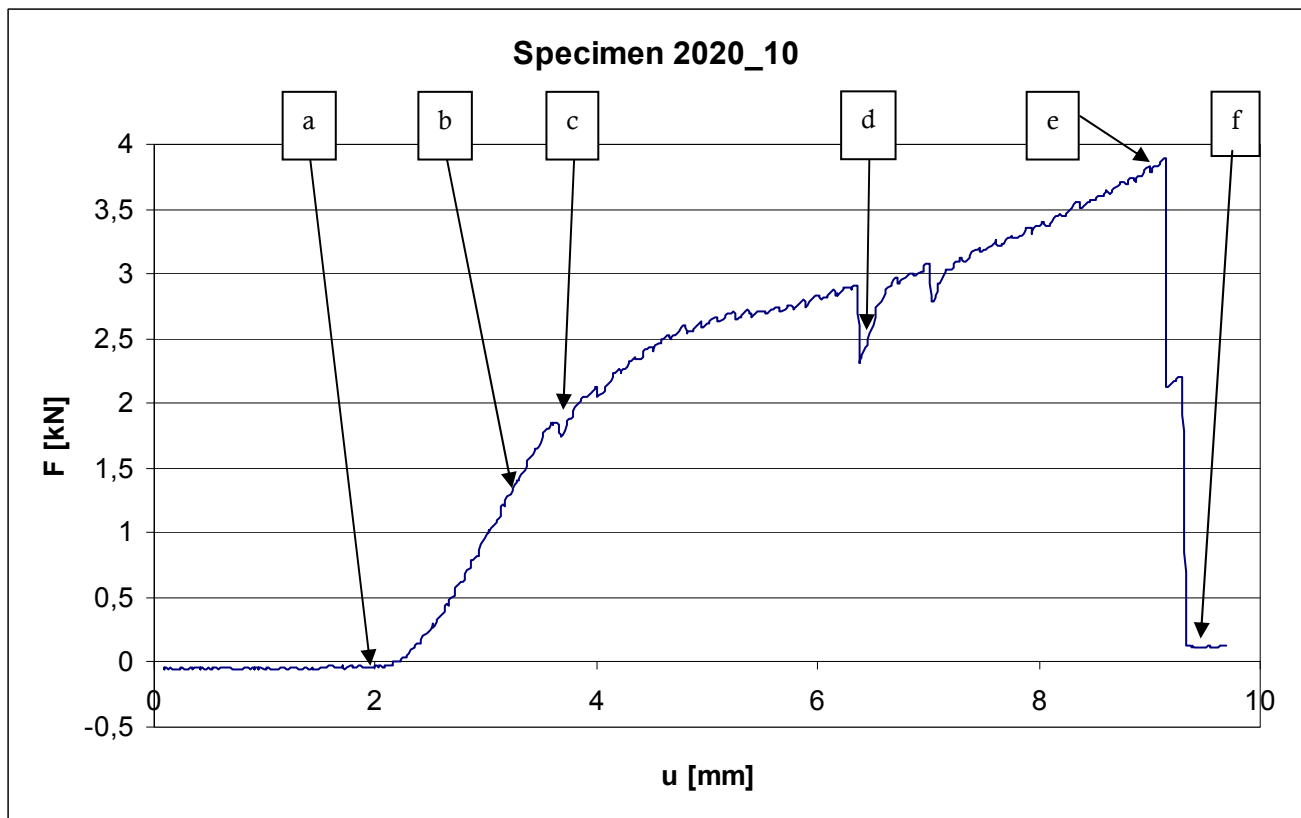


Figure 63, Force-displacement diagram of specimen 2020_10.

Specimen 2020_10

The configuration of this specimen is geometry 1.

This adhesive does not appear suitable for a thicker adhesive layer. This is endorsed by the outcome of the previous test, where the adhesive failed cohesively.

Hypothesis is therefore that the glass will remain intact and that the adhesive will fail in a comparable way as specimens 2020_01 to 2020_03, but at a lower shear force.

This did not happen. Failure of the adhesive is not observed. The glass pane started fracturing at a force of 1,3 kN. More fractures occurred as the force increased, until ultimate failure at 3,9 kN.

Table 27, summary of specimens 2020_10

Specimen	2020_10	
Configuration	6x0,6	[mm]
Anchorage length	150	[mm]
First adhesive failure	-	[kN]
First glass failure	1,3	[kN]
Ultimate strength	3,9	[kN]

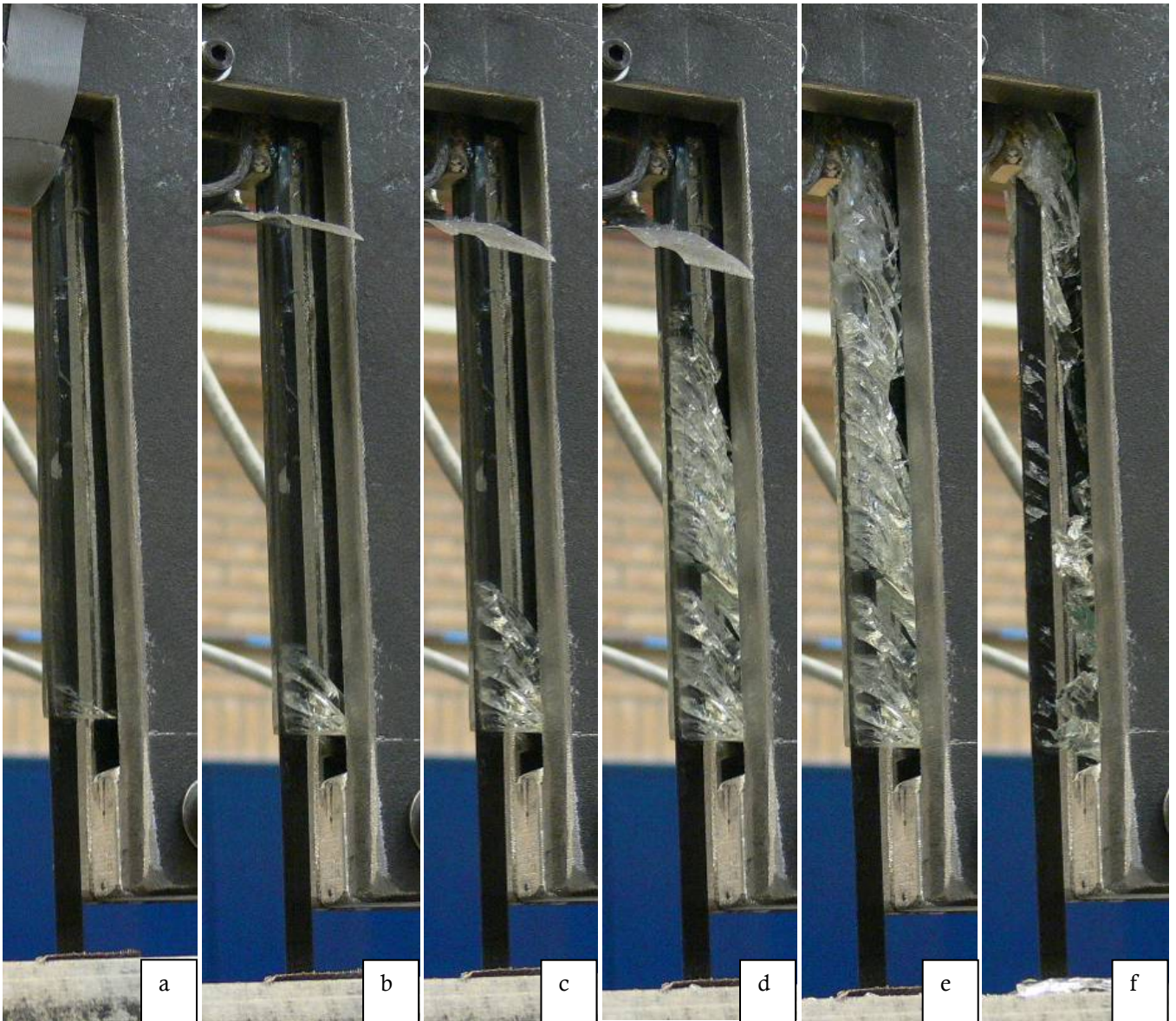
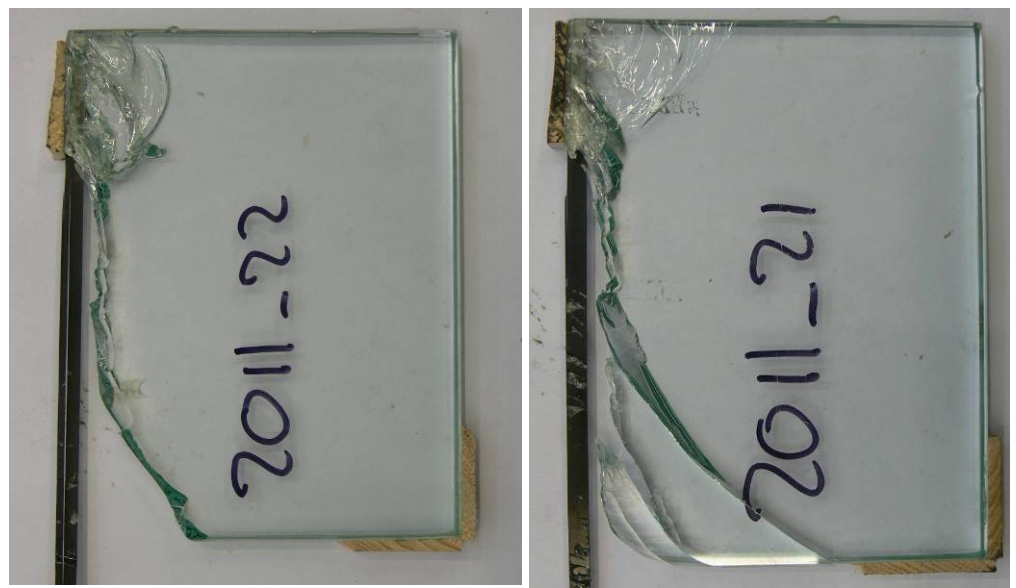


Figure 64

Above: specimen 2011_21 at different moments during the test.

Right: after the test.



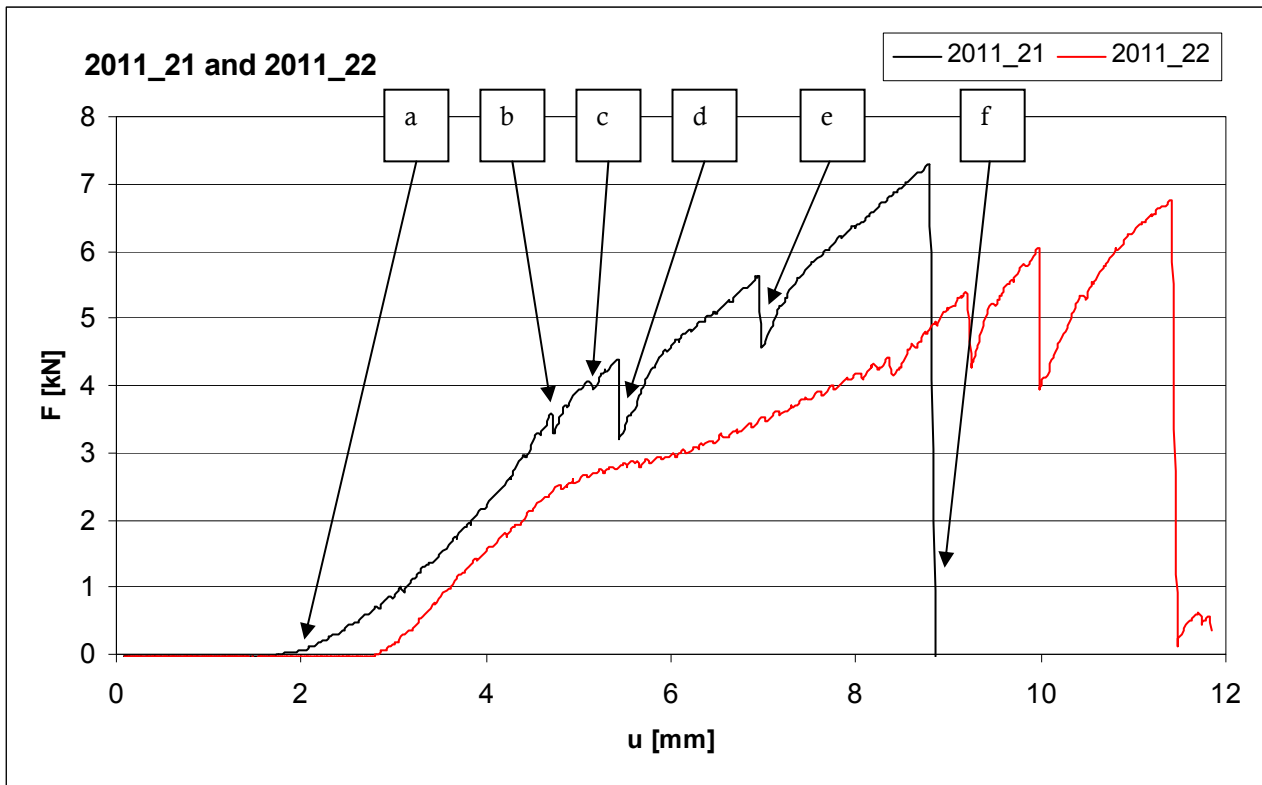


Figure 65, force-displacement diagram of specimen 2011_21 and 2011_22.

Specimens 2011_21 and 2011_22

Specimen 2011_21 was slightly fractured when test commenced (see Figure 64).

Both specimens have comparable failure behavior; progressive glass failure, failure of the adhesive is not observed.

Note that the highest force, 7,3 kN, was gained with a totally fractured glass pane.

Table 28, summary specimens 2011_21 and 2011_22

Specimen	2011_21		2011_22	
Configuration	6x0,8	[mm]	6x0,8	[mm]
Anchorage length	150	[mm]	150	[mm]
First adhesive failure	-	[kN]	2,5 (left)	[kN]
First glass failure	3,4	[kN]	3,2	[kN]
Ultimate strength	7,3	[kN]	6,75	[kN]

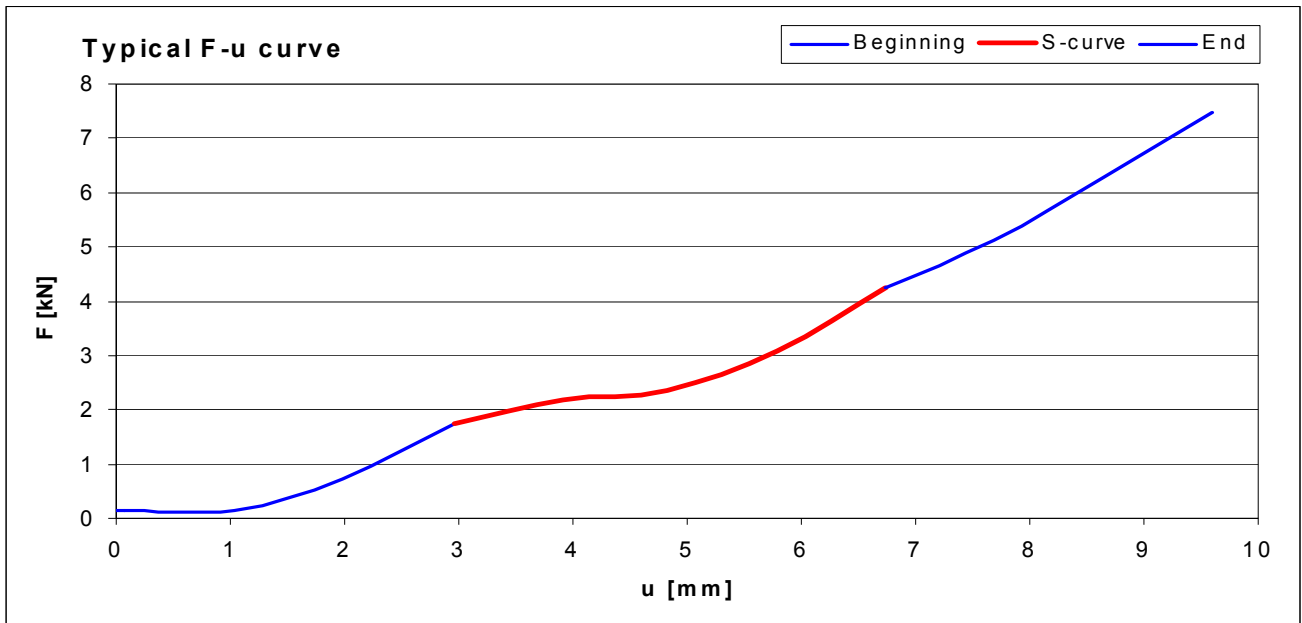
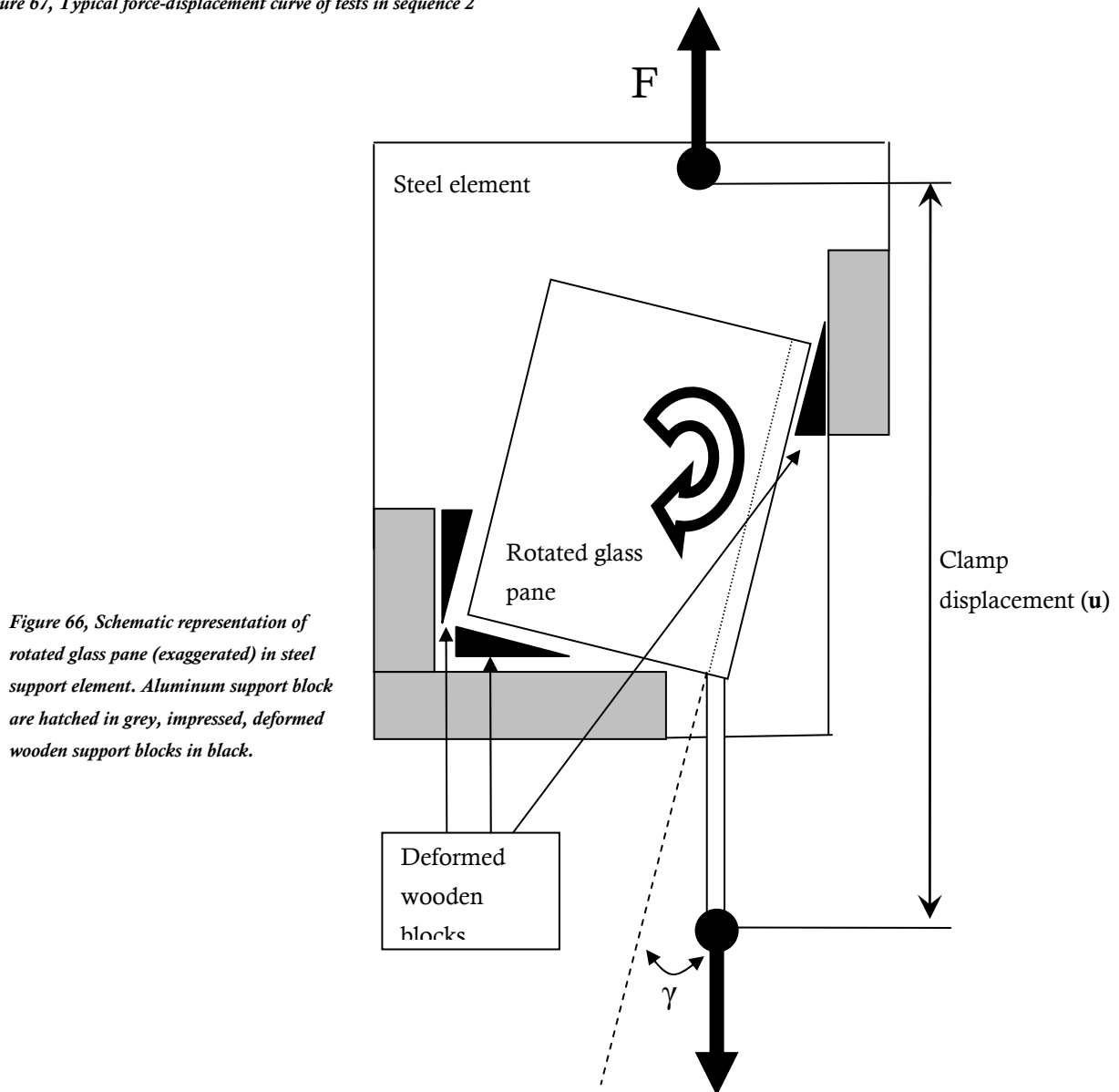


Figure 67, Typical force-displacement curve of tests in sequence 2



Discussion

The maximum displacement caused by extension of the carbon fiber is for example for specimen 2011_09:

$$N_{\max} = EA\varepsilon_{\max}$$

$$N_{\max} = 8000N$$

$$E = 145.000N / mm^2$$

$$A = 6 * 0,6 = 3,6mm^2$$

$$l = l_{\text{glasspane}} + l_{\text{glass-clamp}} \approx 150mm + 40mm = 190mm$$

$$\varepsilon_{\max} = \frac{\Delta l}{l} = \frac{u_{\max}}{190mm}$$

$$u_{\max} = \frac{8000N * 190mm}{145000N / mm^2 * 3,6mm^2} = 2,9mm$$

The measured clamp displacement is approximately 9mm. The other 6mm have to be caused by distortions in the setup.

Every force-displacement curve shows a similar S-curve between 2 and 4 kN (see red part of curve in *Figure 67*).

This is caused by rotation of the specimens.

The wooden blocks, with which the specimens are mounted, are impressed by the supporting force of the setup (*Figure 68*). The resin channels in the wood (*Figure 69*) are crushed between 2 and 4 kN. This causes the wood to impress and the specimen to drop (slightly) and rotate.

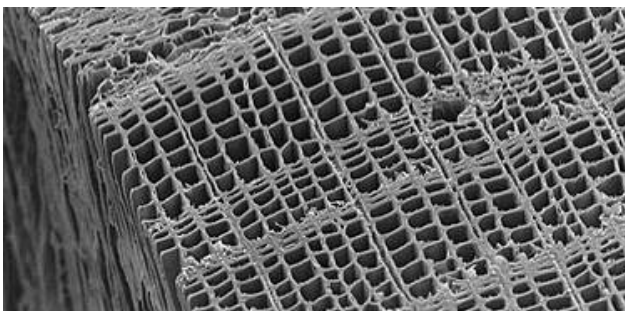


Figure 69, Coniferous wood seen under an electron microscope.

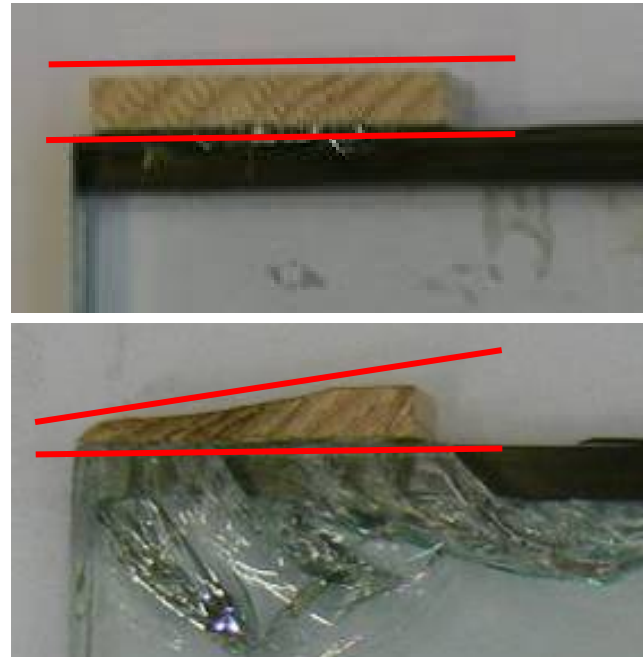


Figure 68, Wooden support block before (above) and after (below) the test. The shape of the blocks is emphasized in red.

The rotation of the glass pane has negative influence on the test results.

Because the glass pane rotates, the carbon strip is pulled out of the glass pane under an angle (γ in *Figure 66*). This could influence the strength of the connection and/or the failure mechanism. Furthermore it troubles the interpretation of the force-displacement curve.

Recommendations

For further testing it is advised to take measures to minimize or prevent rotation of the specimen.

For interpreting the deformation of the carbon fiber strip in the glass pane, the measuring of the clamp to clamp distance is not accurate enough. It is advised to add equipment that measures the displacement of the carbon strip against the glass pane more directly and not via the clamp-to-clamp distance.

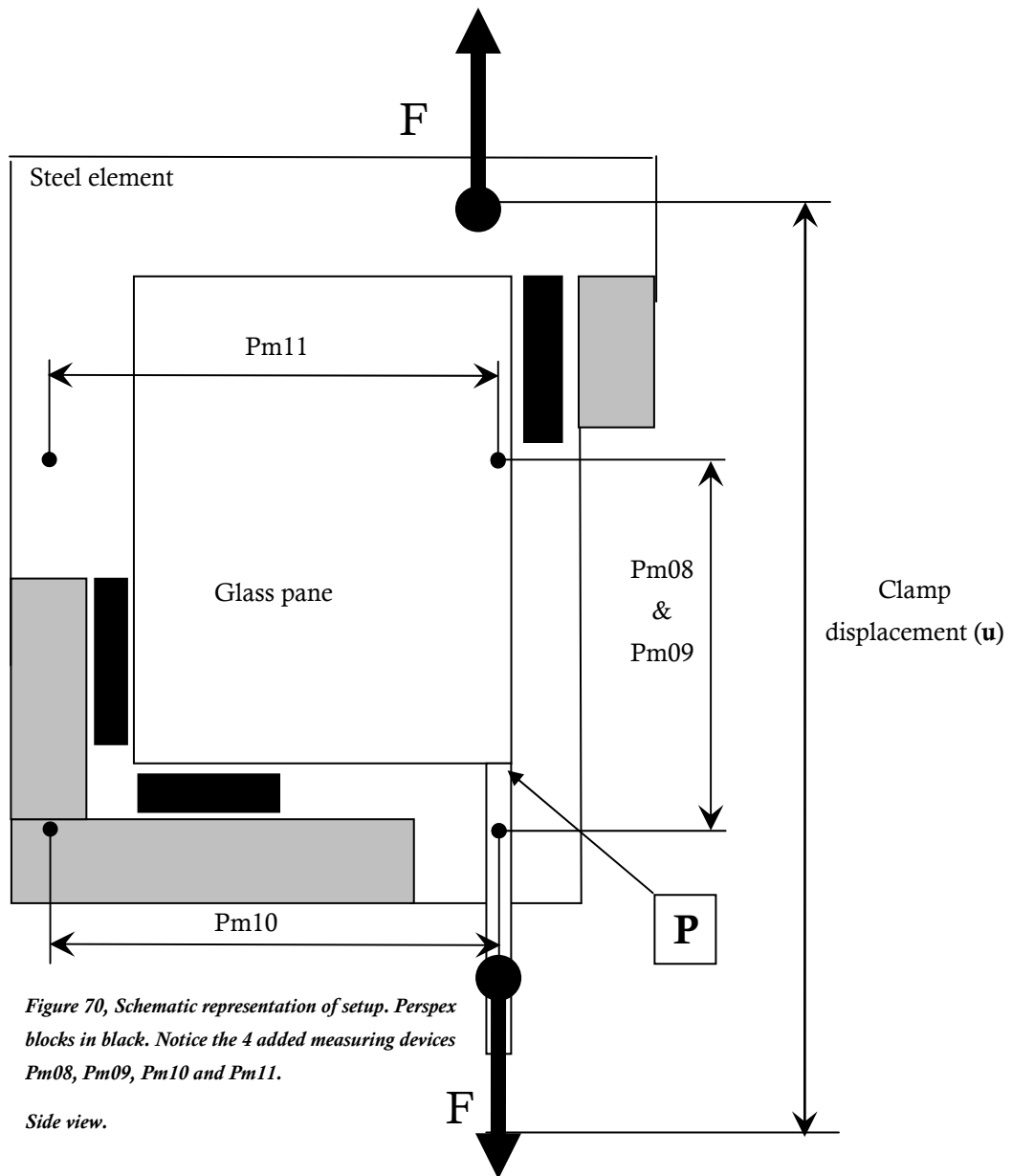


Figure 70, Schematic representation of setup. Perspex blocks in black. Notice the 4 added measuring devices Pm08, Pm09, Pm10 and Pm11.

Side view.

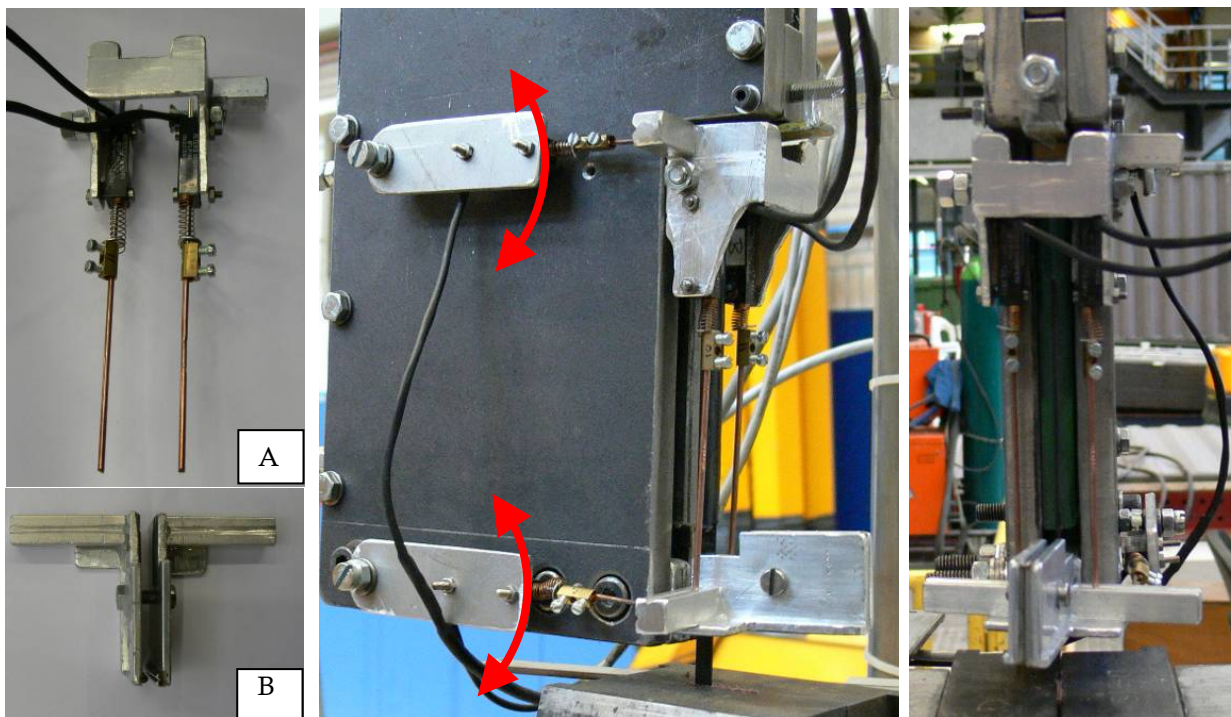


Figure 71. Left: frog clamping A and B isolated. Middle: mounted in setup (mirrored), side view, the red arrows indicate possible rotation of the sensors. Right: front view.

Test sequence 3

Method

The setup is adjusted according to the recommendations on page 69: (see *Figure 70*)

The wooden blocks are replaced by perspex blocks of the same dimensions.

4 elongation meters are added:

- Pm08 & Pm09 measure the displacement of the carbon strip against the glass pane.
- Pm10 & Pm11 monitor the rotation of the glass pane in the steel element.

The mounting of Pm08 and Pm09 is done by aluminum frog clamps.

Clamp A can be mounted to the glass pane by screwing the bolt by hand. This does not damage the glass, yet is tight enough to prevent the clamp from slipping.

Clamp B is firmly mounted on the carbon strip by screwdriver.

Clamp B has two aluminum blocks with a small gutter in which Pm08, Pm09 and Pm10 are placed. The displacement of clamp B against the glass pane is the average between Pm08 and Pm09, settled for the possible difference between x and y .

The exact displacement of the carbon strip at the edge of the glass pane equals the displacement of clamp B settled for the elongation of the carbon strip over distance z (δz). This can be calculated as follows:

$$N = EA\varepsilon = E_{carbon} A_{strip} \frac{\delta z}{z} = F_{clamp}$$

$$\delta z = \frac{F * z}{EA}$$

Pm10 and Pm11 are attached to the steel element so that they can rotate and allow vertical movement of the

specimen. The sensors are placed in the gutters of clamp A and B. If the extension of Pm10 and Pm11 is concurrent, the specimen lowers straight. If Pm10 is impressed and Pm11 extends, the specimen rotates. The hypothesis that the rotation is minimal due to the perspex blocks can be (dis)confirmed by this.

Note that Pm10 is placed on clamp B at distance 'y' to the carbon strip.

Point 'P' marks the carbon strip at the edge of the glass where the adhesive connection begins.

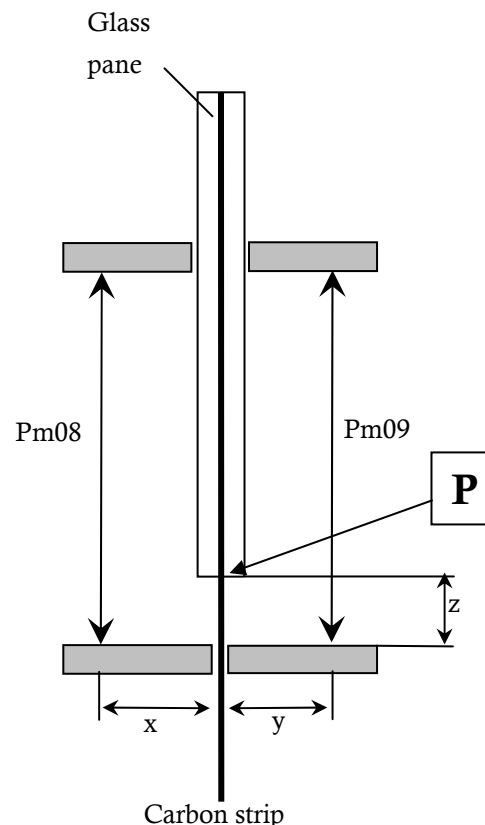


Figure 72, Schematic representation of specimen with position of measuring devices Pm08 and Pm09.

a, b and c are measured prior to testing.

Front view

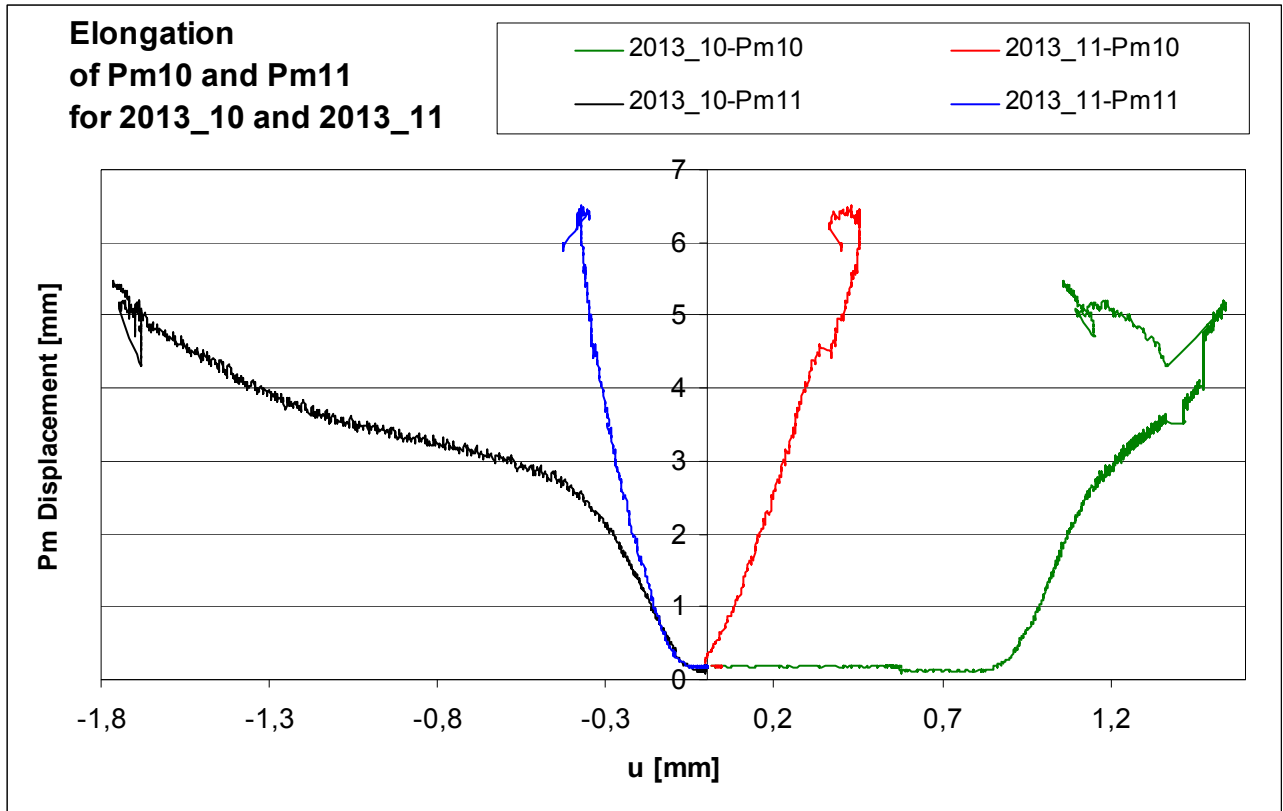


Figure 74, Elongation of Pm10 and Pm11 for 2013_10 (black) and 2013_11 (red). Note that the extension is marked negative and shortening marked positive.

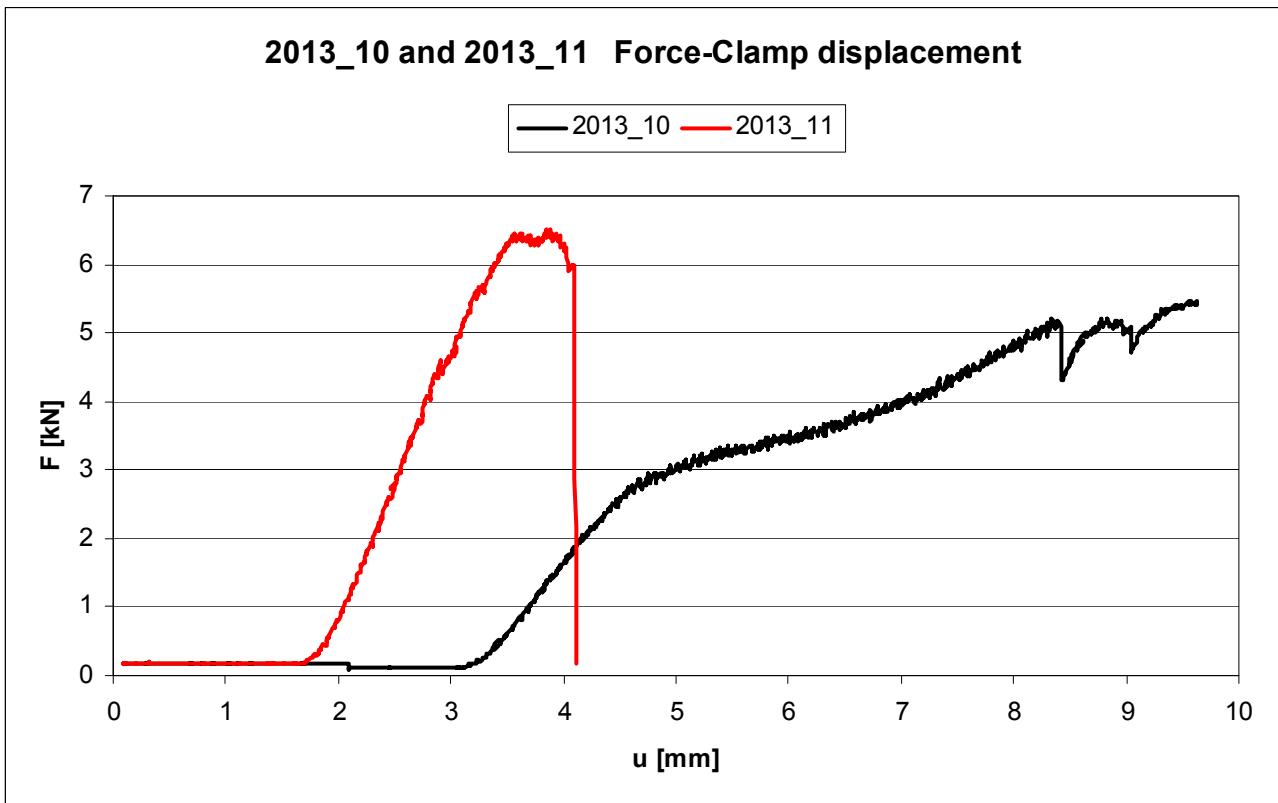


Figure 73, Force displacement diagram for 2013_10 and 2013_11.

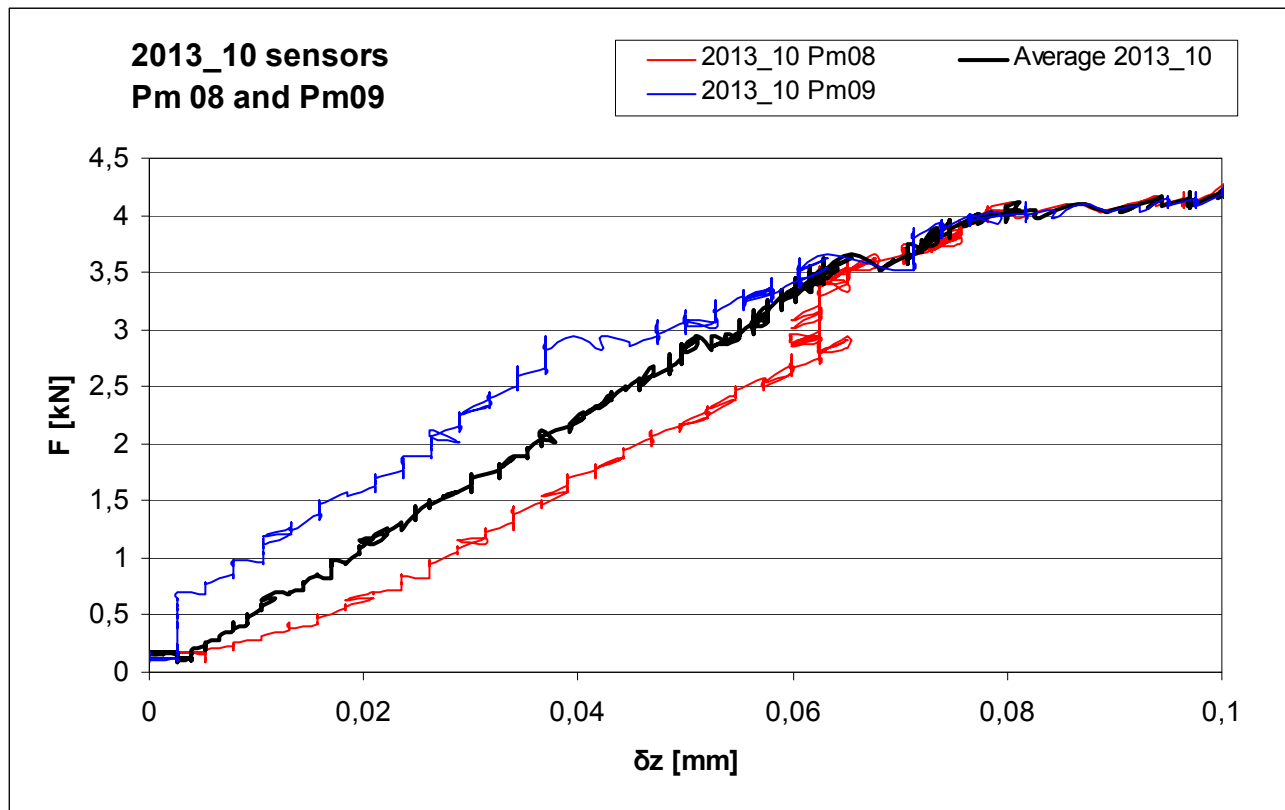


Figure 75, Force-elongation of sensors Pm08 and Pm09. In blue Pm08 and Pm09 for 2013_10 and their average value in black. Average value for Pm08 and Pm09 of 2013_11 in red.

Results

Interpretation of renewed setup

First the results from the added sensors are interpreted for specimen 2013_10 and 2013_11. 2013_10 is mounted with wooden blocks; 2013_11 is mounted with perspex blocks.

See Figure 73. 2013_10 was mounted high; it lowered 3mm before the glass pane rested on the setup and the build-up of force started. This is visible in Figure 74 by the displacement of 0,8mm of Pm10 when force was not build up yet.

The build-up of force is faster (curve is steeper) for 2013_11 than for 2013_10. This implies that the perspex blocks are stiffer than the wooden blocks. This is confirmed by the difference in E-modulus of 12 times: approximately 250 MPa for Pine wood perpendicular to the grain and approximately 3000 MPa for perspex.

The hypothesis that the S-curve in the force-displacement diagram is caused by rotation of the specimen due to impression of the wooden blocks is confirmed by Figure 74. Pm10 and Pm11 sense this rotation for 2013_10 by opposite displacement: similar S-curves occur in Pm10 and 11 at the same force as visible in Figure 73. This S-curve does not occur for 2013_11, which is mounted by perspex blocks.

The displacement of clamp B against the glass pane is monitored by Pm08 and Pm09. This displays the distortion of the carbon fiber in the glass pane more directly than the clamp-to-clamp displacement u . The rotation or crookedness of clamp B is visible by the difference in length between Pm08 and Pm09 of approximately 0,02mm (Figure 75). This rotation is compensated by taking the average value.

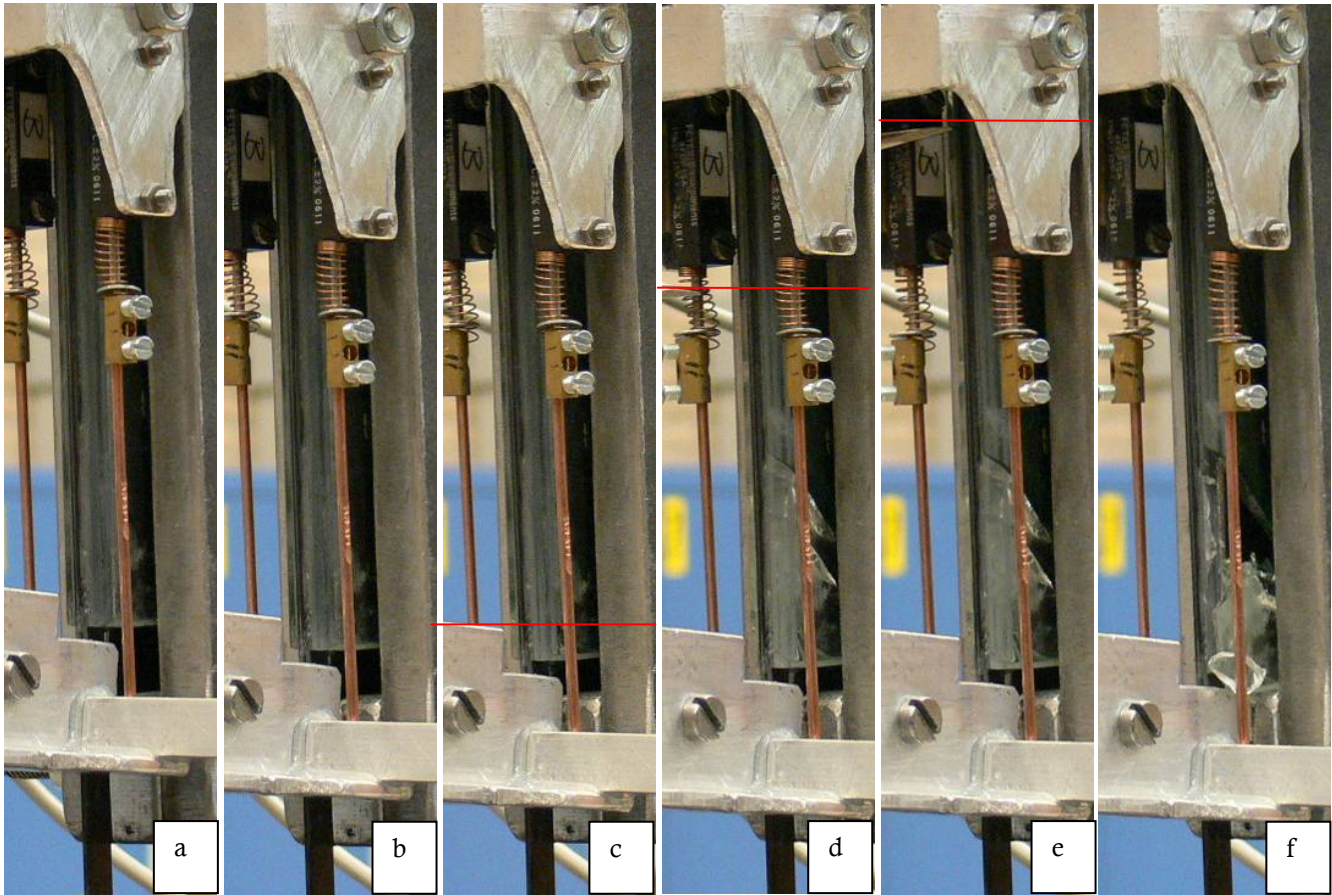
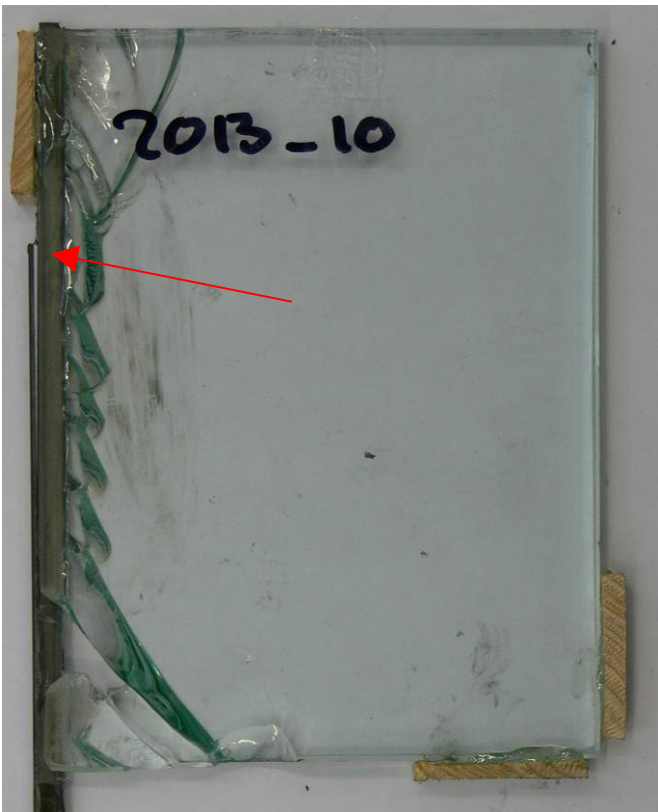


Figure 76, Above: specimen 2013_10 at different moments during the test. The letters correspond to the moments marked in Error! Reference source not found.. Below: Specimens 2013_10 and 2013_11 after the test.



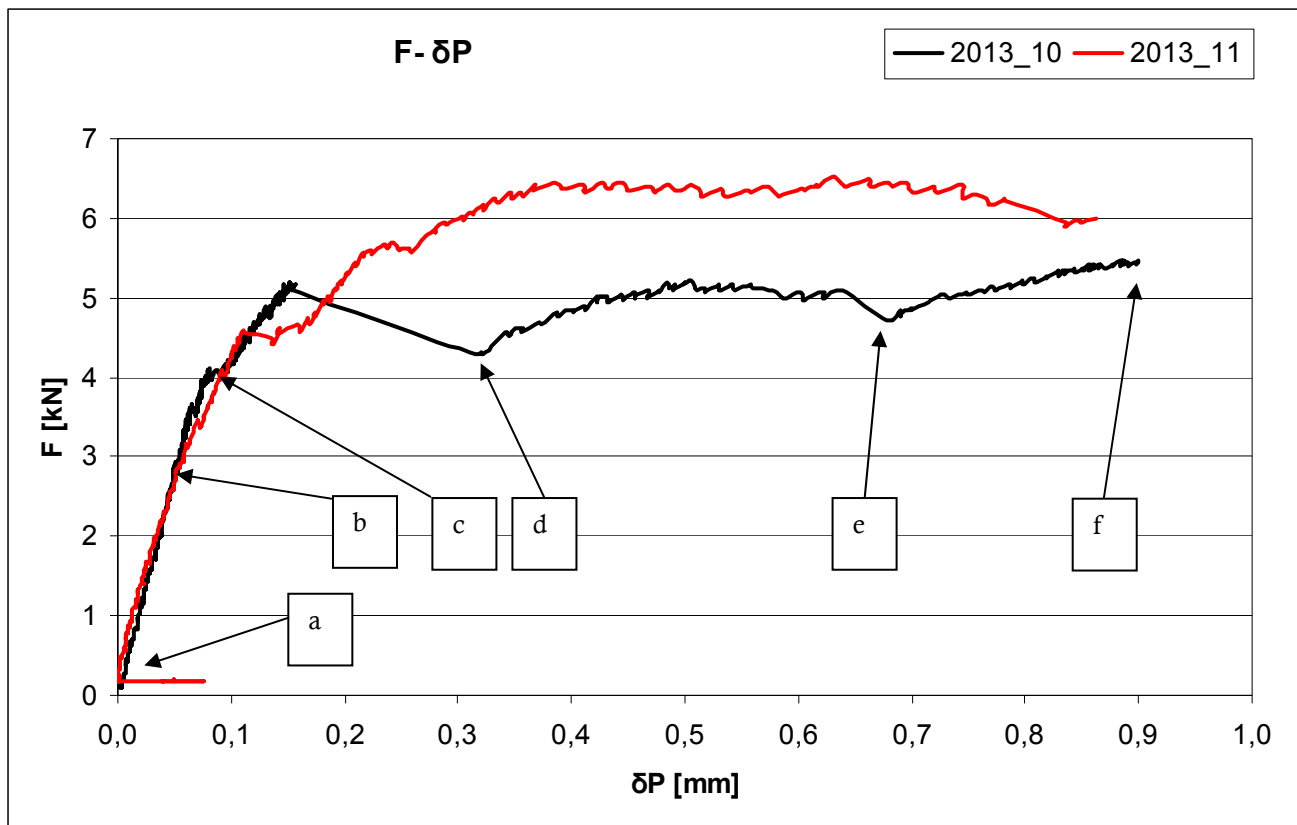


Figure 77, Force-displacement diagram for point P of specimens 2013_10 and 2013_11.

Specimens 2013_10 and 2013_11

Failure pattern of both specimens is comparable. Although *Figure 73* shows a difference in stiffness (steepness of the curve), this is not noticed in **Error!** Reference source not found..

Error! Reference source not found. shows that the tensile force in the carbon strip builds up to the maximum strength of the connection and then levels

out as fracturing of the glass pane progresses. If the specimen would be longer than 150mm the strength would probably not increase.

The red lines in *Figure 76c,d&e* emphasize the level of glass fracture in the picture. This is not clearly visible on the pictures because fractures occurred on the left side of the glass pane.

The fallback marked by *Figure 76e* is due to partial shattering and therefore drop in stiffness, of the carbon strip. This is visible in *Figure 76* by the red arrow

Table 29, summary specimens 2013_10 and 2013_11

Specimen	2013_10				2013_11			
Configuration	6x0,6 6x0,8			[mm]	6x0,6 6x0,8			[mm]
Support blocks	Wood				Perspex			
Positions (<i>Figure 72</i>)	x	y	z	[mm]	x	y	z	[mm]
	11	11	4,2		11	11	4,6	
Anchorage length	150			[mm]	150			[mm]
First adhesive failure	2,7			[kN]	4,0			[kN]
First glass failure	3,0			[kN]	4,5			[kN]
Ultimate strength	5,47			[kN]	6,51			[kN]

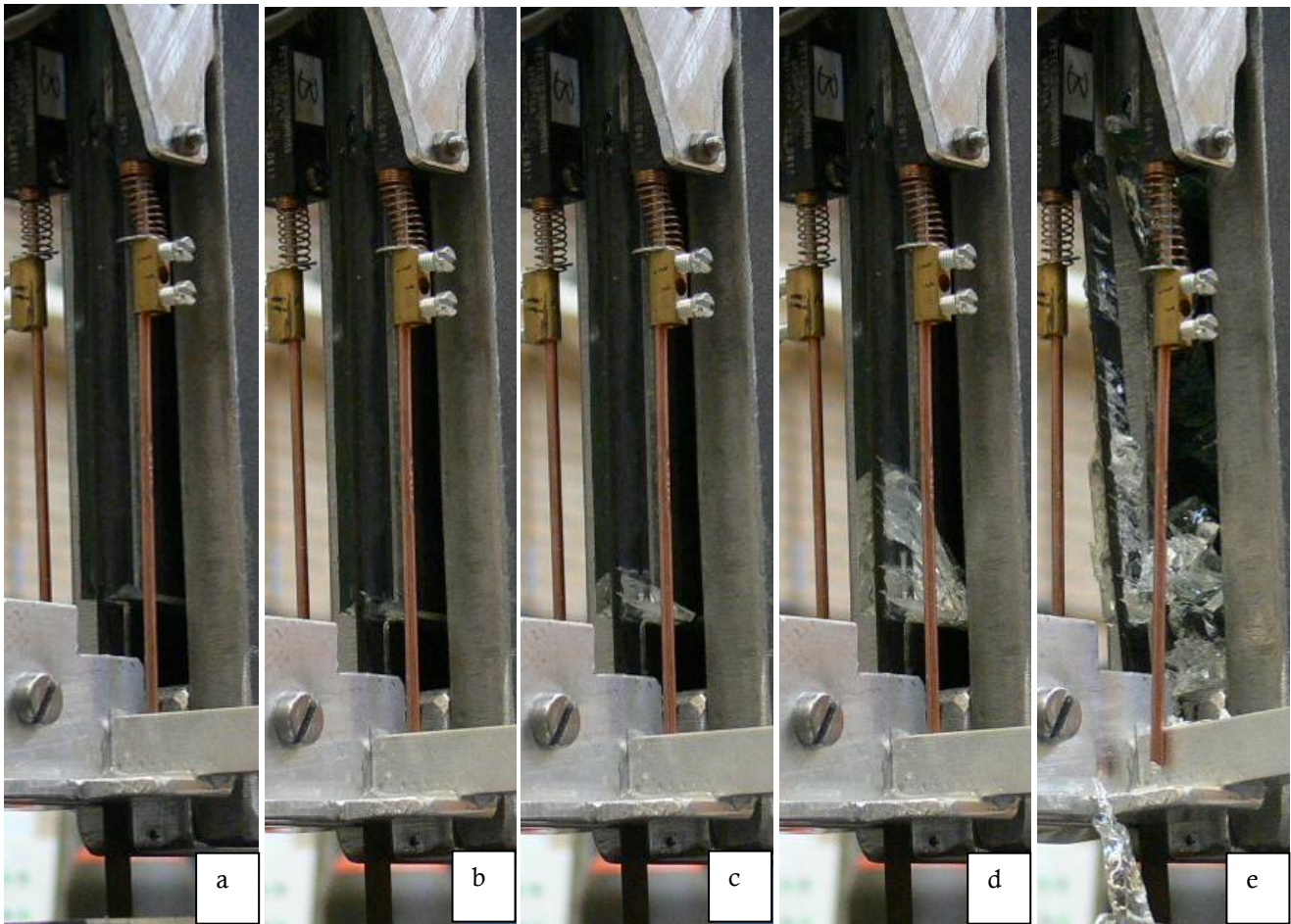
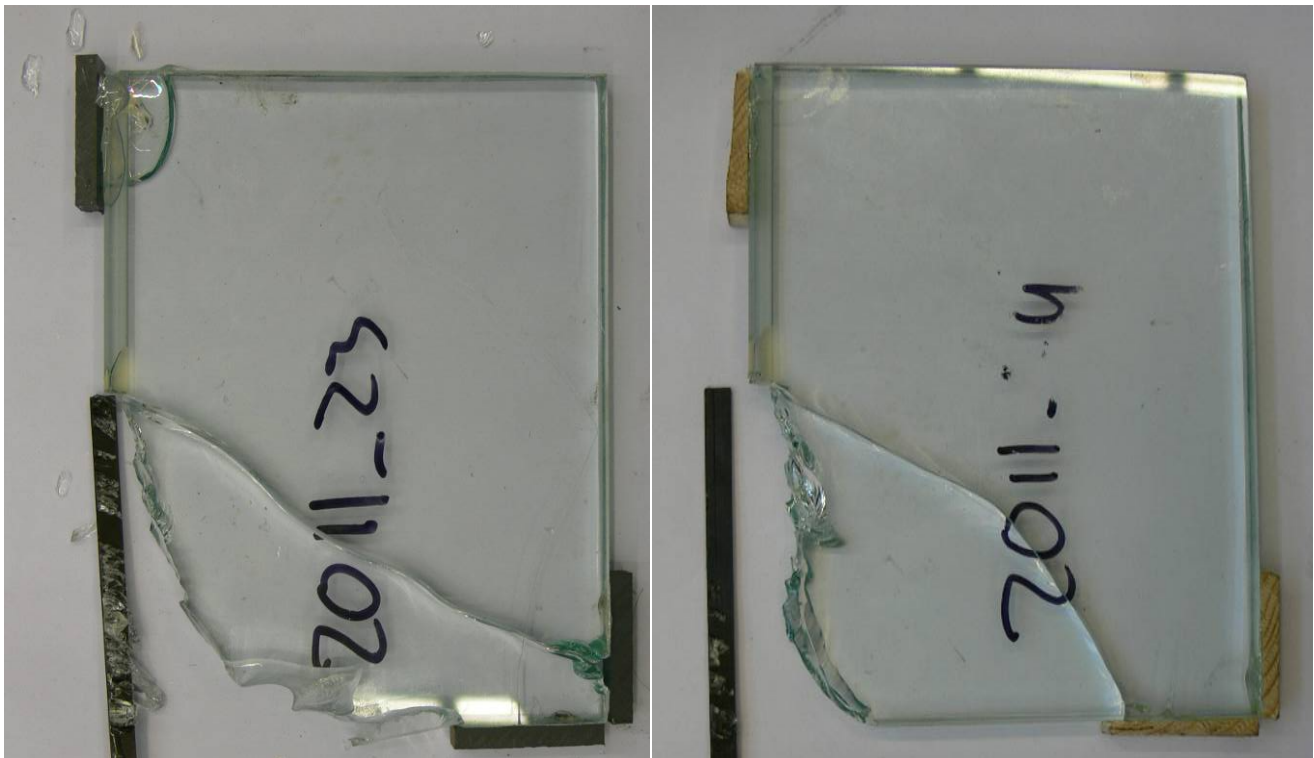


Figure 78, Above: specimen 2011_23 at different moment during the test. The letters correspond to the moments marked in Figure 79. Below: Specimens 2011_23 and 2011_24 after the test.



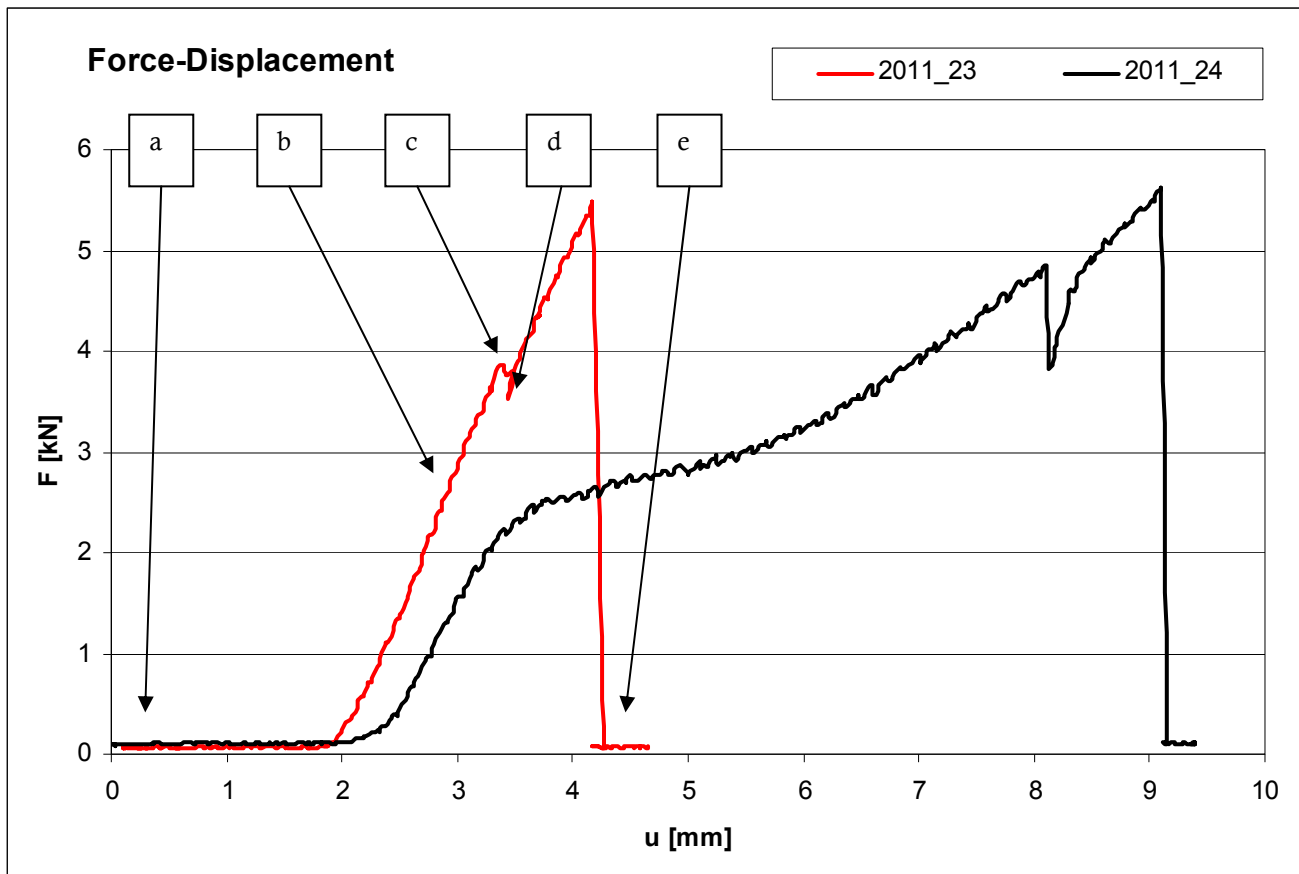


Figure 79, Force-displacement diagram of specimen 2011_23 and 2011_24.

Specimens 2011_23 and 2011_24

Unfortunately Pm08 was malfunctioning during the test. The results from Pm09 are therefore unreliable as well. A diagram like **Error! Reference source not found.** cannot be presented.

The extension of Pm09 at 4,5 kN is however approximately 0,4mm for both specimens and the fallbacks in *Figure 79* are visible as jumps as well (moment 'd' for 2011_23 and $u=8\text{mm}$ for 2011_24).

First crack in specimen 2011_23 occurred at moment 'b'. This is a small fracture that arose from the carbon strip, approximately 2mm from the edge of the glass, to the edge of the glass. Moment 'c' and 'd' occur almost directly after each other.

Table 30, summary specimens 2011_23 and 2011_24

Specimen	2011_23				2011_24			
Configuration	6x0,6			[mm]	6x0,6			[mm]
Support blocks	Perspex				Wood			
Positions (<i>Figure 72</i>)	x	y	z	[mm]	x	y	z	[mm]
	12,4	8,1	11,2		10,5	10,5	7,8	
Anchorage length	75			[mm]	75			[mm]
First adhesive failure	-			[kN]	4,0			[kN]
First glass failure	2,8			[kN]	4,7			[kN]
Ultimate strength	4,5			[kN]	4,6			[kN]

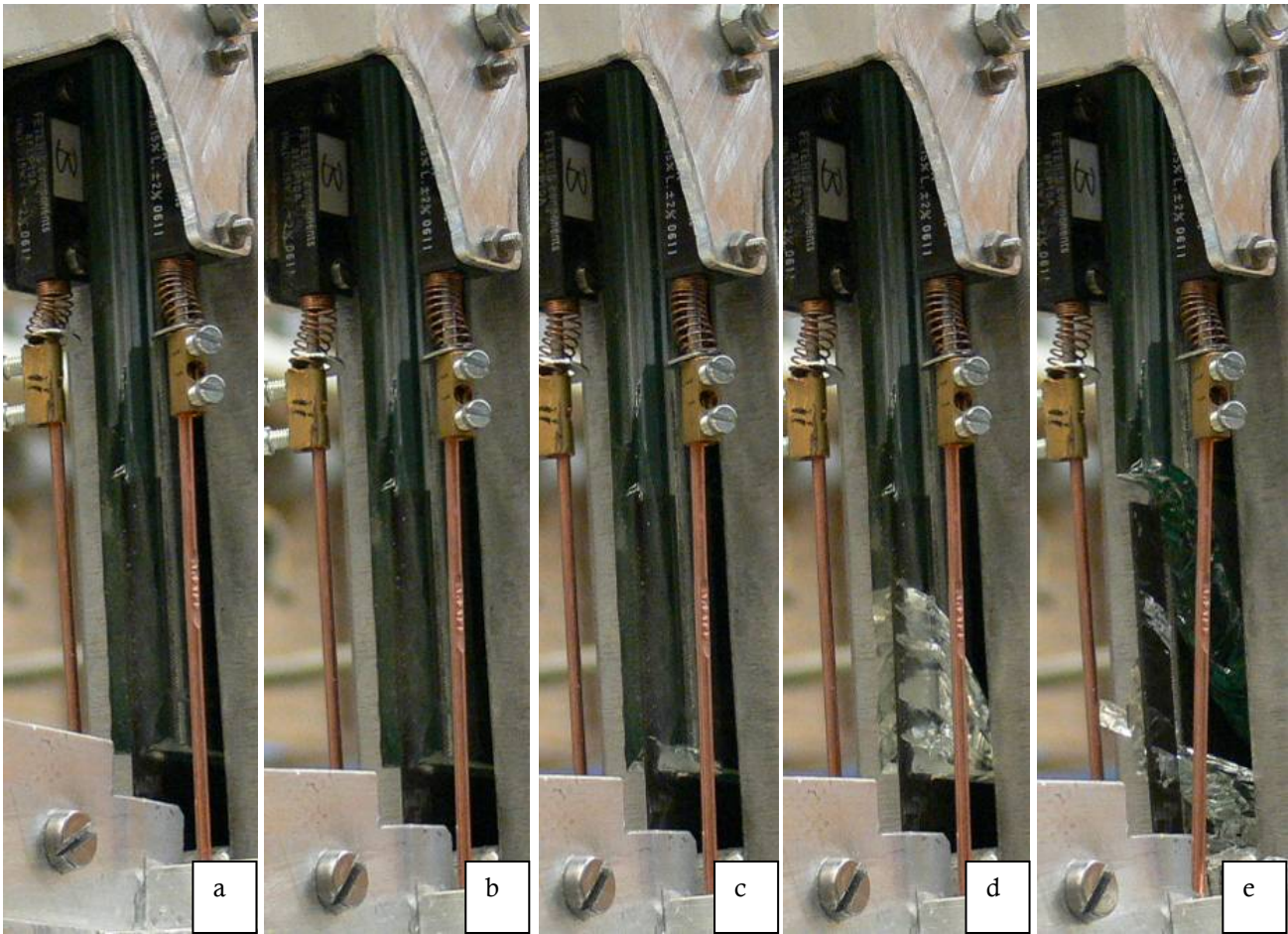
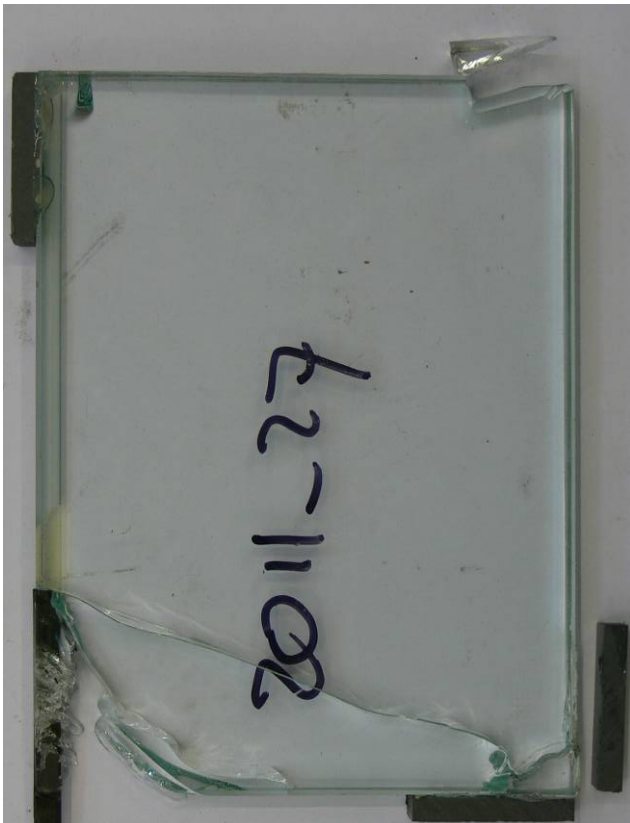


Figure 80, Above: Specimen 2011_26 at different moments during the test. Below: 2011_26 and 2011_27 after the test.



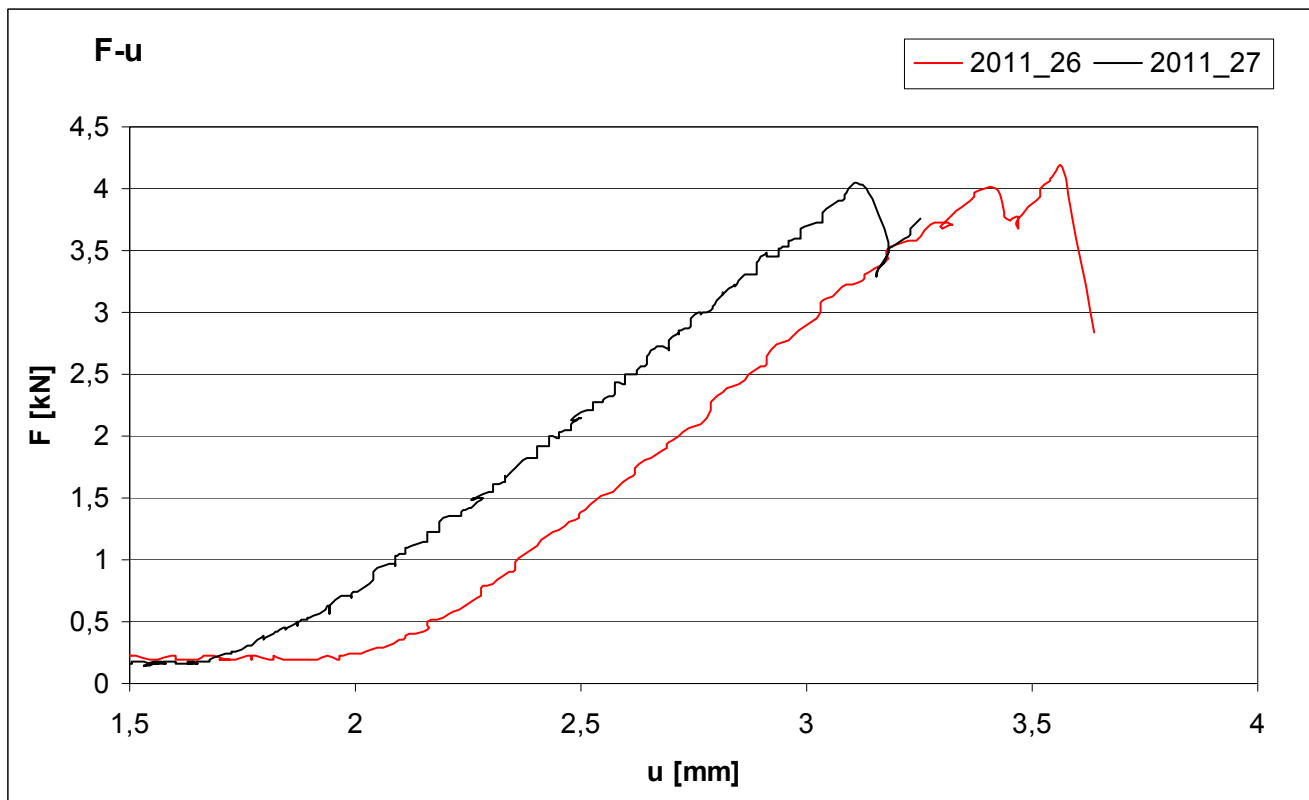


Figure 81, force-displacement diagram of specimens 2011_26 to 2011_28.

Specimens 2011_26 to 2011_28

2011_28 is discussed on the following page. Specimens 2011_26 and 2011_27 are mounted with perspex blocks, 2011_28 with wooden blocks.

Notice the fracture in the top-right corner of specimen 2011_27, this is caused after the test and has no further influence on the test results.

The support force q_1 (see *Figure 47*) at the perspex support block is suddenly released when the reinforcement bursts out of the glass pane. The impressed perspex block functions as a spring and releases all its stored energy at once. The specimen is launched back with the edge against the steel element.

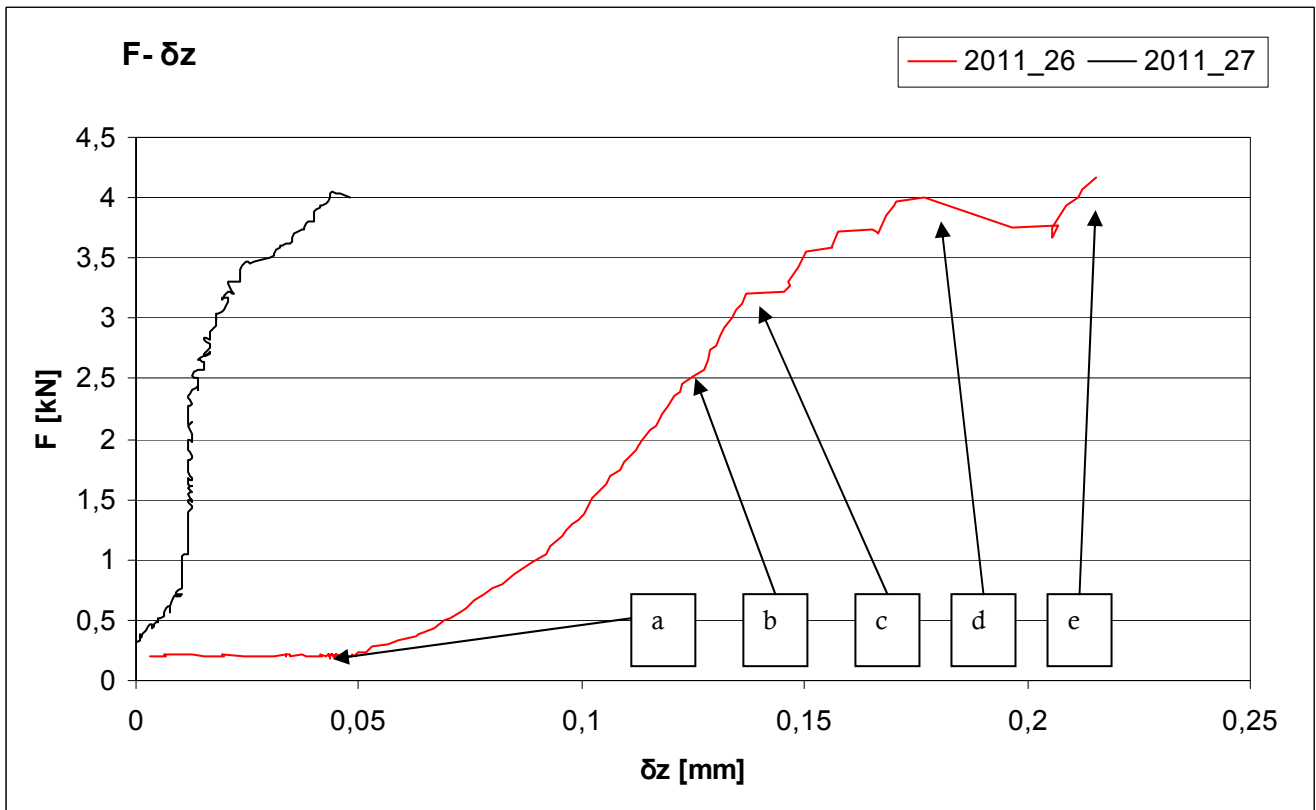
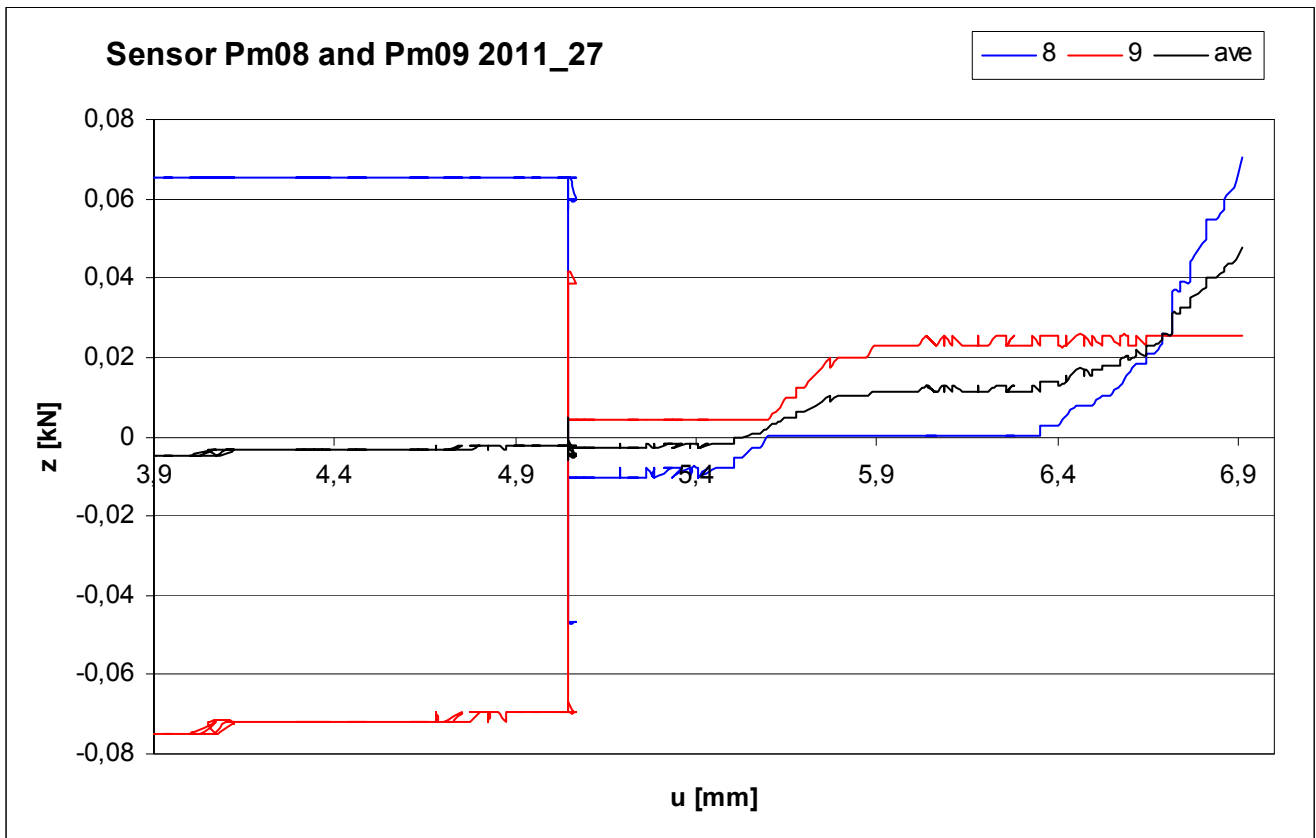


Figure 82, Above (a): F-z diagram for specimen 2011_26 and 2011_27.

Below (b): z-u diagram 2011_27 for Pm08, Pm09 and their average value.



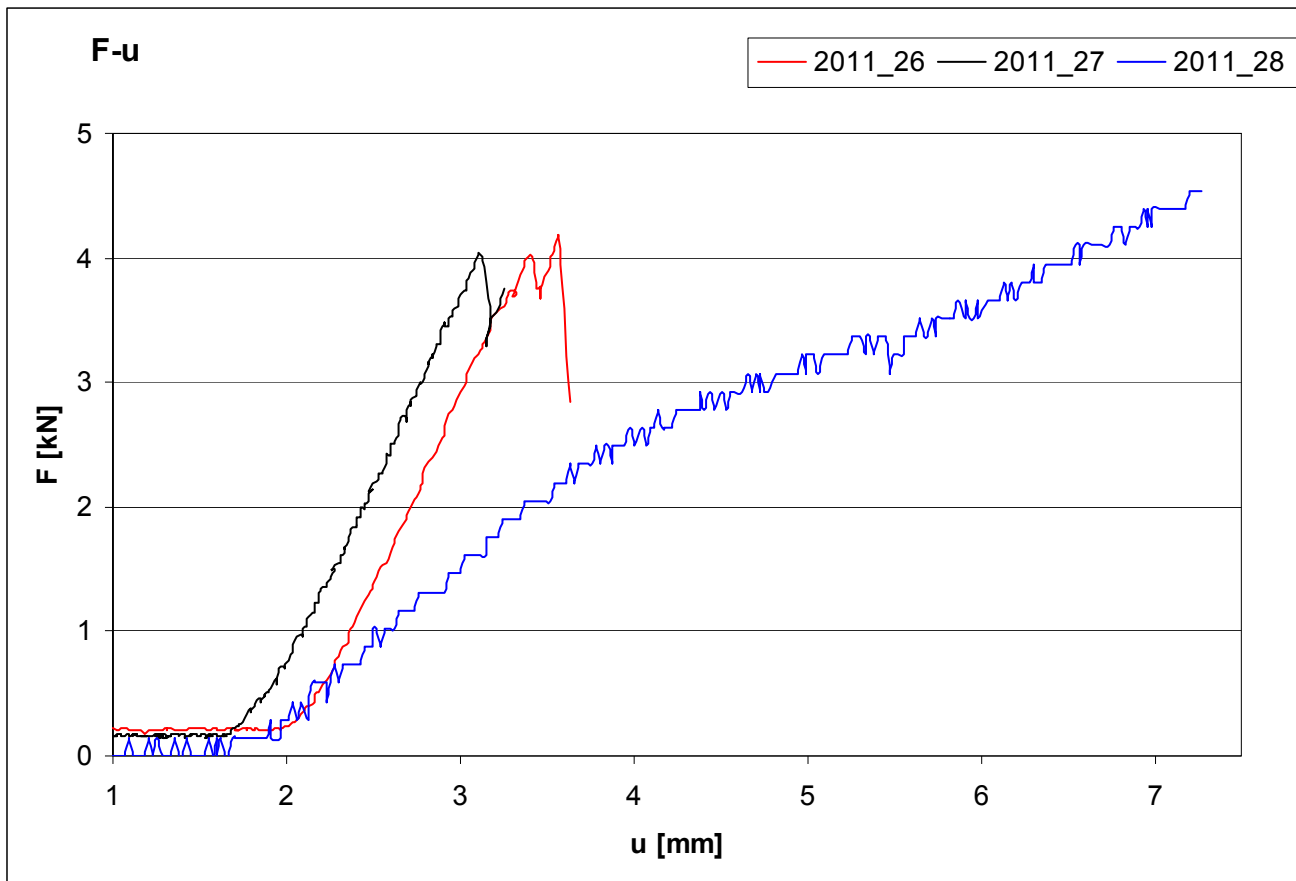


Figure 83, Force-displacement diagram for specimens 2011_26 to 2011_28.

Figure 82a shows the displacement of point P for specimens 2011_26 and 2011_27.

Figure 82b shows that the sensors Pm08 and Pm09 give strange results for specimen 2011_27: the sensors seem to be stuck during the test and make a jump at $u \approx 5,0$ mm. These results will be discarded.

The $F-\delta z$ curve of 2011_26 in Figure 82a shows a typical loss of stiffness after moment 'b'. This corresponds with the first failure of the adhesive connection.

Specimen 2011_28 showed a typical $F-u$ diagram with the S-curve up to total failure. The specimen exploded hard at 4,5 kN. Unfortunately pictures are not available.

Table 31, summary specimens 2011_26 to 2011_28

Specimen	2011_26				2011_27				2011_28		
Configuration	6x0,6			[mm]	6x0,6			[mm]	6x0,6		[mm]
Support blocks	Perspex				Perspex				Wood		
Positions (Figure 52)	x	y	z	[mm]	x	y	z	[mm]	N/A		
	10	10	10,0		10	10	4,1				
Anchorage length	40			[mm]	40			[mm]	40	[mm]	
First adhesive failure	-			[kN]	-			[kN]	-	[kN]	
First glass failure	3,2			[kN]	2,5			[kN]	2,3	[kN]	
Ultimate strength	4,2			[kN]	4,0			[kN]	4,5	[kN]	

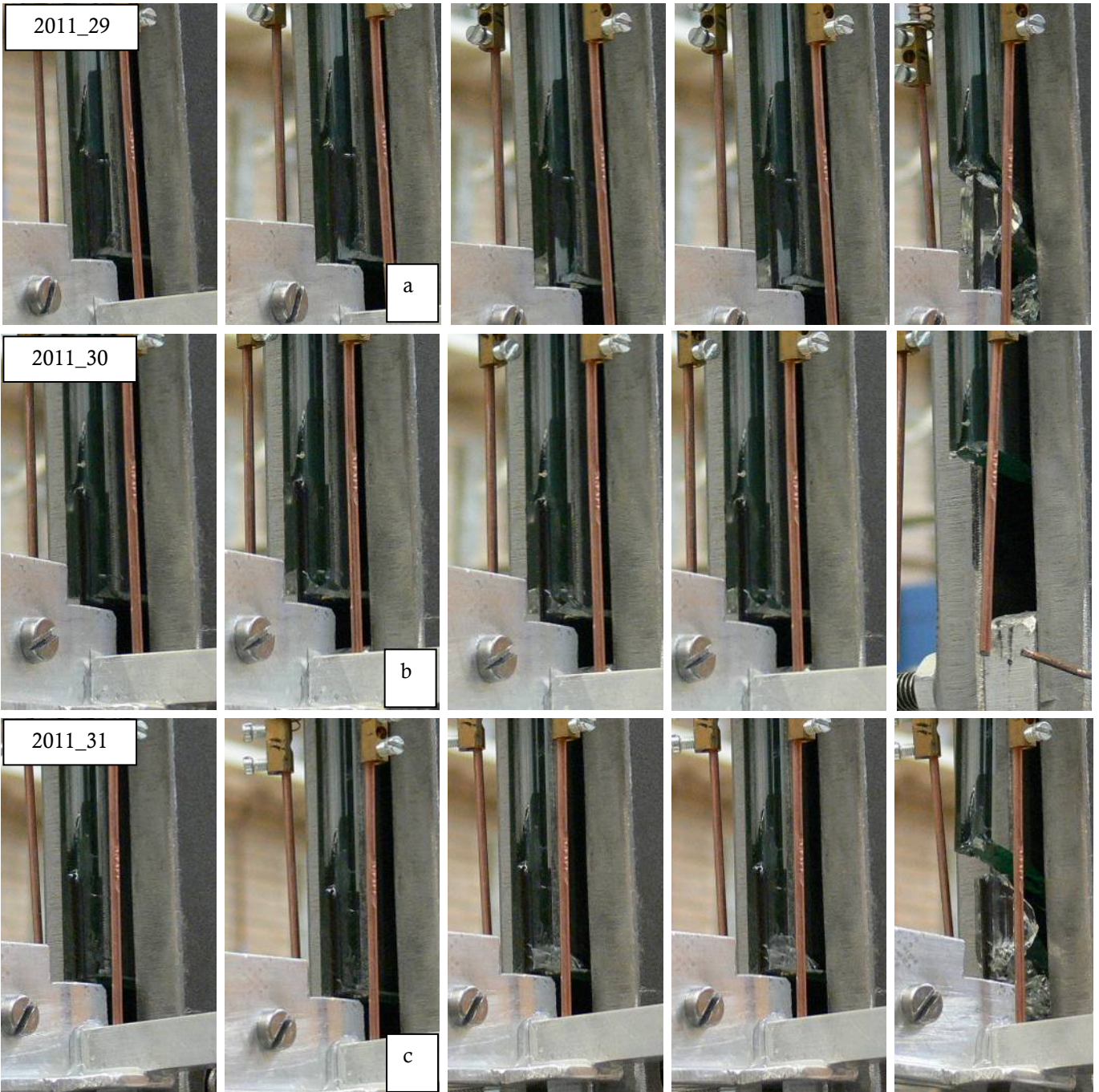


Figure 84, Above: Specimens 2011_29 (top row), 2011_30 (middle row) and 2011_31 (bottom row) at different moment during the tests. Below: close-up of specimen 2011_29 after the test.



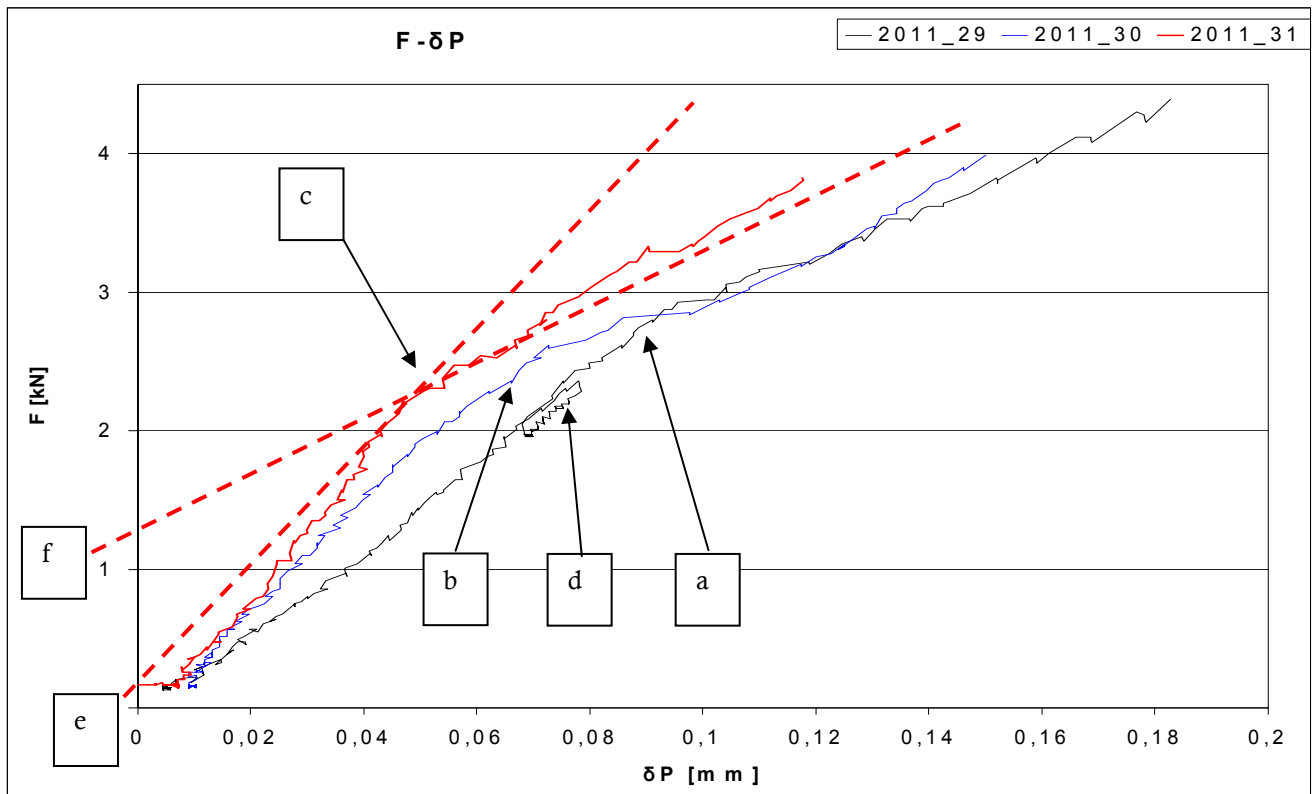


Figure 85, Force-strip displacement for specimens 2011_29 to 2011_30.

Specimens 2011_29 to 2011_31

Figure 84 displays all failure modes for the specimens. The fracture pattern after the test is comparable for all three specimens.

The diagram in Figure 85 represents the displacement of the carbon strip at the edge of the glass. This is calculated from the displacement of clamp B, compensated for the extension of the carbon over length 'z'.

Notice the loop in the curve of 2011_29, marked by 'd' in Figure 85. The test was interrupted for a short while to replace the battery of the camera. This did not have influence on the test results.

Specimen 2011_29: first the adhesive starts to fail (picture 'a') and then a fracture occurs in the glass pane (next picture in line).

Specimen 2011_30: A small fracture occurs (picture 'b'), at the same time the adhesive starts progressive failure at the left side of the carbon strip (not visible on the photo's).

Specimen 2011_31: The glass fractures at the right side of the carbon strip (picture 'c'). No visible failure of the adhesive is noticed.

Remarkable is the change in stiffness of the specimens after the first failure of the joint, marked by 'a', 'b' and 'c'.

This is emphasized in Figure 85 with two tangent lines 'e' and 'f' for the curve of 2011_31. 'e' marks the stiffness for the intact adhesive connection, 'f' marks the stiffness for the failing connection.

Similar crossing tangents could be drawn for 2011_29 (crossing in point 'a') and 2011_30 (crossing in point 'b').

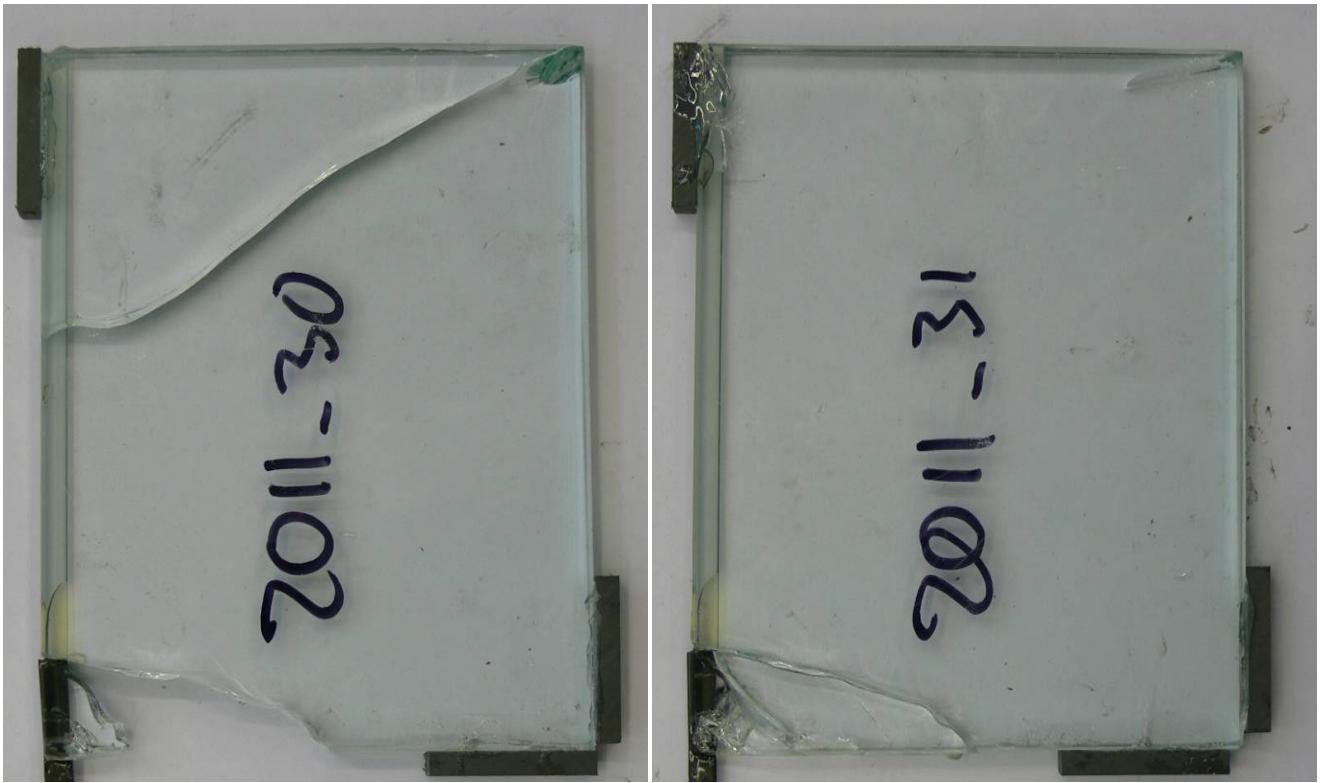


Figure 86, Specimens 2011_30 and 2011_31 after the test.

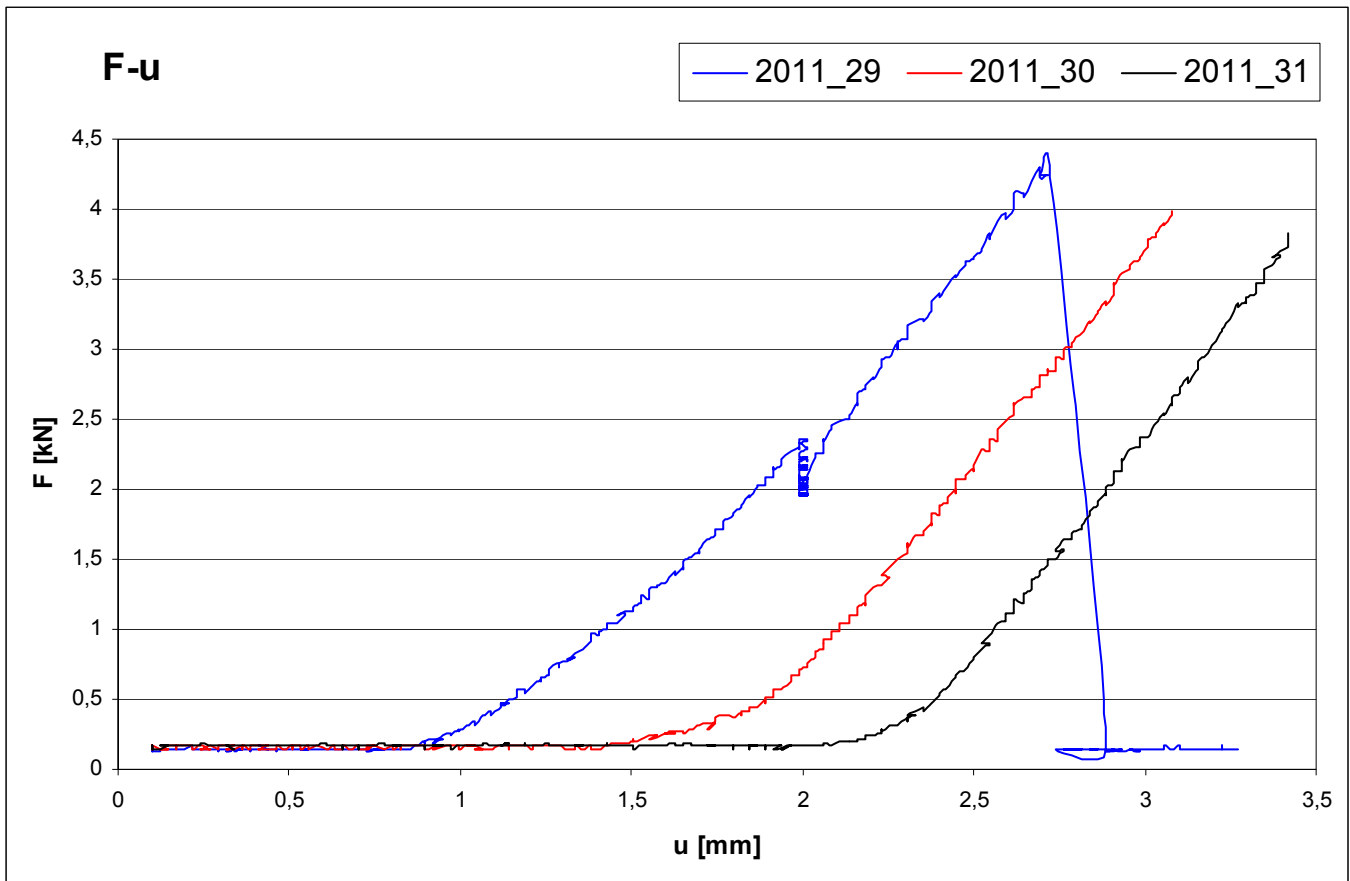


Figure 87, Force-displacement diagram for specimens 2011_29 to 2011_31.

All three specimens show similar force-displacement diagrams. The fallback in 2011_29 is caused by a short pause in the test.

Table 32, summary specimens 2011_29 to 2011_31

Specimen	2011_29				2011_30				2011_31			
Configuration	6x0,6			[mm]	6x0,6			[mm]	6x0,6			[mm]
Support blocks	Perspex				Perspex				Perspex			
Positions (Figure 52)	x	y	z	[mm]	x	y	z	[mm]	x	y	z	[mm]
	10	10	3,1		10	10	3,6		10	10	3,0	
Anchorage length	20			[mm]	20			[mm]	20			[mm]
First adhesive failure	2,0			[kN]	2,5			[kN]	-			[kN]
First glass failure	3,1			[kN]	2,7			[kN]	2,5			[kN]
Ultimate strength	4,4			[kN]	4,0			[kN]	3,8			[kN]

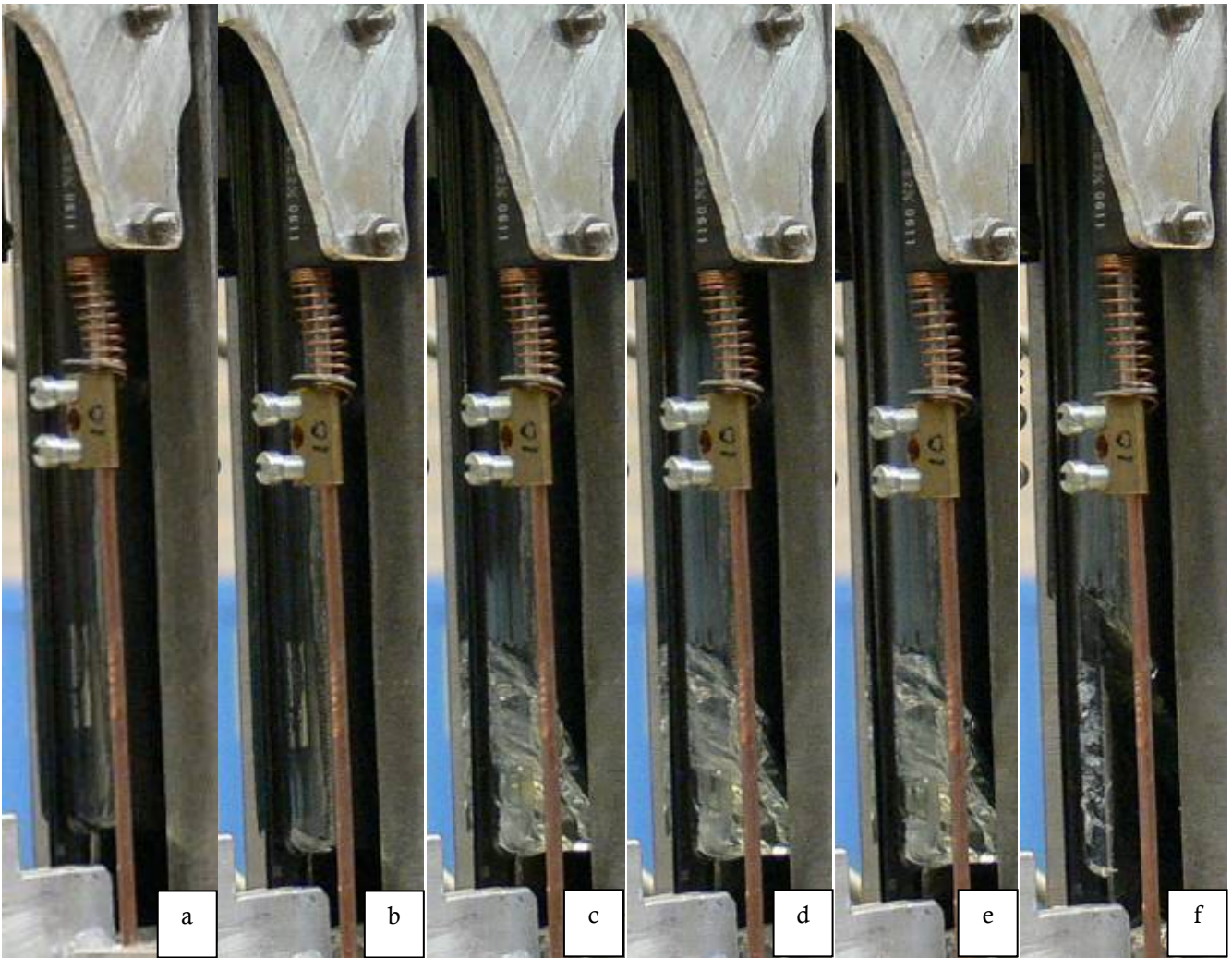


Figure 88, Above: specimen 2011_32 at different moments during the test, corresponding to the moments in Error! Reference source not found.. Picture 'f' was taken after total failure. Below: Specimen 2011_32 and 2011_34 after the test.



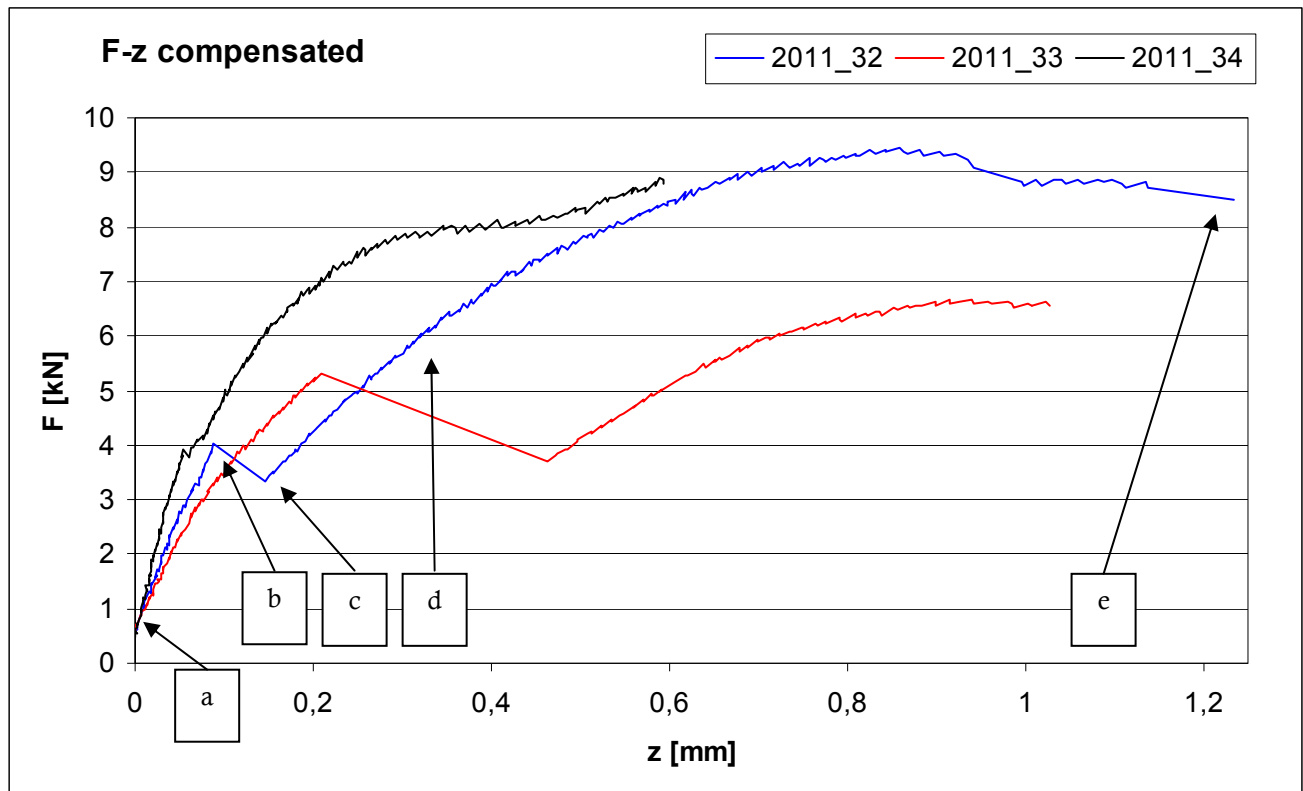


Figure 89, Force-displacement diagram for point 'P' of specimens 2011_32 to 2011_34. Moment 'P' is after total failure.

Specimens 2011_32 to 2011_34

Specimens 32 and 34 have similar failure patterns; 2011_33 is discussed on the next page.

First visible failure is adhesive failure (picture 'b'). Note that pictures 'b' and 'c' are taken seconds after each other.

The progression of adhesive failure in picture 'd' is approximately 60mm.

2011_34 is stiffer than 32 and 33. This is because the failure of the glass, at approximately 4,0 kN is over approximately 5 mm. This is a smaller length than with 2011_32 (picture 'b') where the glass failed over 30mm.

From *Figure 89* it is clear that stiffness decreases as force increases. The specimens have a certain maximum force to which they level out. This maximum force is different for each specimen. Anticipation is that the maximum force would not rise if the specimen was larger and had a longer carbon strip.

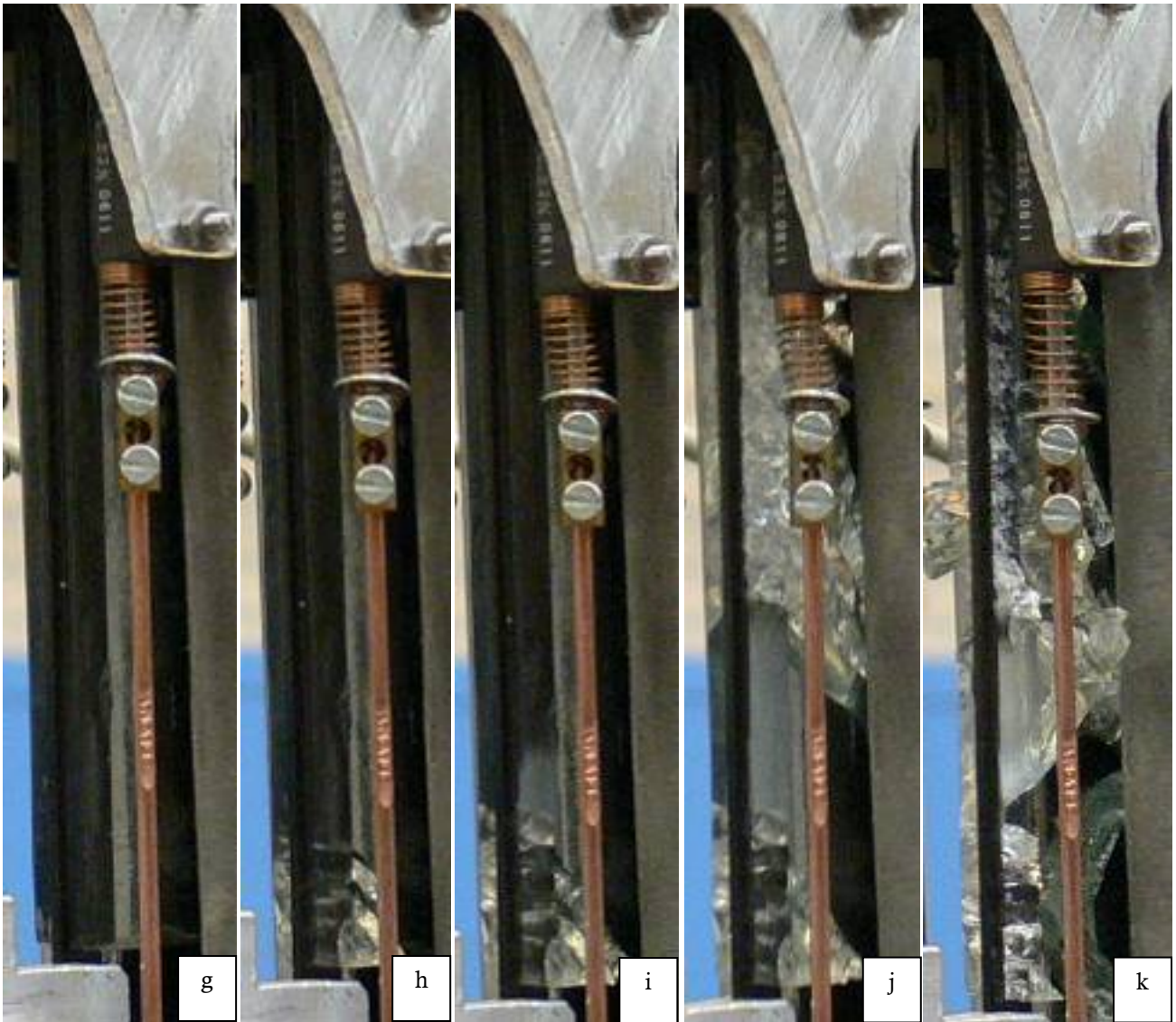


Figure 90,

Above: Specimen 2011_33 at different moments during the test. Moment correspond to Figure 91. Note that pictures 'g' and 'h' are referring the beginning of the test, approximately the same point as 'a' in Figure 88.

Right: after the test.



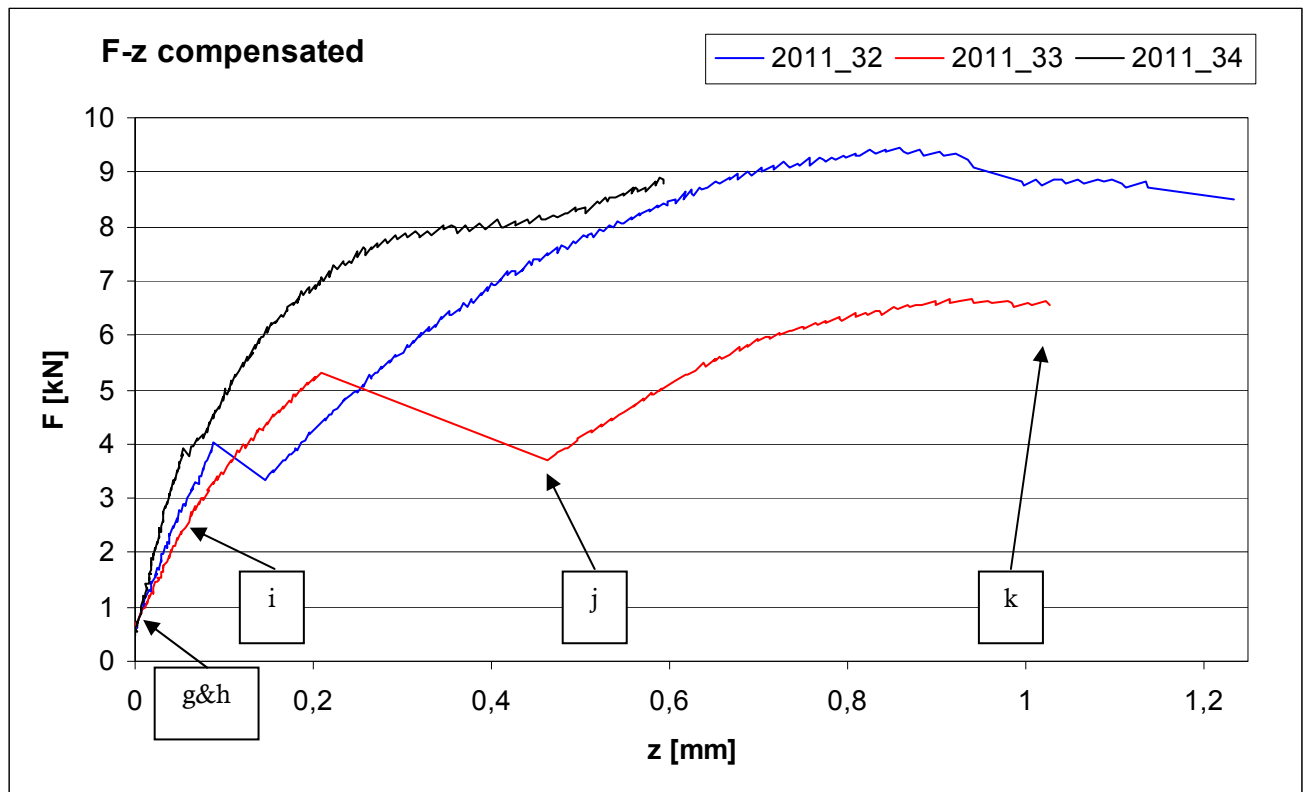


Figure 91, Force-displacement diagram for point 'P' of specimens 2011_32 to 2011_34. Moment 'k' is after total failure.

Remarkable difference in failure pattern of 2011_33 with 32 and 34 is the failure of the glass at 1,7 kN, in the beginning of the test.

Table 33, summary specimens 2011_32 to 2011_34

Specimen	2011_32				2011_33				2011_34			
Configuration	6x0,6			[mm]	6x0,6			[mm]	6x0,6			[mm]
	6x0,8				6x0,8				6x0,8			
Support blocks	Perspex				Perspex				Perspex			
Positions (Figure 52)	x	y	z	[mm]	x	y	z	[mm]	x	y	z	[mm]
	11	11	6,3		11	11	3,2		11	11	4,5	
Anchorage length	150			[mm]	150			[mm]	150			[mm]
First adhesive failure	1,7			[kN]	-			[kN]	2,0			[kN]
First glass failure	4,0			[kN]	0,4			[kN]	4,0			[kN]
Ultimate strength	9,4			[kN]	6,7			[kN]	8,9			[kN]

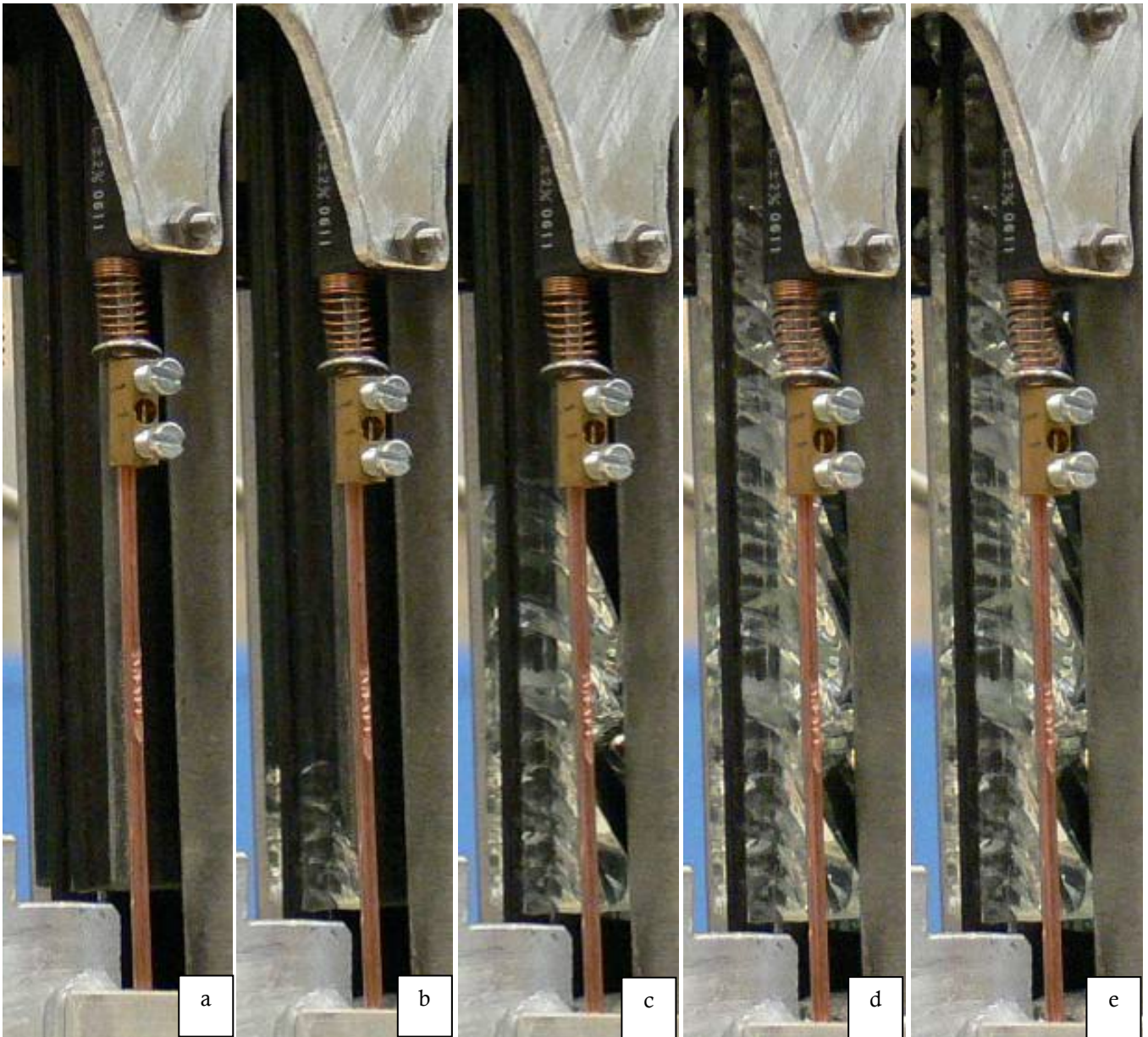


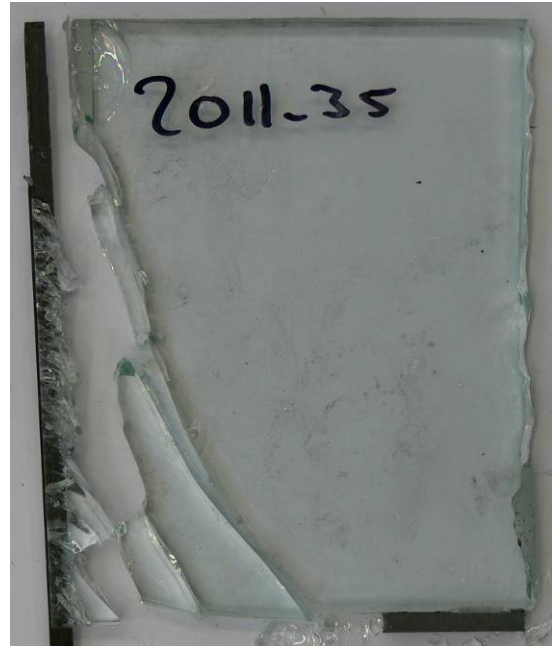
Figure 92,

Above: specimen 2011_35 at different moments during the test.

Right: after the test.

Table 34, summary specimen 2011_35

Specimen	2011_35	
Configuration	6x0,6 2x(0,4x3) 0,5/0,7x3	[mm]
Support blocks	Perspex	
Length z	2,8	[mm]
Anchorage length	150	[mm]
First adhesive failure	-	[kN]
First glass failure	0,4	[kN]
Ultimate strength	4,3	[kN]



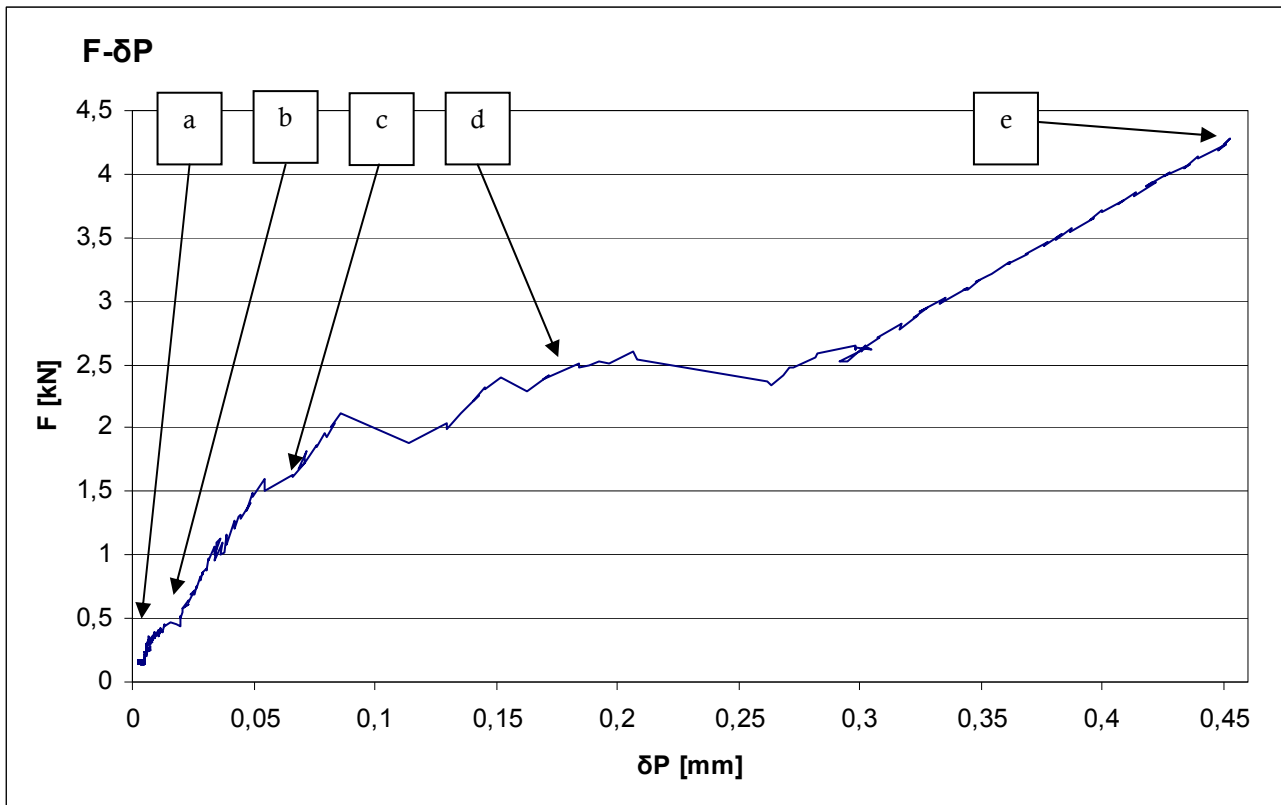
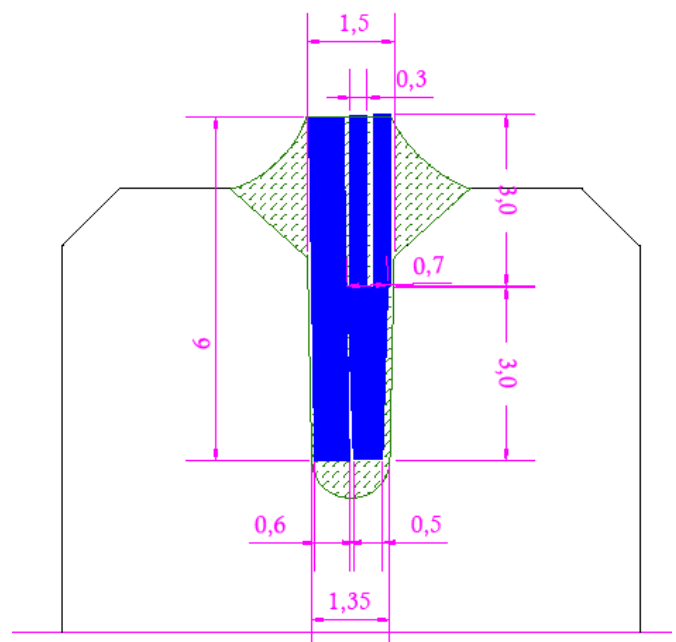


Figure 94, Force-displacement diagram for point P for specimen 2011_35.

Specimen 2011_35

This specimen has a different carbon strip configuration (see Figure 93), this results in a constant thin adhesive layer.

In the bottom of the groove the adhesive layer is approximately 0,1mm thick, in the top of the groove it is approximately 0,075mm thick.



$$0,6 \times 6 \text{ mm} + 2 \times (0,4 \times 3) + 0,5 / 0,7 \times 3$$

Figure 93, configuration of carbon strips in specimen 2011_35. Not to scale, measurements in mm.

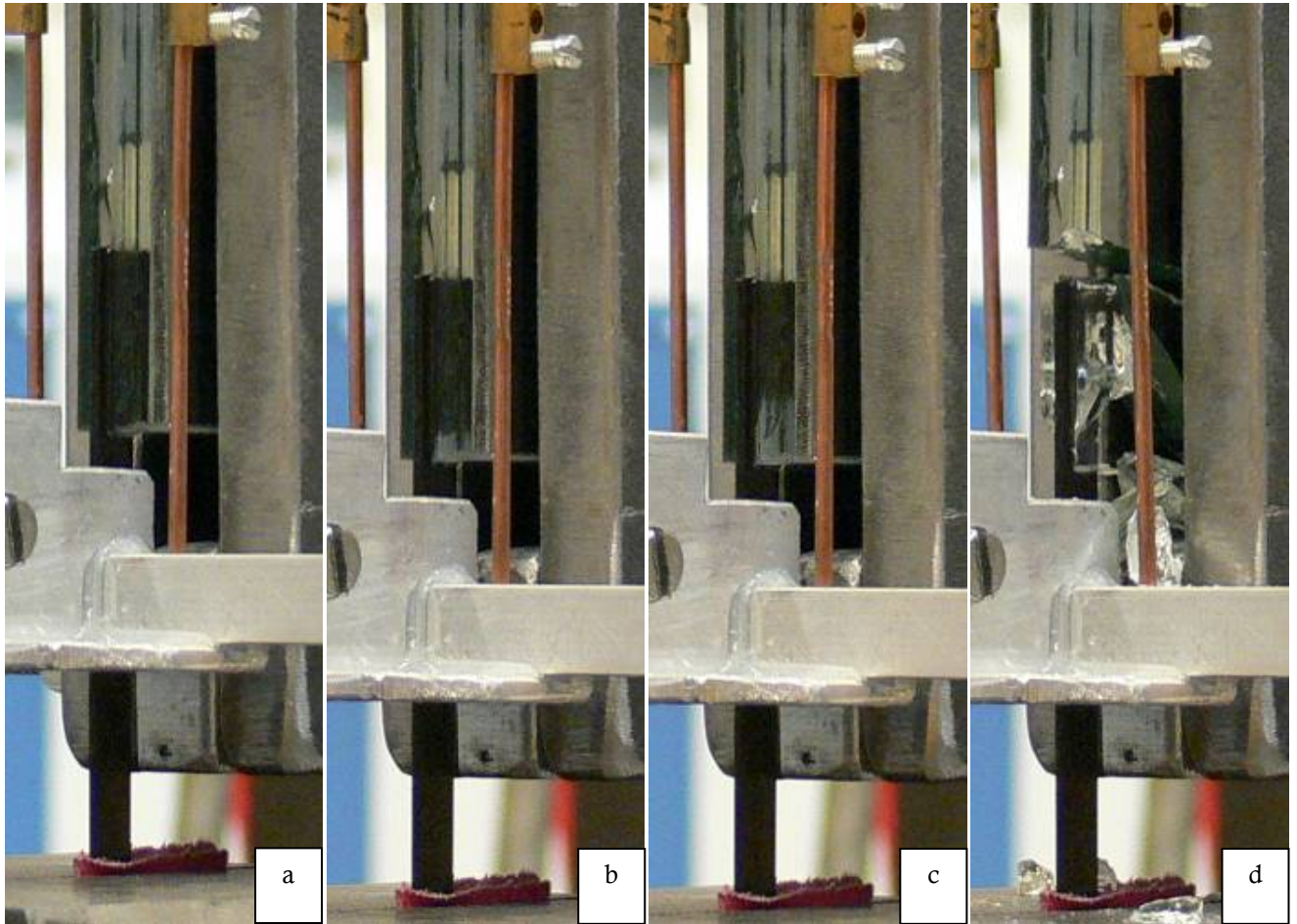


Figure 95,

Above: specimen 2011_35 at different moments during the test.

Right: After the test.

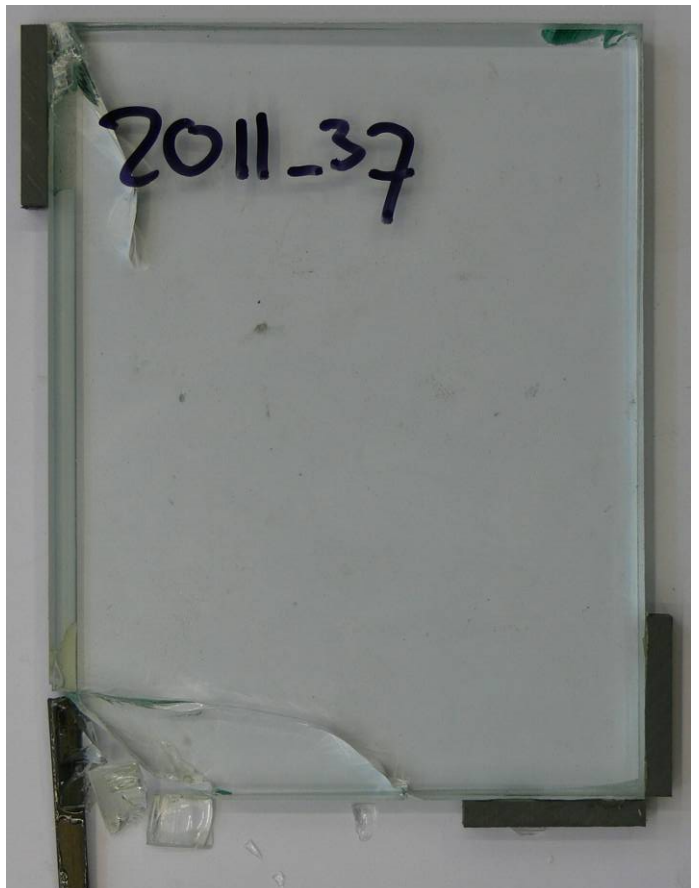


Table 35, summary specimen 2011_37

Specimen	2011_37	
Configuration	0,6x6 0,8x6	[mm]
Support blocks	Perspex	
Positions (Figure 52)	z	[mm]
	6,3	
Anchorage length	20	[mm]
First adhesive failure	3,1	[kN]
First glass failure	-	[kN]
Ultimate strength	4,5	[kN]

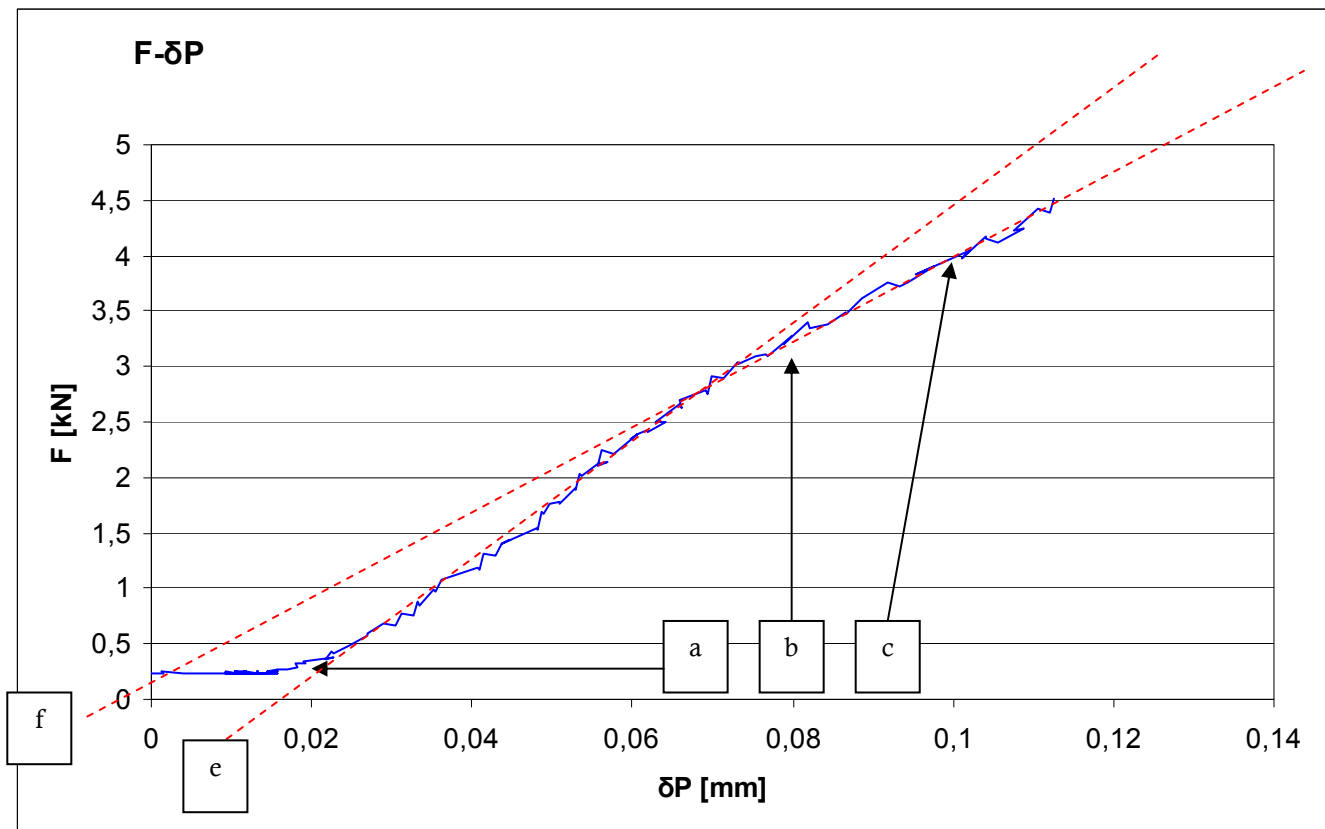


Figure 96, Force displacement diagram for point P for specimen 2011_37.

Specimen 2011_37

The specimen is identical to 2011_16 to 2011_18, but with perspex blocks. The maximum force is considerably higher (4,5kN in stead of 3,3kN average) due to the lack of rotation of the specimen.

At the same time of picture 'b' at a force of 3,1 kN there was a loud crack indicating fracturing of the glass pane. This must have been the crack visible in the top-left corner of the specimen as visible in *Figure 95*.

At this same moment the adhesive started progressive failure and the specimen reduced in stiffness. This is emphasized by lines 'e' and 'f' (*Figure 96*).

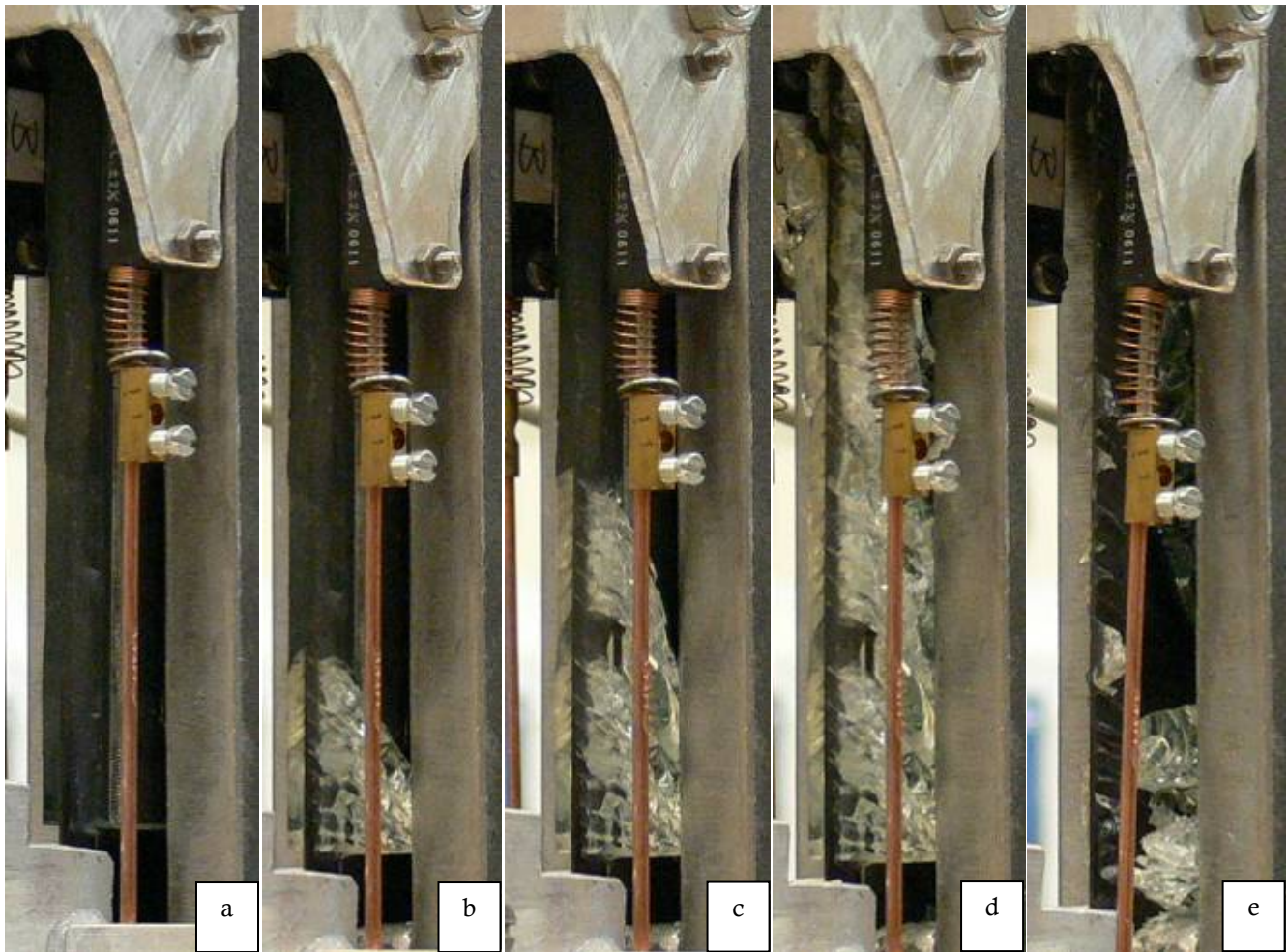


Figure 97, Above: specimen 2011_40 at different moment during the test. Below left: obliqueness of carbon strip, denoted by red lines. Middle: after the test.

Below right: specimen 2011_41 before the test. The red arrows indicate the beginning and end of the fissure.



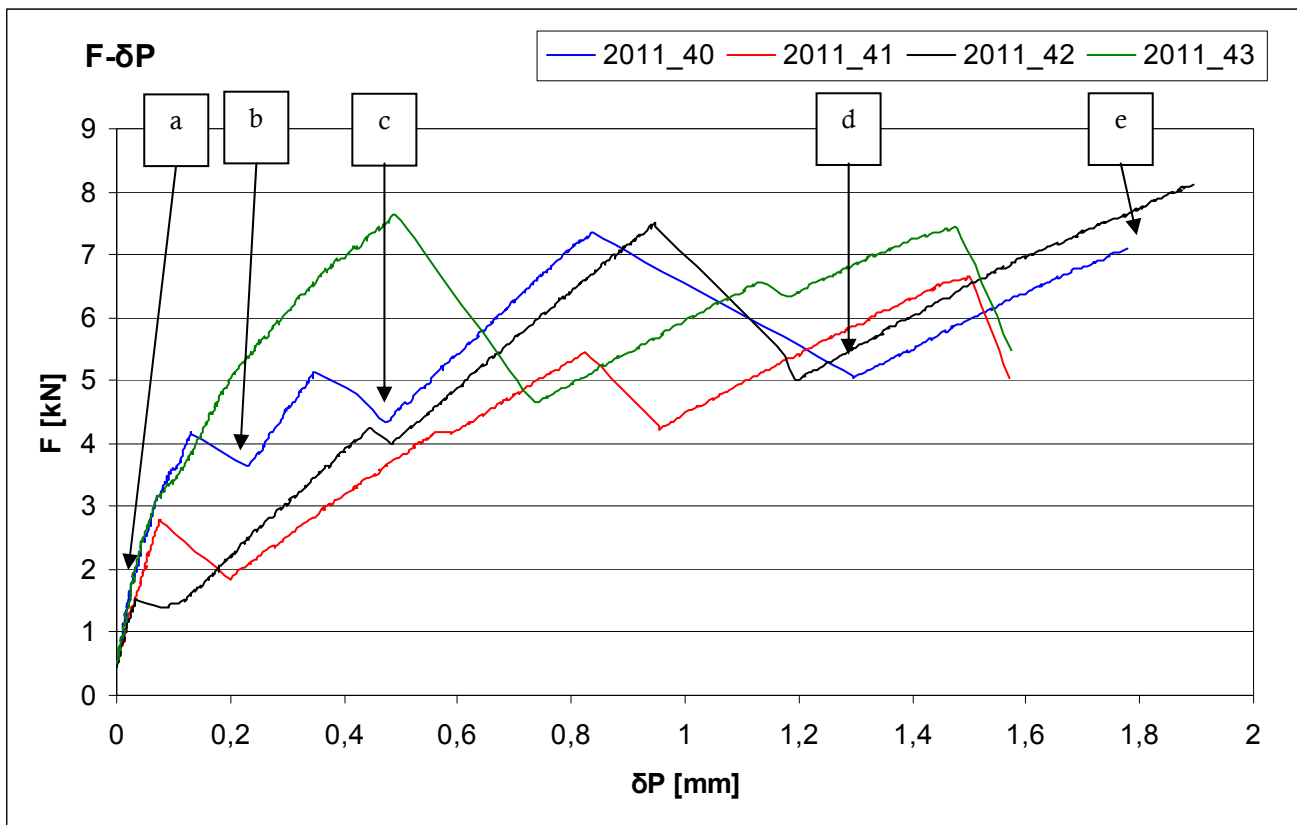


Figure 98, Force-displacement diagram for point P for specimens 2011_40 to 2011_43.

Specimens 2011_40 to 2011_43

The specimens are discussed individually.

2011_40:

The carbon strip is not straight in the groove (see Figure 97, bottom left).

Force buildup until 1,7 kN; the adhesive starts failing at the left side of the glass pane (not visible on photo's). At 4,0 kN the glass pane starts fracturing.

2011_41 & 2011_42 (see next pages):

The failure patterns of the specimens are alike.

To shorten curing time the specimens were cured in an oven under 50°C. Specimens 2011_41 and 42 fractured because of the difference in coefficient of expansion between glass, adhesive and the carbon strip. Both glass panes had a fissure from point P along the groove with a length of 40mm.

Force buildup until approximately 2,5 kN. Then, shortly after small adhesive failure is observed, the glass

fractured over the exact length of the fissure; 40mm. Then progressive fracturing of the glass occurred until total failure.

2011_43 (see next pages):

The specimen is undamaged and the carbon strip is positioned straight up and in the middle of the groove.

Force buildup until adhesive failure starts at 1,7 kN, only on the right side of the carbon strip. At 3,1 kN the left side of the glass cracks for over the same distance as the adhesive failure has progressed; approximately 8mm. Adhesive failure progresses for up to 20mm at 7,5 kN, then a large crack occurs (Figure 99b).

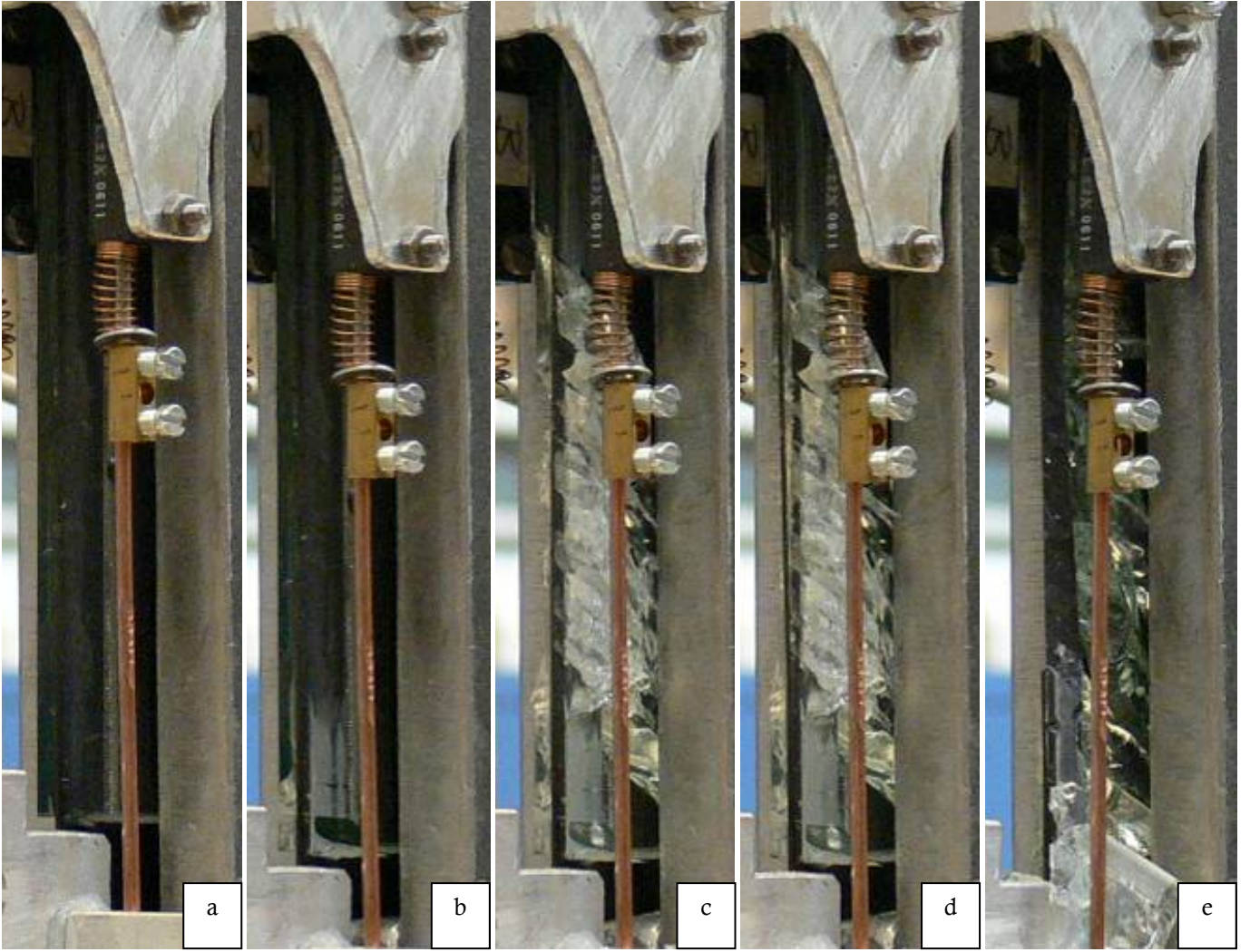


Figure 99, Above: specimen 2011_43 at different moments during the test. Below: specimens after the test.



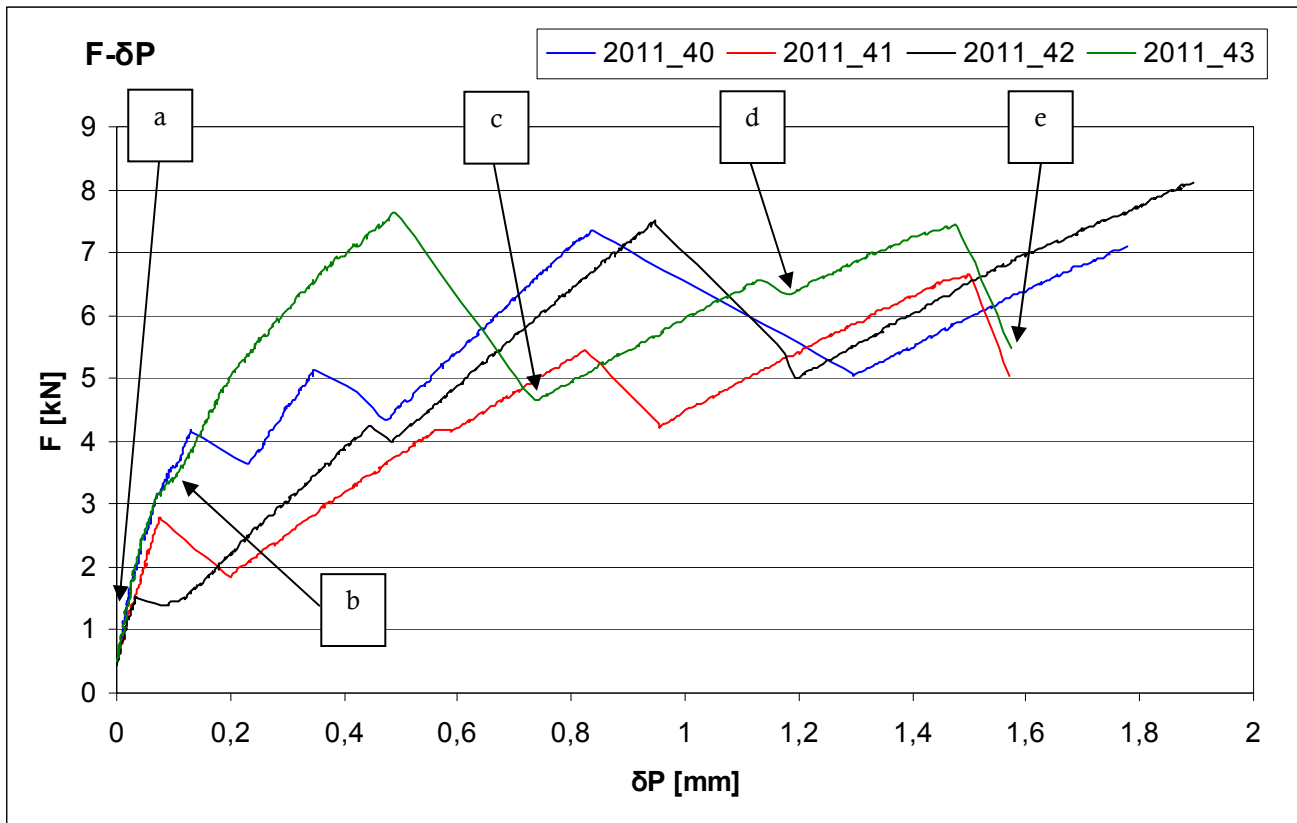


Figure 100, Force-displacement diagram for point P for specimens 2011_40 to 2011_43.

This crack is square to the ‘usual’ cracks and denoted by the red arrow in *Figure 99* (bottom right).

The small fallback denoted by picture ‘d’ is due to the partial failure of the carbon strip.

Summarizing:

All specimens failed due to glass fracturing. It is remarkable that every specimen seems to level out at approximately the same maximum force, regardless of irregularities like fissures (specimens 41 and 42) or obliqueness of the carbon strip (specimen 40). 2011_43,

the specimen that was most perfect by sight; undamaged and the strip straight in the middle of the groove, did not reach the highest force.

Table 36, summary specimens 2011_40 to 2011_43

Specimen	2011_40		2011_41		2011_42		2011_43	
Configuration	6x0,6	[mm]	6x0,6	[mm]	6x0,6	[mm]	6x0,6	[mm]
Support blocks	Perspex		Perspex		Perspex		Perspex	
Positions (<i>Figure 52</i>)	z	[mm]	z	[mm]	z	[mm]	z	[mm]
	3,8		4,3		4,3		2,7	
Anchorage length	150	[mm]	150	[mm]	150	[mm]	150	[mm]
First adhesive failure	1,7	[kN]	2,6	[kN]	2,5	[kN]	1,7	[kN]
First glass failure	4,1	[kN]	2,8	[kN]	1,3	[kN]	3,1	[kN]
Ultimate strength	7,4	[kN]	6,7	[kN]	8,1	[kN]	7,6	[kN]

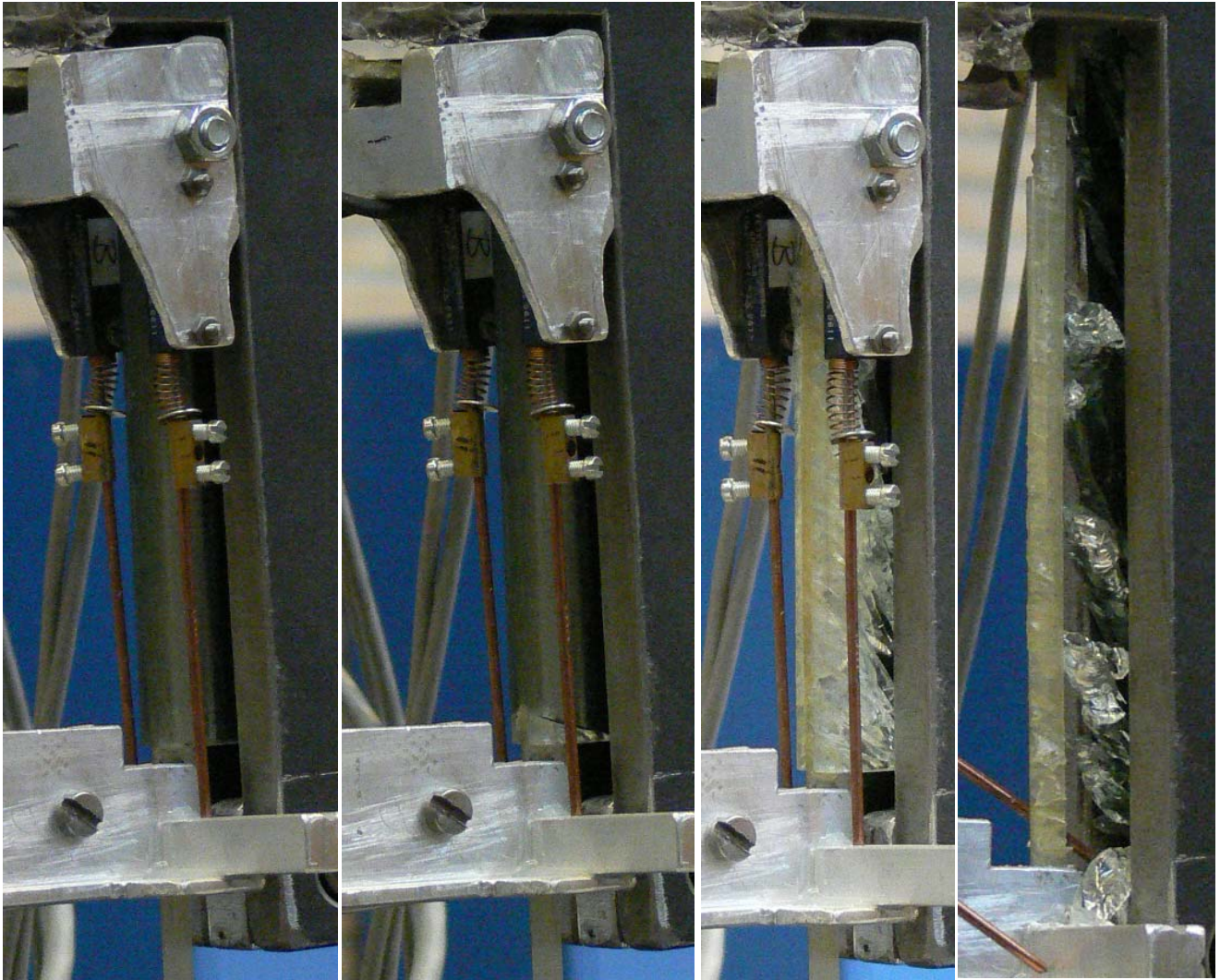


Figure 101, Above: specimen 2011_GF1 at different moments during the test. Below: specimens after the test.



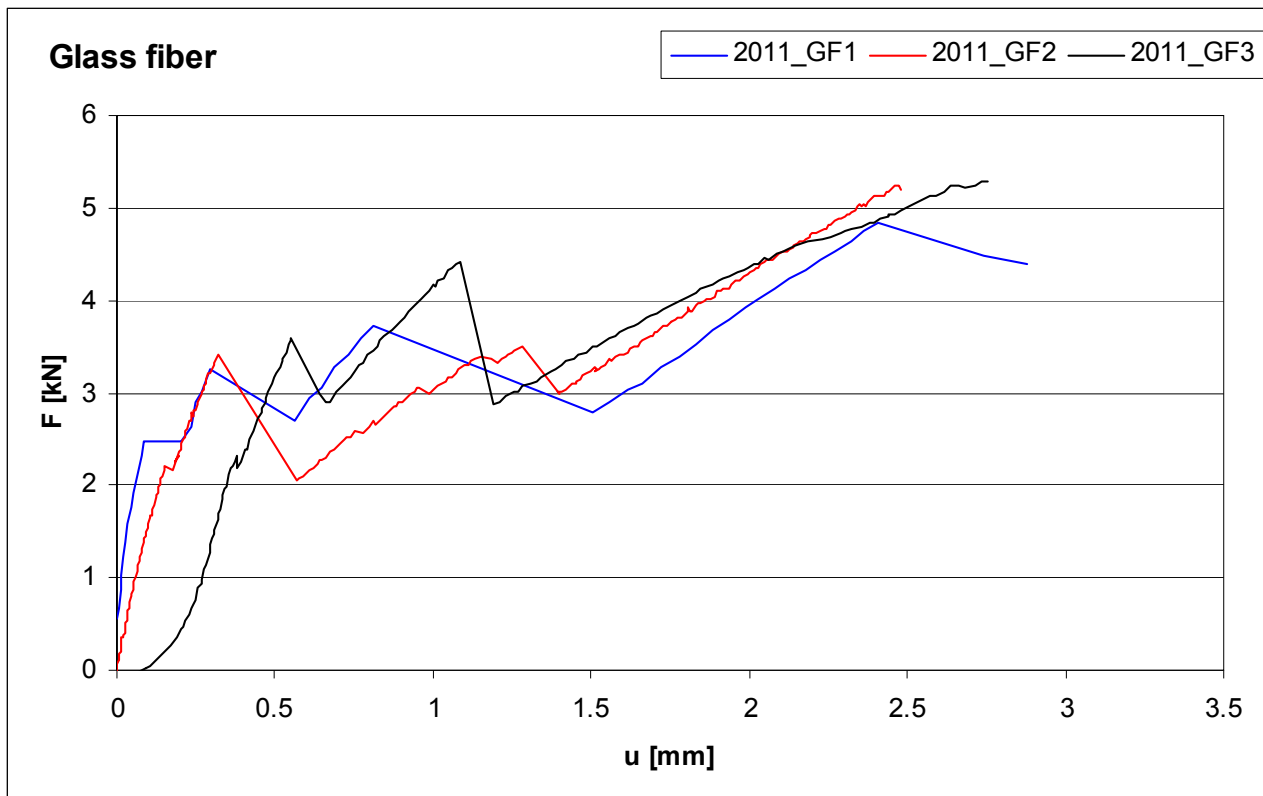


Figure 102, Force-Displacement curves of specimens 2011_GF1/GF3

Specimens 2011_GF1/GF3

The geometry of reinforcement used in specimens 2011_GF1 to 2011_GF3 is comparable to geometry 1, but the reinforcement is not 0,6 mm thick, but 0,8mm. This results in a slightly thinner adhesive layer.

Failure of the adhesive was not observed, the specimens failed due to progressive glass failure.

Table 37, summary specimens 2011_40 to 2011_43

Specimen	2011_GF1		2011_GF2		2011_GF3	
Configuration	6x0,8	[mm]	6x0,8	[mm]	6x0,8	[mm]
Support blocks	Perspex		Perspex		Perspex	
Anchorage length	150	[mm]	150	[mm]	150	[mm]
First adhesive failure	-	[kN]	-	[kN]	-	[kN]
First glass failure	2,5	[kN]	2,1	[kN]	2,2	[kN]
Ultimate strength	4,8	[kN]	5,3	[kN]	5,3	[kN]

5.5 Preliminary beam tests

Introduction & Method

Three glass girders are reinforced and tested by a displacement controlled bending test up to total failure.

Description of adhesives

The first two specimens have been prepared with the adhesive 'DELO Rapid 03 Thix', the third is prepared with Huntsman Araldite 2013.

Rapid 03 Thix is a transparent two-component adhesive with a relatively short handling time of 3-10 minutes (depending on the temperature). It is a relatively tough adhesive with a long elongation at break of 20 %. It can be applied as so called 'ready-mix'. The 'ready-mix' system is based on a special mixing nozzle. The adhesive components are pressed out of a cartridge in the right proportion by a glue squirt into a nozzle. In this nozzle they are mixed together and applied thru a mouth. This mouth can be varied in diameter to adjust the amount of adhesive that is applied.

Araldite 2013 is a grey-colored two-component epoxy adhesive, specially designed for use with stainless steel. It has a curing time of around 30 minutes, which makes it more user-friendly. The adhesive is quite stiff compared to the DELO adhesive although the E-modulus is comparable. Unfortunately the elongation at break is not specified.

Araldite can also be applied as ready-mix.



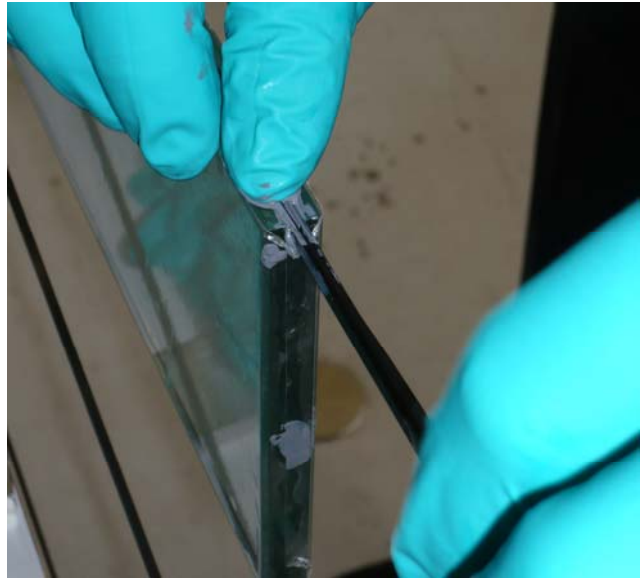
a: Cleaning procedure of glass specimen.



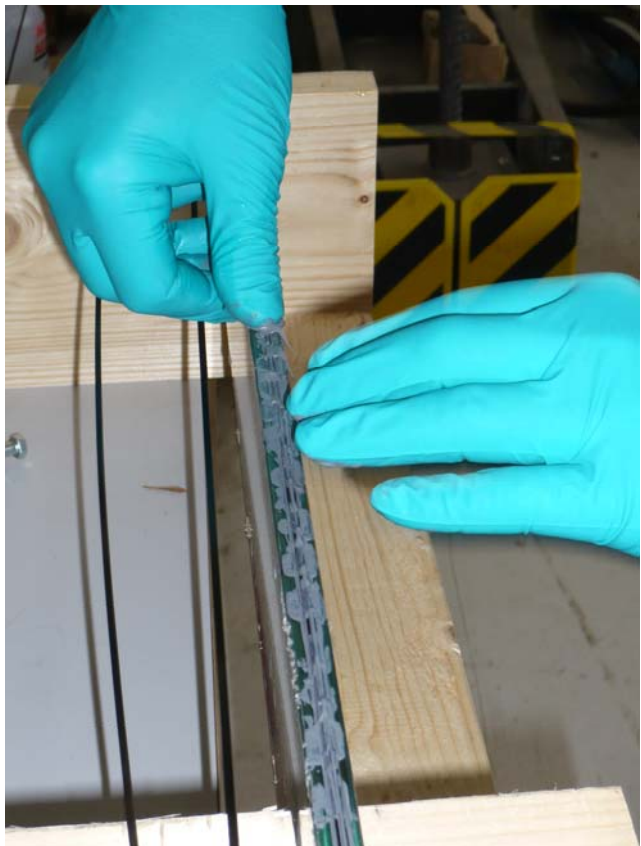
b: Application of adhesive at specimen 3



e: Ready-mix nozzle, adhesive cartridges of both adhesives and glue squirt.



c: Application of reinforcing elements at specimen 3



d: further stage of application of reinforcing elements at specimen 3

Specimen preparation

The side panes of the specimens are covered with thin transparent plastic foil. On this foil horizontal lines are placed with a marker to easily measure crack depth during the experiment. Another important reason for the foil is to prevent glass fractures to explode thru the whole laboratory at breaking. The structural strength of this foil can be neglected compared to the glass.

The specimens as well as the reinforcing elements are thoroughly degreased with an acetone suspension and cleaned with a paper towel.

For gaining practical skill in the gluing, three test samples of MDF (wood) plates with similar groove where made. Relevant observations with this were that the DELO adhesive is indeed quite fast curing. There is not much time between the mixing, or application of the adhesive and the point at which it becomes too tough to handle.

The first specimen is prepared with 2 Ø 2,0 mm Carbon fiber. After the application of the adhesive and the reinforcing elements a tape and a aluminum u-profile is placed over the reinforcement and clamped with frame clamps. After 15 minutes the clamps, profile and tape are removed and the result is visible.

It seems that little or no air has been encapsulated in the specimen.

The other two specimens are done in the same way. The third specimen was bonded with Araldite 2013. This allowed much more handling time which was comfortable but not necessary for these specimens.

The measurements of the groove do not comply with the manufacturers specifications. The measured deviations in dimensions are given in *Table 38*. This does have a large effect on the layer thickness of the adhesive and therefore on the strength of the adhesive bond. This is not studied further.

Table 38, Deviation of SGG Clip-in groove

Measured deviation of SGG clip-in groove			
	Given by manufacturer	Maximum anomaly measured in specimens	Maximum deviation
Depth [mm]	3	3,3	0,3
Width of bottleneck [mm]	2,1	2,25	0,15
Width of inner part [mm]	2,59	N/A	N/A

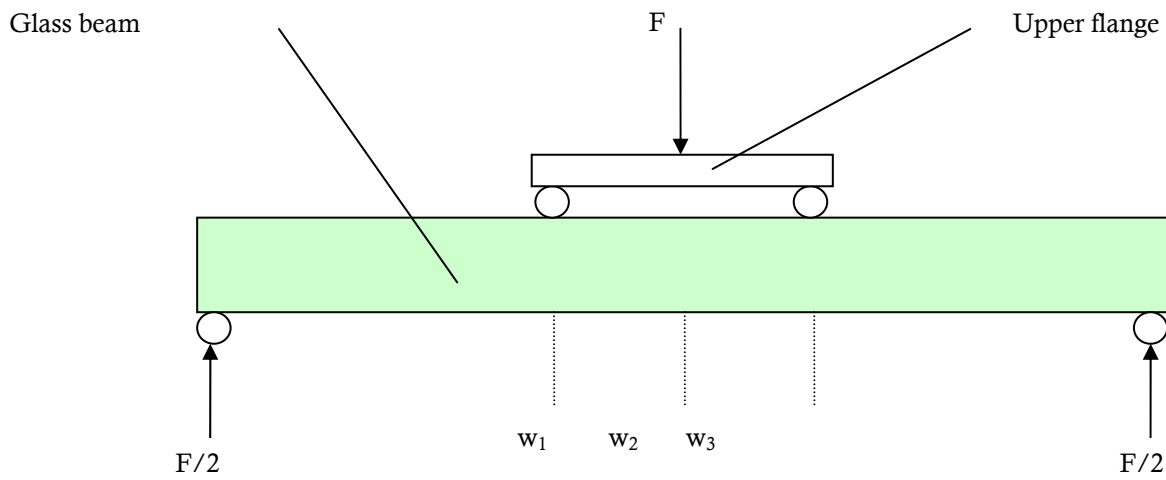
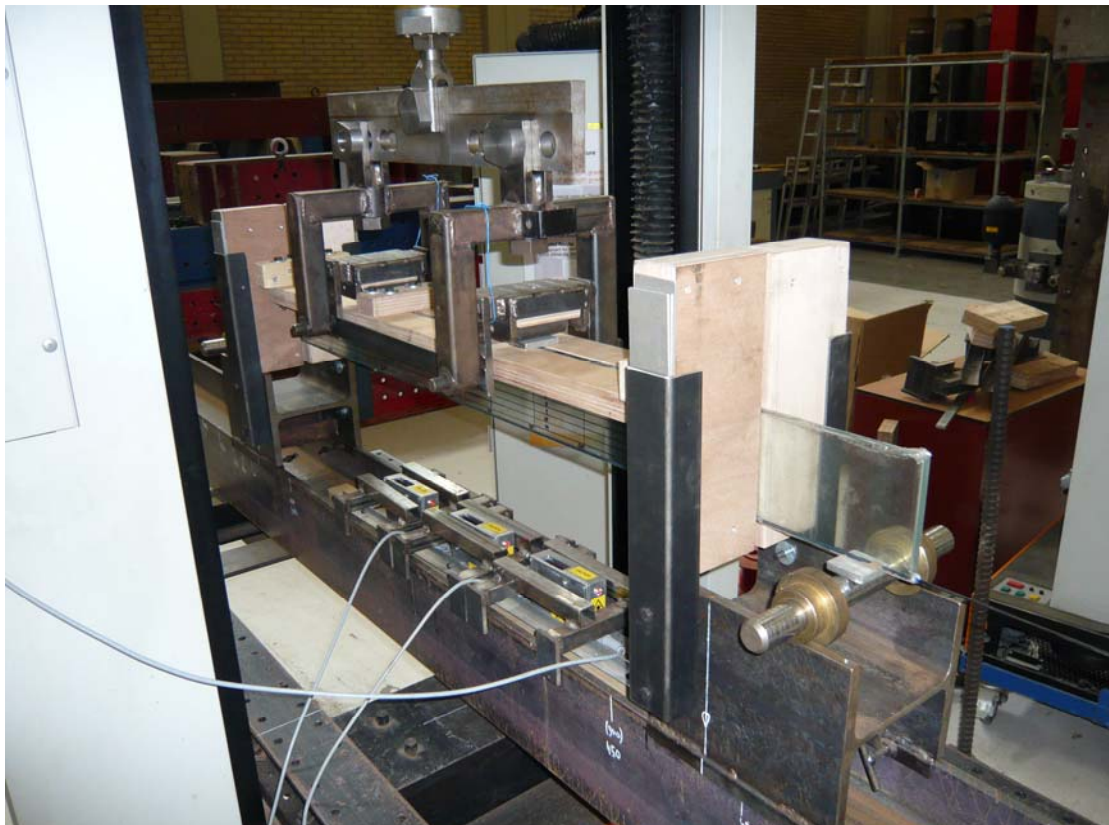


Figure 104, Schematic representation of test setup. The force F is varied to gain a constant displacement of the upper flange of ca. 1 mm/min. The displacement of the girder is measured at three positions: w_1 , w_2 and w_3 .



(Left) Figure 103, Photo of test setup for test 1. This setup was slightly modified after test 1.

Setup

To avoid lateral torsional buckling the top of the girder is fixed horizontally by two wooden flanges that are connected to each other (support 2). These flanges lie on the girder and are not fixed by external forces. This way the glass has a vertical degree of freedom, but is constraint in transversal direction.

Initially the ends of the wooden flanges were connected to external supports (similar to 1 & 3) which were supposed to have a vertical degree of freedom. It turned out that the friction was too large and the support got stuck. Decided was to remove the supports. This way the compression zone of the girder is not constraint globally in horizontal direction by this flange. Buckling of the compression zone however is constraint and transversal support is given by supports X&Y.

To avoid stress peaks where the forces from the four supports are introduced into the glass girder, aluminum plates of 8mm thick are placed between the glass and the steel rolls. This way the pressure is applied over a larger area and the stress is reduced.

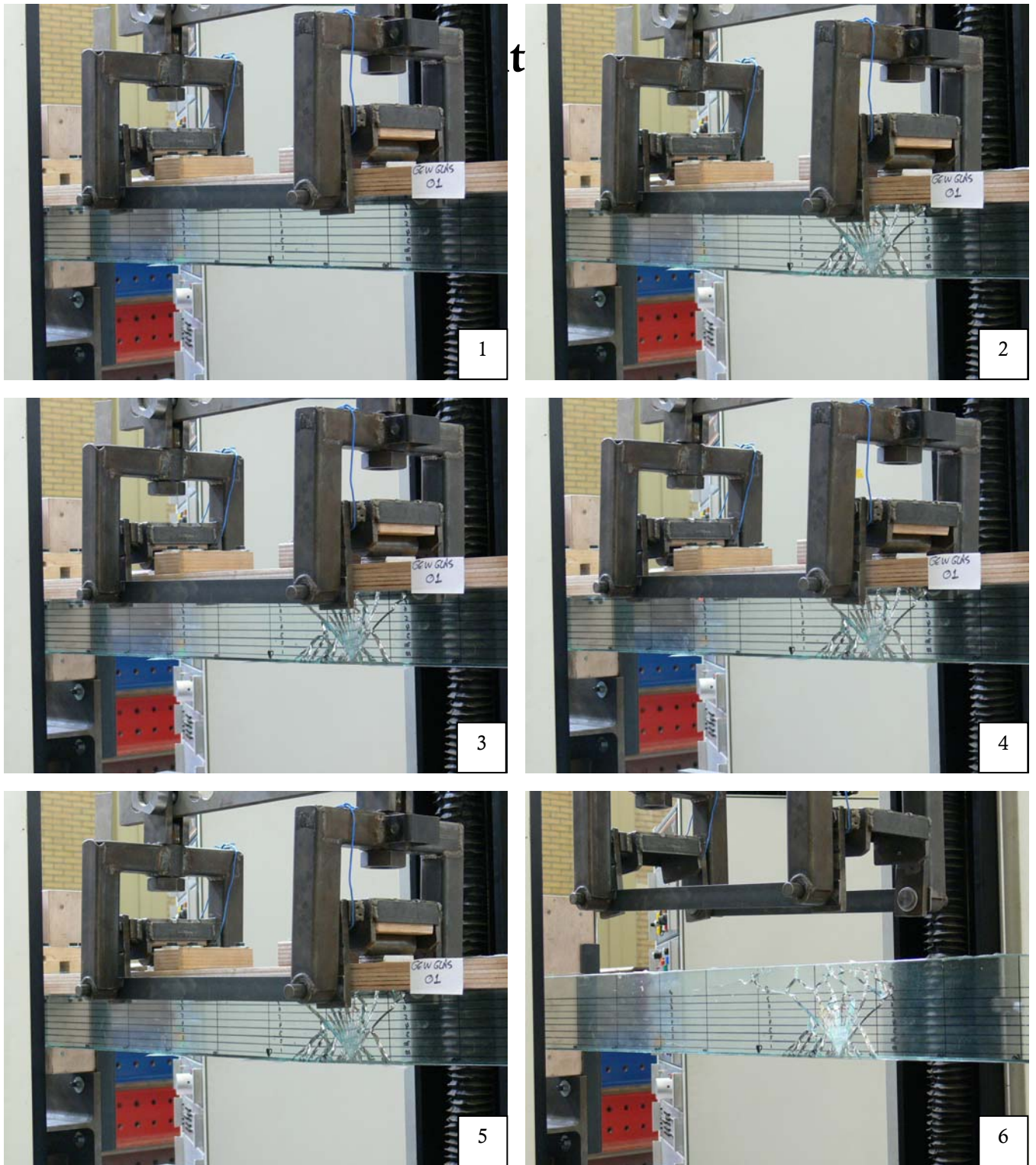
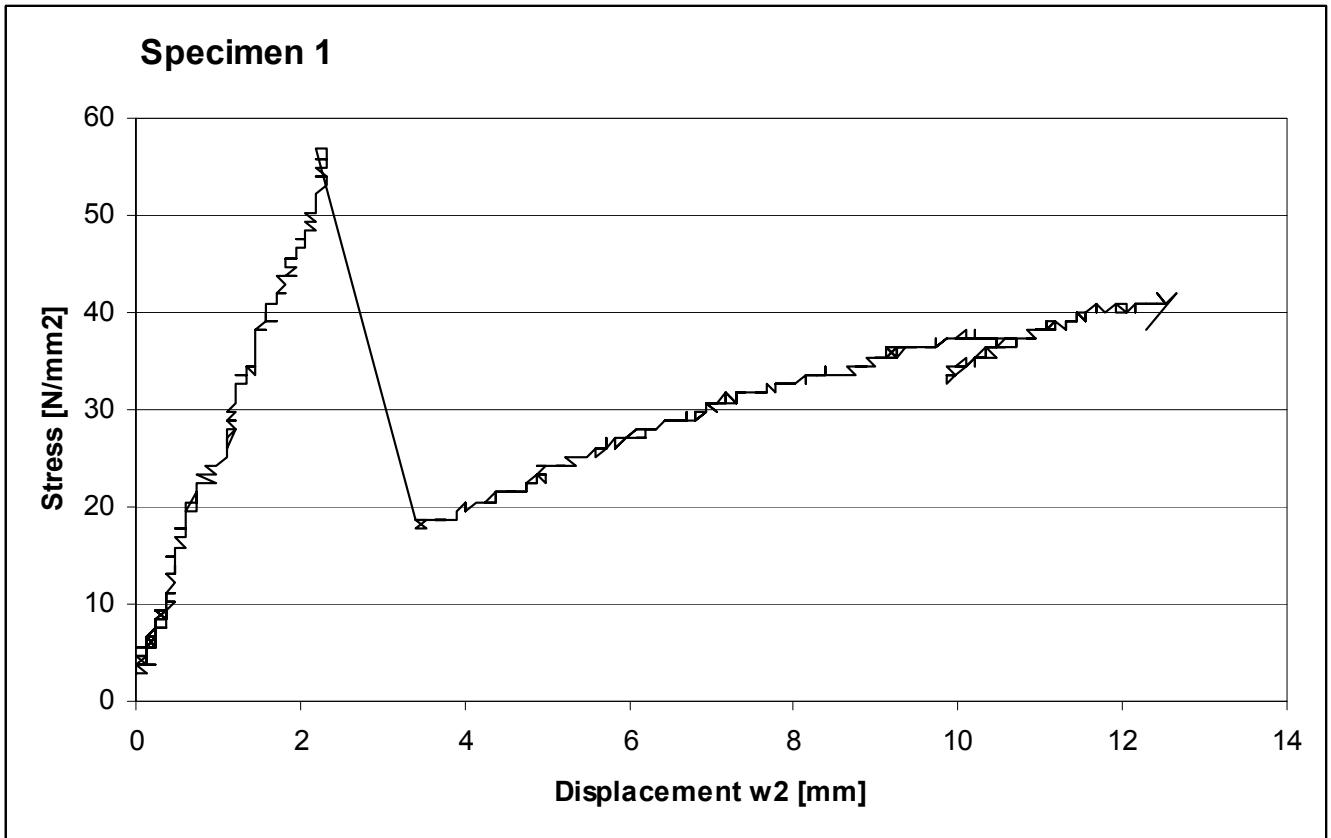


Figure 105, Test 1 on 6 different stages of the test. First crack is visible on picture 2. When examined closely the sliding of the upper support is visible on photos 3, 4 and 5. Photo 6 is taken when the test was complete.



Specimen 1

Dimensions:

Reinforcement:

2x $\text{Ø}2$ mm Carbon Fiber (see *Figure 106*)

Total area of cross section reinforcement:

6,28 mm²

Adhesive:

DELO Rapid 03 Thix

Due to the deviation in the depth of the groove, the surface with which the most superficially positioned carbon fiber rod is bonded to the glass, is not constant.

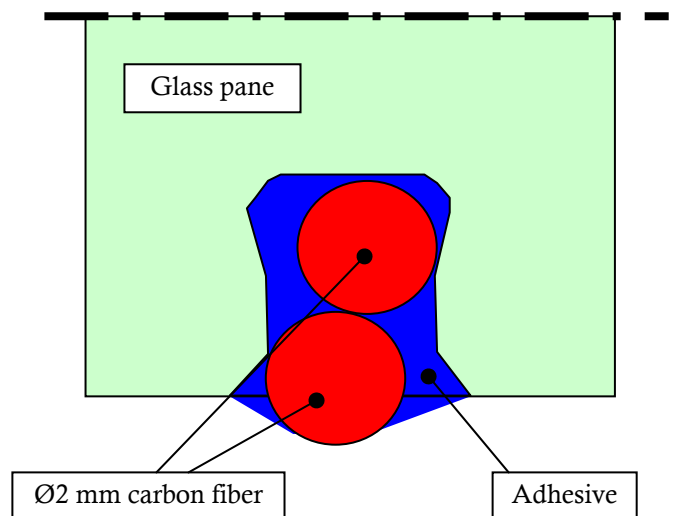


Figure 106, Close-up of bottom of girder cross-section with reinforcement geometry for specimen 1.

Light green: Glass pane.

Blue: Adhesive.

Red: Reinforcement

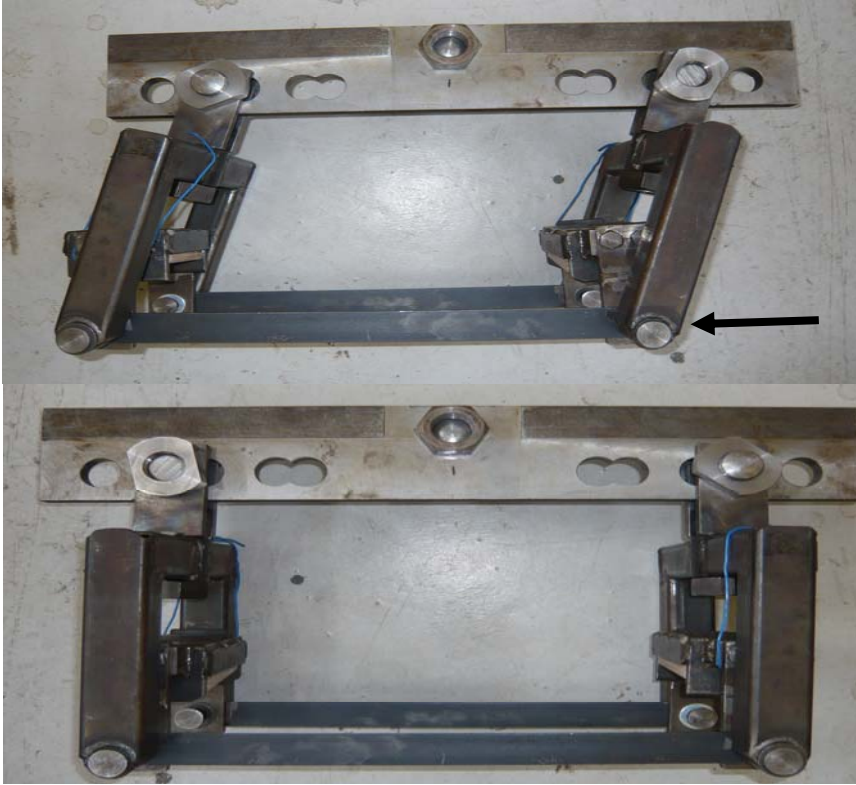


Figure 107, the hinged-roll supports at the top of the girder. Bottom as they should be, on the top is shown how they slid away during the first test (see black arrow).

Results

The girder shows a linear elastic behavior up to initial failure. Then a regression in force and stiffness is observed. The test was aborted because the hinged supports slid horizontally from their position.

Lateral torsional buckling does not occur, so the wooden flanges are performing as planned.

The glass does not fracture at the supports. Introduction of stresses is ok; the stress-peaks are sufficiently reduced by the aluminum plates.

First crack at a force of 5 kN and a displacement of 2,2 mm of the middle of the beam. The crack occurs 150mm from the centre of the beam and has a depth of 115mm, the full height of the beam.

After the first crack the stiffness of the beam is greatly reduced. The applied load falls back to 2,0 kN.

After the first crack the hinged-roll supports are rolling sideways towards the end of the beam (see Figure 107). The test is being aborted at a displacement of 12 mm because the results are no longer relevant. A modification of the test setup is necessary to avoid this in the future.

Discussion

The First crack occurs when the tensile bending stress in the bottom fiber of the girder has reached 57 N/mm². This is comparable to previous tests with glass girders of the same dimensions without a groove milled in the bottom. This implies that the cutting of the SGG Clip-in groove does not have a large negative effect on the practical tensile bending strength of this glass girder.

When the glass fails the girder expands locally due to the cracking. At the vertical supports this could result in clenching. The test results could be influenced by this. To allow vertical freedom several layers of Teflon film should be put between the wood and the glass.



Figure 108, Altered upper support flange.

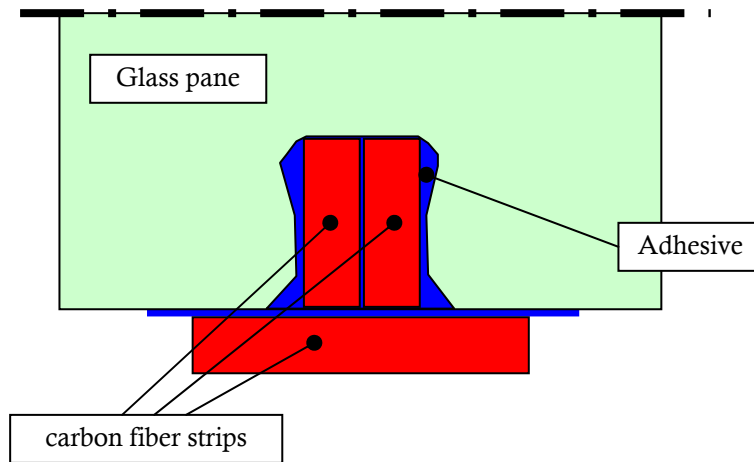


Figure 109, Close-up of bottom of girder cross-section with reinforcement geometry for specimen 2.

Light green: Glass pane.

Blue: Adhesive.

Red: Reinforcement

Specimen 2

Dimensions

Reinforcement:

2x 3x0,8 mm Carbon Fiber

1x 6x0,8 mm Carbon Fiber

Total area of reinforcement cross section:

9,6 mm²

Adhesive:

DELO Rapid 03 Thix

Curing time before testing:

29 hours

Method

To prevent the rolling of the supports after the first crack, the hinged steel construction is simplified (see *Figure 108*).

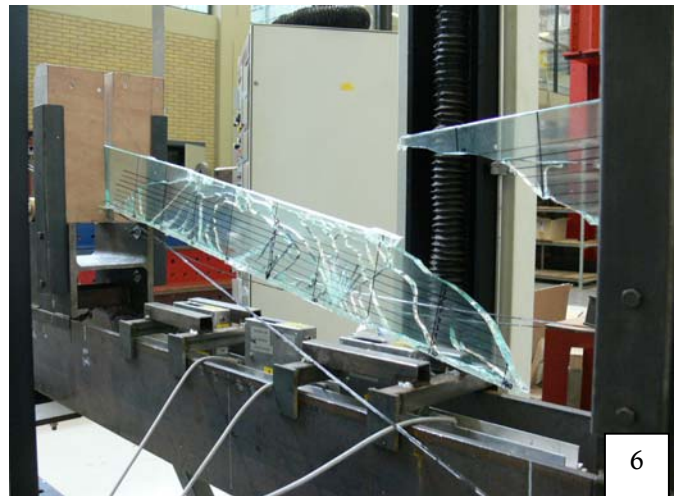


Figure 110, Test 2 on 6 different stages of the test. First crack is visible on picture 2. Further cracks are visible on photos 3 and 4. Total failure has occurred on photo 5. The final result of test 2 is visible on photo 6.

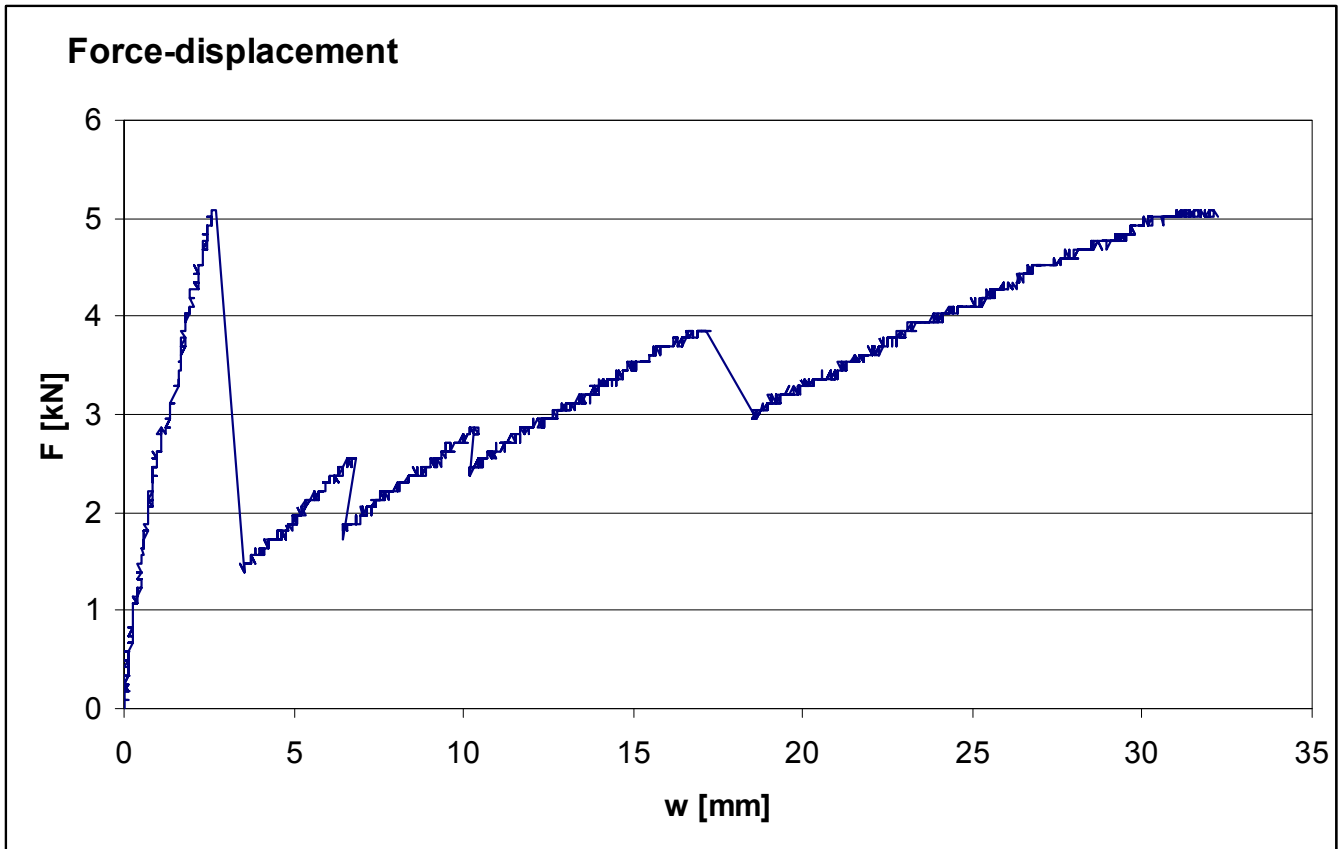


Figure 111, Force- displacement diagram. Each fallback in applied force represents a new crack in the glass.

Results

The girder performs a linear elastic behavior up to initial failure. Then multiple fractures occur until total failure due to shear force.

Lateral torsional buckling is not governing. There is failure due to local stress peaks at the supports.

First crack at 5,0 kN, 3mm deflection, 150 mm right of middle.

Second crack at 2,5 kN, 7,7 mm deflection, 250 mm left of middle.

Third crack at 2,7 kN, 12,5 mm deflection, 450 mm right of middle.

Total collapse at 5,0 kN, 32 mm deflection, 400-500 mm right of middle.

The stiffness of the beam is greatly reduced after the first crack.

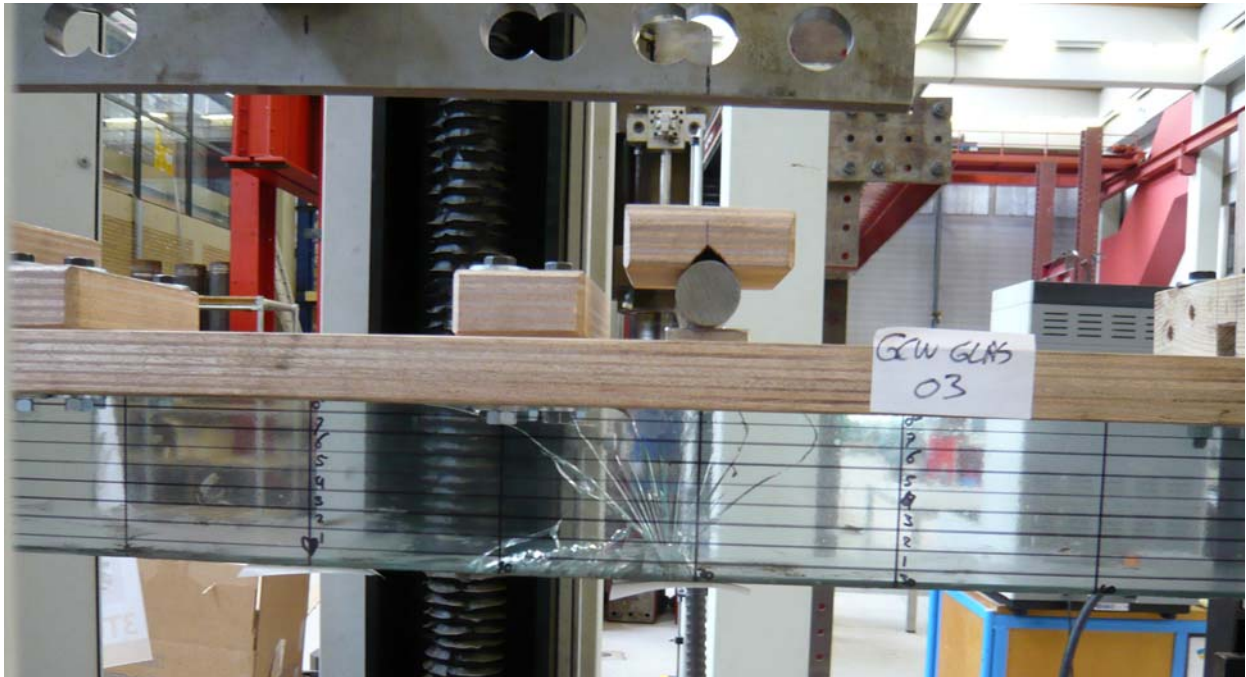


Figure 113, Test 3 at begin.

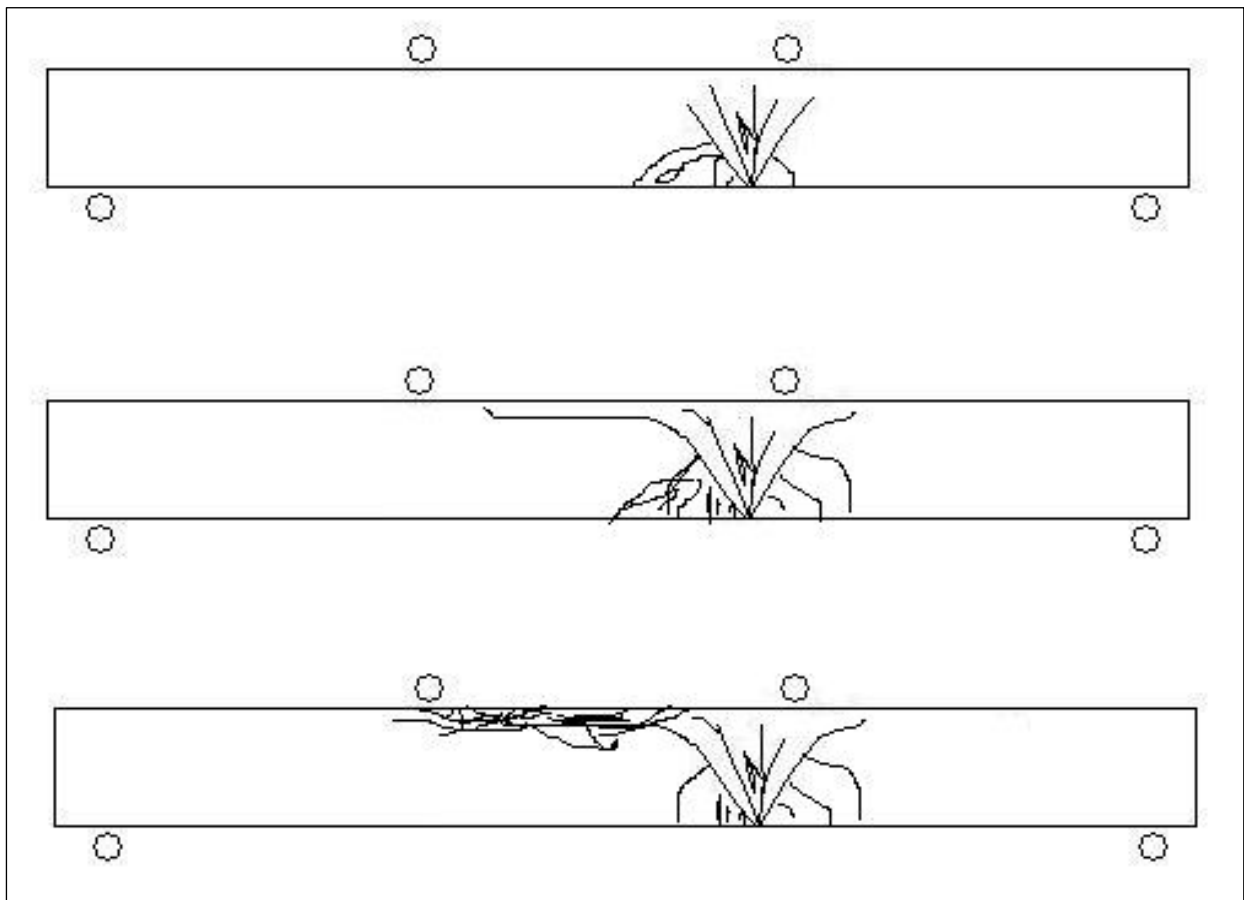


Figure 112, Crack growth during test 3.

Specimen 3

Dimensions

Reinforcement:

2x 3x0,8 mm Carbon Fiber

2x 3x0,13 mm Carbon Fiber

Total area of reinforcement cross section:

5,58 mm²

Adhesive:

Huntsman Araldite 2013

Curing time before testing:

3 days

The setup is enhanced with Teflon foil between the supports and the glass.

A mechanical failure of the testing machine damaged the beam (*Figure 113*). No data was recorded during this. Because it is unsure what load is applied, it is not clear to which degree the specimen is damaged. This makes it useless for testing.

The test is still performed to measure the residual load bearing capacity, but the test can not be regarded as representative.

Results

The first crack occurred at 180 mm from the centre of the girder.

Second crack occurred near first crack at 160 mm from the middle of the beam.

Total collapse due to compressive failure of the top of the girder occurred at an applied force of 2,7 mm and a deflection of 5,7 mm. The point of failure is 170 mm right of the middle, near the upper support.

At the maximum applied load of 2,7 kN the adhesive was still intact.

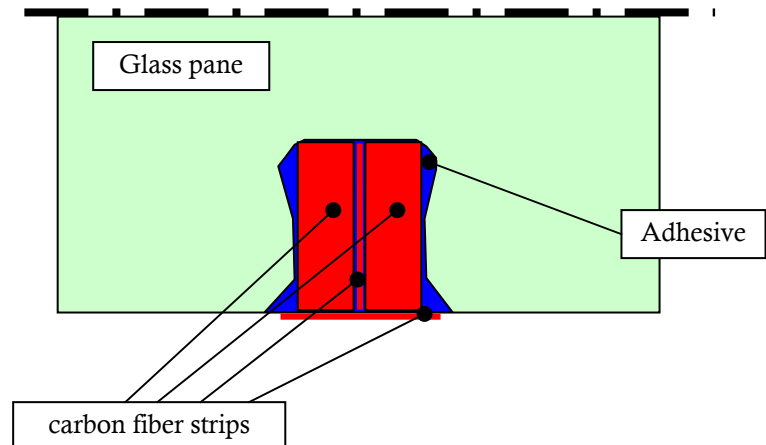


Figure 114, Close-up of bottom of girder cross-section with reinforcement geometry for specimen 2.

Light green: Glass pane.

Blue: Adhesive.

Red: Reinforcement

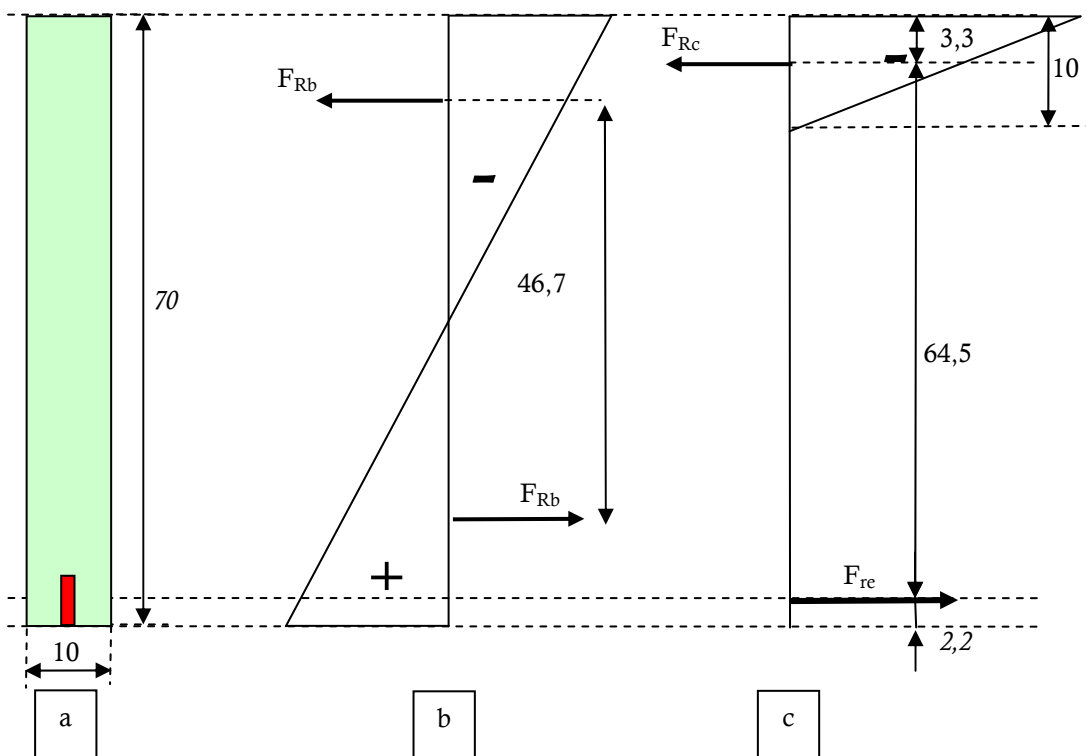
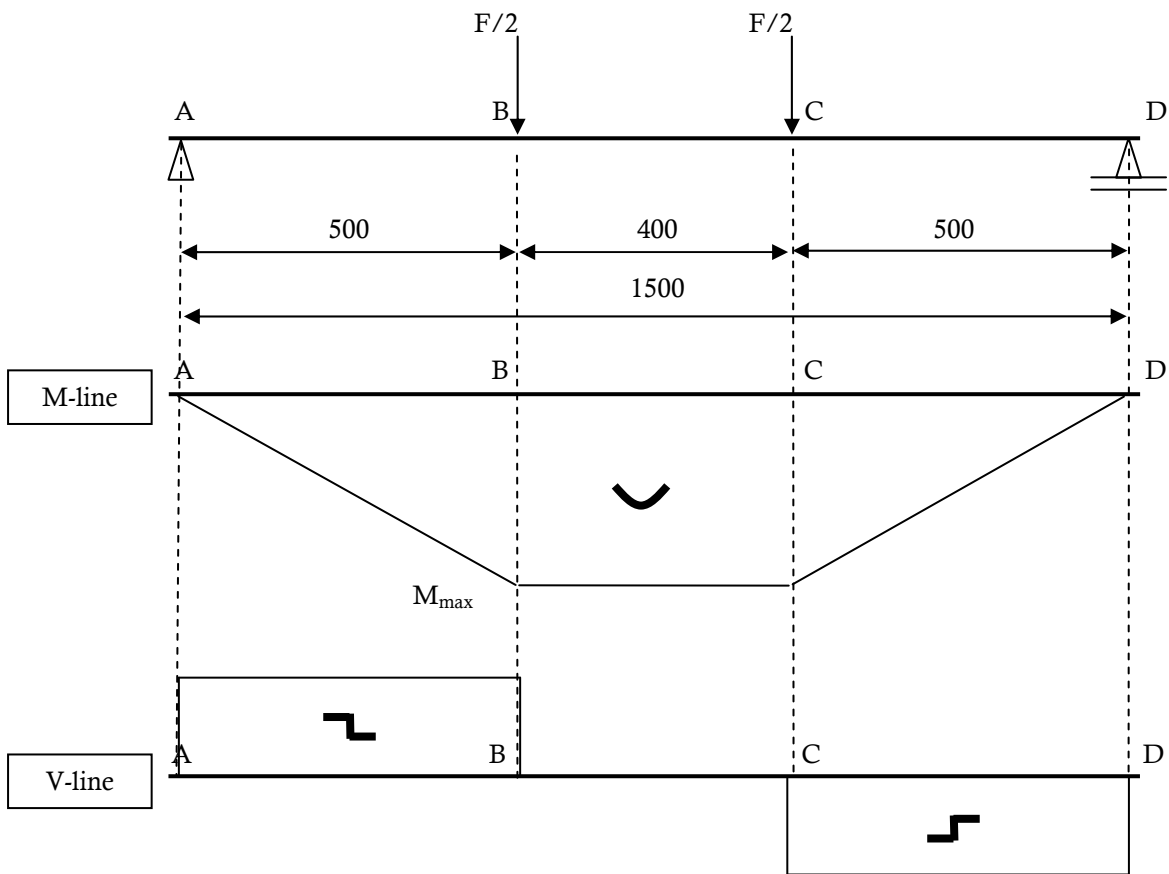


Figure 115 a-c, Stress diagram of girder cross-section between B and C. Measurements in mm.

a: Girder cross-section. Glass fiber in red, glass panes in light green.

b: Stress diagram before initial glass failure

c: Stress diagram at crack location after initial glass failure.

6. Beam tests

Determination relevant moments & stresses

Specimens 70-01 to 70-03

Determination moments of inertia:

$$I_{zz} = \frac{1}{12}bh^3 + e_z^2bh$$

Glass pane:

$$I_{gl.} = \frac{1}{12} * 10 * 70^3 - (\frac{1}{12} * 1,4 * 5,4^3 - 33^2 * 1,4 * 5,4)$$

$$I_{gl.} = 277.582mm^4$$

$$EI_{gl.} = 70.000 * 277.582 = 19,431 * 10^9$$

Reinforcement:

$$I_{re.} = (\frac{1}{12} * b * 6^3) + (33^2 * b * 6)$$

$$I_{re.geom.1} = 3931,2mm^4$$

$$EI_{re.geom.1} = 145.000 * 3931,2 = 570,024 * 10^6$$

Stresses at initial failure, 70-01&70-02:

$$M_i = \frac{1.558N}{2} * 500mm = 389.500Nmm$$

$$M_{i.gl.} = \frac{EI_{gl.}}{EI_{girder}} * M_i = \frac{19,431 * 10^9}{20,000 * 10^9} * 389.500Nmm = 378.399Nmm$$

$$\sigma_{i.gl.} = \frac{M_{i.gl.} * z}{I_{gl.}} = \frac{378.399Nmm * 35mm}{277.582mm^4} = 47,7N/mm^2$$

$$M_{i.re.} = \frac{EI_{re.}}{EI_{girder}} * M_i = \frac{570,024 * 10^6}{20,000 * 10^9} * 389.500Nmm = 11.101Nmm$$

$$\sigma_{i.re.} = \frac{M_{i.re.} * z}{I_{re.}} = \frac{11.101Nmm * 33mm}{3.931mm^4} = 98,8N/mm^2$$

Stresses at initial failure 70-02&70-03

$$M_i = \frac{1.231N}{2} * 500mm = 307.500Nmm$$

$$M_{i.gl.} = \frac{EI_{gl.}}{EI_{girder}} * M_i = \frac{19,431 * 10^9}{20,000 * 10^9} * 307.500Nmm = 298.736Nmm$$

$$\sigma_{i.gl.} = \frac{M_{i.gl.} * z}{I_{gl.}} = \frac{298.736Nmm * 35mm}{277.582mm^4} = 37,7N/mm^2$$

$$M_{i.re.} = \frac{EI_{re.}}{EI_{girder}} * M_i = \frac{570,024 * 10^6}{20,000 * 10^9} * 307.500Nmm = 8.764Nmm$$

$$\sigma_{i.re.} = \frac{M_{i.re.} * z}{I_{re.}} = \frac{8764Nmm * 33mm}{3.931mm^4} = 78,0N/mm^2$$

Maximum stresses 70-02&70-03

$$M_{max} = \frac{2.133N}{2} * 500mm = 533250Nmm$$

$$F_{re} = \frac{533250Nmm}{64,5mm} = 8267N$$

$$\sigma_{re} = \frac{8267N}{0,6mm * 6mm} = 2296N/mm^2$$

Table 39, Dimensions

Glass pane		Reinforcement		Girder	
l	1.500 mm	l	1.500 mm	l	1.500 mm
h	70 mm	h	6 mm	h	71 mm
b	10 mm	b	0,6 mm	b	10 mm
E	$70 * 10^3 N/mm^2$	E	$145 * 10^3 N/mm^2$	EI	$20.000 * 10^6$
I	$278 * 10^3 mm^4$	I	$3.931 mm^4$		
EI	$19.431 * 10^6$	EI	$570 * 10^6$		

Table 40, Relevant bending moments, forces and stresses

70-01			70-02			70-03		
F_i	1558 [#]	[N]	F_i	1558 [#]	[N]	F_i	1231 [#]	[N]
M_i	$0,390 \cdot 10^3$	[Nmm]	M_i	$0,390 \cdot 10^6$	[Nmm]	M_i	$0,308 \cdot 10^6$	[Nmm]
$\sigma_{i.gl.}$	47,7	[N/mm ²]	$\sigma_{i.gl.}$	47,7	[N/mm ²]	$\sigma_{i.gl.}$	37,7	[N/mm ²]
$\sigma_{i.re.}$	98,8	[N/mm ²]	$\sigma_{i.re.}$	98,8	[N/mm ²]	$\sigma_{i.re.}$	78,0	[N/mm ²]
			F_{max}	2,13 [#]	[N]	F_{max}	2,13 [#]	[N]
			M_{max}	$0,533 \cdot 10^6$	[Nmm]	M_{max}	$0,533 \cdot 10^6$	[Nmm]
			$F_{max.re.}$	8267	[N]	$F_{max.re.}$	8267	[N]
			$\sigma_{max.re.}$	2296	[N/mm ²]	$\sigma_{max.re.}$	2296	[N/mm ²]

Sensitivity load cell = 82N

Specimens 70-04 to 70-06

Determination moment of inertia reinforcement:

$$I_{re,geom.1} = \left(\frac{1}{12} * 1,4 * 6^3\right) + (33^2 * 1,4 * 6) = 9172,3mm^4$$

$$EI_{re,geom.1} = 145.000 * 9172,3 = 1330 * 10^6$$

Initial failure:

$$M_i = \frac{1.887N}{2} * 500mm = 471.750Nmm$$

$$M_{i,gl.} = \frac{EI_{gl.}}{EI_{girder}} * M_i = \frac{19,431 * 10^9}{20,760 * 10^9} * 471.750Nmm = 441.526Nmm$$

$$\sigma_{i,gl.} = \frac{M_{i,gl.} * z}{I_{gl.}} = \frac{441.526Nmm * 35mm}{277.582mm^4} = 55,7 N/mm^2$$

$$M_{i,re.} = \frac{EI_{re.}}{EI_{girder}} * M_i = \frac{1.330 * 10^6}{20,760 * 10^9} * 471.750Nmm = 30.223Nmm$$

$$\sigma_{i,re.} = \frac{M_{i,re.} * z}{I_{re.}} = \frac{30.223Nmm * 33mm}{9.172mm^4} = 108,7 N/mm^2$$

Ultimate failure, 70-04:

$$M_{max} = \frac{2.871N}{2} * 500mm = 717.800Nmm$$

$$F_{re} = \frac{717.800Nmm}{64,5mm} = 11.128N$$

$$\sigma_{re} = \frac{11.128N}{1,4mm * 6mm} = 1325 N/mm^2$$

Ultimate failure, 70-05:

$$M_{max} = \frac{3.117N}{2} * 500mm = 779.328Nmm$$

$$F_{re} = \frac{779.328Nmm}{64,5mm} = 12.082N$$

$$\sigma_{re} = \frac{12.082N}{1,4mm * 6mm} = 1438 N/mm^2$$

Ultimate failure, 70-06:

$$M_{max} = \frac{3.035N}{2} * 500mm = 758.818Nmm$$

$$F_{re} = \frac{758.818Nmm}{64,5mm} = 11.765N$$

$$\sigma_{re} = \frac{11.765N}{1,4mm * 6mm} = 1401 N/mm^2$$

Table 42, Dimensions

Glass pane		Reinforcement		Girder	
1	1.500 mm	1	1.500 mm	1	1.500 mm
b	10 mm	h	6 mm	h	71 mm
h	70 mm	b	1,4 mm	b	10 mm
E	$70 * 10^3 N/mm^2$	E	$145 * 10^3 N/mm^2$		
I	$278 * 10^3 mm^4$	I	$9172 mm^4$		
EI	$19.431 * 10^6$	EI	$1330 * 10^6$	EI	$20.760 * 10^6$

Table 42, Relevant bending moments, forces and stresses

70-04			70-05			70-06		
F_i	1887 [#]	[N]	F_i	1887 [#]	[N]	F_i	1887 [#]	[N]
M_i	$0,472 * 10^6$	[Nmm]	M_i	$0,472 * 10^6$	[Nmm]	M_i	$0,472 * 10^6$	[Nmm]
$\sigma_{i,gl.}$	55,7	[N/mm ²]	$\sigma_{i,gl.}$	55,7	[N/mm ²]	$\sigma_{i,gl.}$	55,7	[N/mm ²]
$\sigma_{i,re.}$	108,7	[N/mm ²]	$\sigma_{i,re.}$	108,7	[N/mm ²]	$\sigma_{i,re.}$	108,7	[N/mm ²]
F_{max}	2871 [#]	[N]	F_{max}	3120 [#]	[N]	F_{max}	3036 [#]	[N]
M_{max}	$0,718 * 10^6$	[Nmm]	M_{max}	$0,779 * 10^6$	[Nmm]	M_{max}	$0,759 * 10^6$	[Nmm]
$F_{max,re.}$	11.129	[N]	$F_{max,re.}$	12.082	[N]	$F_{max,re.}$	11.764	[N]
$\sigma_{max,re.}$	1325	[N/mm ²]	$\sigma_{max,re.}$	1438	[N/mm ²]	$\sigma_{max,re.}$	1401	[N/mm ²]

Sensitivity load cell = 82N

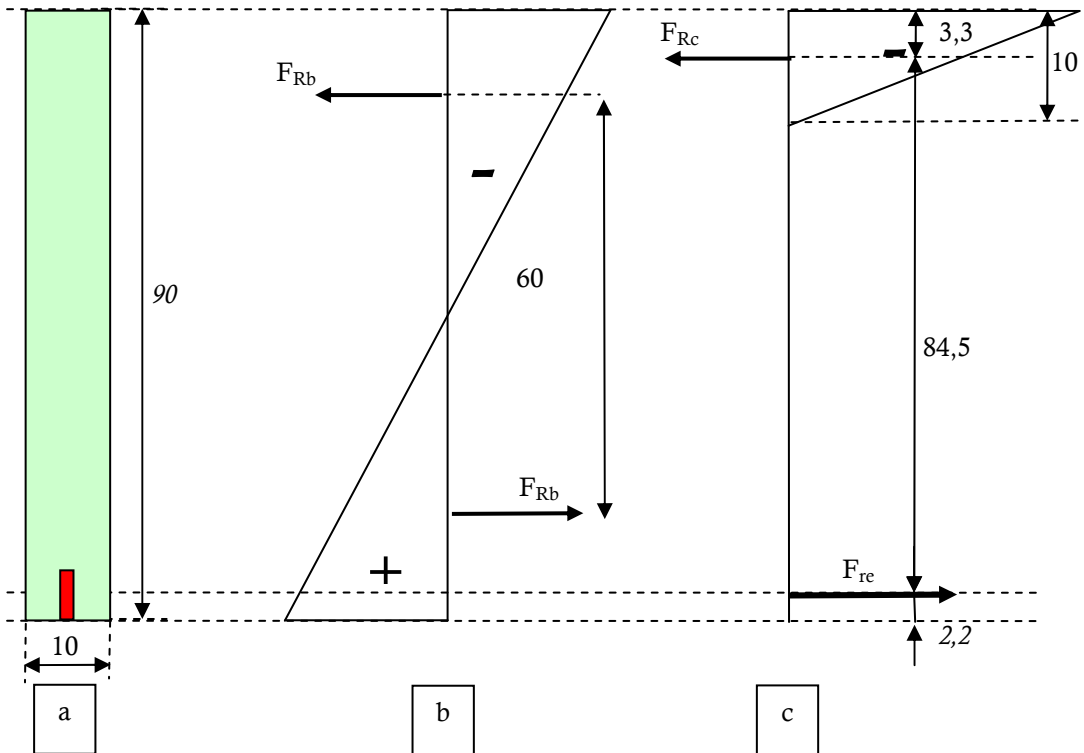


Figure 116 a-c, Stress diagram of girder cross-section. Measurements in mm

a: Girder cross-section. Glass fiber in red, glass panes in light green.

b: Stress diagram before initial glass failure

c: Stress diagram at crack location after initial glass failure.

Table 44, Dimensions

Glass pane		Reinforcement		Girder	
l	1.500 mm	l	1.500 mm	l	1.500 mm
h	90 mm	h	6 mm	h	91 mm
B	10 mm	b	1,4 mm	b	10 mm
E	$70 \cdot 10^3 \text{ N/mm}^2$	E	$145 \cdot 10^3 \text{ N/mm}^2$	EI	$43,8 \cdot 10^9$
I	$594 \cdot 10^3 \text{ mm}^4$	I	15.557 mm^4		
EI	$41,6 \cdot 10^9$	EI	$2,256 \cdot 10^9$		

Table 44, Relevant bending moments, forces and stresses

90-01			90-02			90-03		
F_i	2.871 [#]	[N]	F_i	3117 [#]	[N]	F_i	2.871 [#]	[N]
M_i	$718 \cdot 10^3$	[Nmm]	M_i	$779 \cdot 10^3$	[Nmm]	M_i	$718 \cdot 10^3$	[Nmm]
$\sigma_{i.gl.}$	51,6	[N/mm ²]	$\sigma_{i.gl.}$	56,0	[N/mm ²]	$\sigma_{i.gl.}$	51,6	[N/mm ²]
$\sigma_{i.re.}$	102	[N/mm ²]	$\sigma_{i.re.}$	111	[N/mm ²]	$\sigma_{i.re.}$	102	[N/mm ²]
F_{max}	3.281 [#]	[N]	F_{max}	3.035 [#]	[N]	F_{max}	3.199 [#]	[N]
M_{max}	$820 \cdot 10^3$	[Nmm]	M_{max}	$759 \cdot 10^3$	[Nmm]	M_{max}	$800 \cdot 10^3$	[Nmm]
$F_{max.re.}$	9.707	[N]	$F_{max.re.}$	8.979	[N]	$F_{max.re.}$	9.464	[N]
$\sigma_{max.re.}$	1.156	[N/mm ²]	$\sigma_{max.re.}$	1.069	[N/mm ²]	$\sigma_{max.re.}$	1.127	[N/mm ²]

Sensitivity of the load cell is 82N

Specimens 90-01 to 90-03

Determination moments of inertia:

$$I_{zz} = \frac{1}{12}bh^3 + e_z^2bh$$

Glass pane:

$$I_{gl.} = \frac{1}{12} * 10 * 90^3 - (\frac{1}{12} * 1,4 * 5,4^3 + 43^2 * 1,4 * 5,4)$$

$$I_{gl.} = 607.500 - 13960 = 593.539mm^4$$

$$EI_{gl.} = 70.000 * 593.539 = 41,55 * 10^9$$

Reinforcement:

$$I_{re.} = (\frac{1}{12} * 1,4 * 6^3) + (43^2 * 1,4 * 6)$$

$$I_{re.} = 15.557mm^4$$

$$EI_{re.} = 145.000 * 15.557 = 2,256 * 10^9$$

Girder:

$$EI_{girder} = EI_{gl.} + EI_{re.} = 41,55 * 10^9 + 2,256 * 10^9 = 43,81 * 10^9$$

Specimen 90-01:

$$M_i = \frac{2.871N}{2} * 500mm = 717.750Nmm$$

$$M_{i.gl.} = \frac{EI_{gl.}}{EI_{girder}} * M_i = \frac{41,55 * 10^9}{43,81 * 10^9} * 717.750Nmm = 680.723Nmm$$

$$\sigma_{i.gl.} = \frac{M_{i.gl.} * z}{I_{gl.}} = \frac{680.723Nmm * 45mm}{593.539mm^4} = 51,6 N/mm^2$$

$$M_{i.re.} = \frac{EI_{re.}}{EI_{girder}} * M_i = \frac{2,256 * 10^9}{43,81 * 10^9} * 717.750Nmm = 36.960Nmm$$

$$\sigma_{i.re.} = \frac{M_{i.re.} * z}{I_{re.}} = \frac{36.960Nmm * 43mm}{15.557mm^4} = 102,2 N/mm^2$$

$$M_{max} = \frac{3.281N}{2} * 500mm = 820.250Nmm$$

$$F_{re} = \frac{820.250Nmm}{84,5mm} = 9.707N$$

$$\sigma_{re} = \frac{9.707N}{1,4mm * 6mm} = 1156 N/mm^2$$

Specimen 90-02:

$$M_i = \frac{3117N}{2} * 500mm = 779.250Nmm$$

$$M_{i.gl.} = \frac{EI_{gl.}}{EI_{girder}} * M_i = \frac{41,55 * 10^9}{43,81 * 10^9} * 779.250Nmm = 739.051Nmm$$

$$\sigma_{i.gl.} = \frac{M_{i.gl.} * z}{I_{gl.}} = \frac{739.051Nmm * 45mm}{593.539mm^4} = 56,03 N/mm^2$$

$$M_{i.re.} = \frac{EI_{re.}}{EI_{girder}} * M_i = \frac{2,256 * 10^9}{43,81 * 10^9} * 779.250Nmm = 40.128Nmm$$

$$\sigma_{i.re.} = \frac{M_{i.re.} * z}{I_{re.}} = \frac{40.128Nmm * 43mm}{15.557mm^4} = 111 N/mm^2$$

$$M_u = \frac{3.035N}{2} * 500mm = 758.750Nmm$$

$$F_{re} = \frac{758.750Nmm}{84,5mm} = 8.979N$$

$$\sigma_{re} = \frac{8.979N}{1,4mm * 6mm} = 1.069 N/mm^2$$

Specimen 90-03:

$$M_i = \frac{2.871N}{2} * 500mm = 717.750Nmm$$

$$M_{i.gl.} = \frac{EI_{gl.}}{EI_{girder}} * M_i = \frac{41,55 * 10^9}{43,81 * 10^9} * 717.750Nmm = 680.723Nmm$$

$$\sigma_{i.gl.} = \frac{M_{i.gl.} * z}{I_{gl.}} = \frac{680.723Nmm * 45mm}{593.539mm^4} = 51,6 N/mm^2$$

$$M_{i.re.} = \frac{EI_{re.}}{EI_{girder}} * M_i = \frac{2,256 * 10^9}{43,81 * 10^9} * 717.750Nmm = 36.960Nmm$$

$$\sigma_{i.re.} = \frac{M_{i.re.} * z}{I_{re.}} = \frac{36.960Nmm * 43mm}{15.557mm^4} = 102 N/mm^2$$

$$M_u = \frac{3.199N}{2} * 500mm = 799.750Nmm$$

$$F_{re} = \frac{799.750Nmm}{84,5mm} = 9.464N$$

$$\sigma_{re} = \frac{9.464N}{1,4mm * 6mm} = 1.127 N/mm^2$$

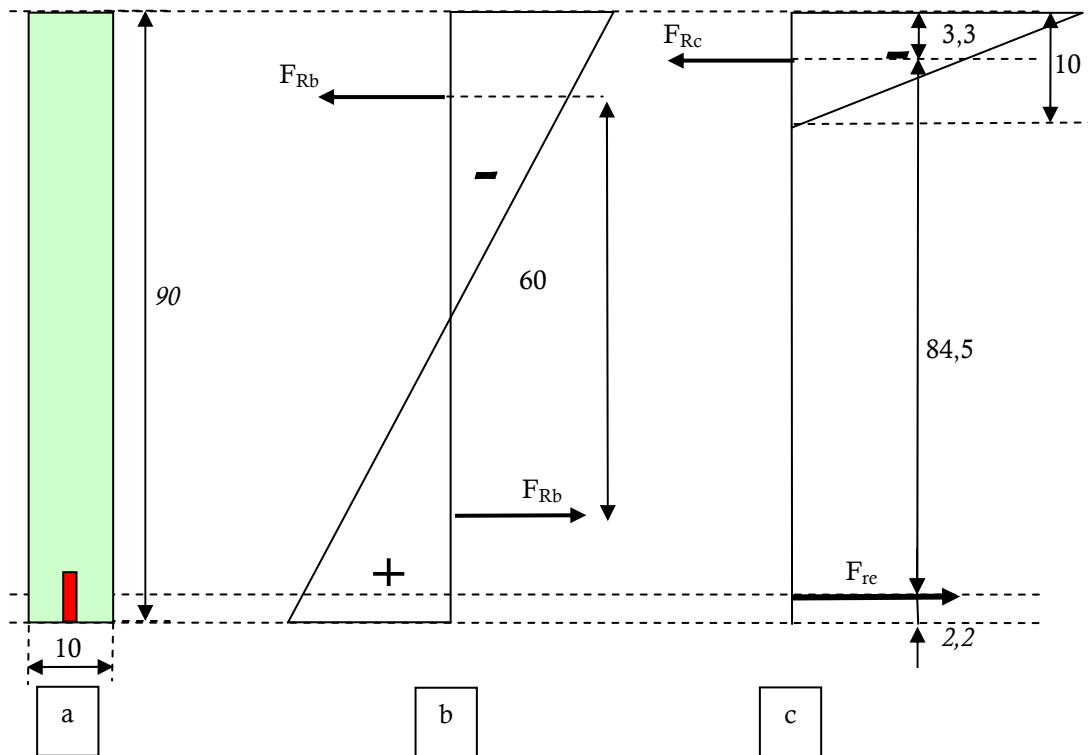


Figure 118 a-c, Stress diagram of girder cross-section. Measurements in mm

a: Girder cross-section. Glass fiber in red, glass panes in light green.

b: Stress diagram before initial glass failure

c: Stress diagram at crack location after initial glass failure.

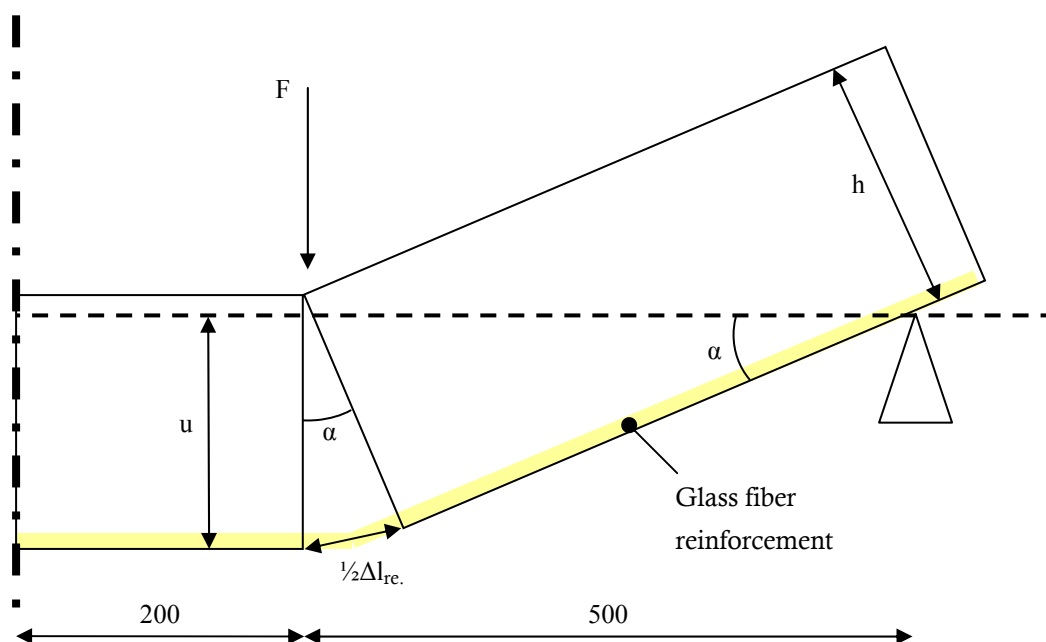


Figure 117, Schematic representation of half of girder in U.L.S.

Hypothesis for additional tests

90mm girder with glass fiber reinforcement

Estimation is made for the ultimate deflection and residual load bearing capacity of the 90mm girder reinforced with a 0,8x6mm glass fiber strip:

Assuming that:

- The fracture pattern will be comparable to specimens 90-01/03
- The E-modulus of the reinforcement is 53.000 N/mm²
- The strength of the connection of the reinforcement to the glass is will allow a tensile force in the reinforcement of 5.500N.
- Shear force will become governing above 3,0 kN.

Initial failure

Compare the results of specimens 70-01/02 to 70-04/06. The initial failure moment of geometry 1 is 18% lower than geometry 2.

In this case the difference in reinforcement geometry and adhesive layer thickness are not the only variables; the Young's modulus of the glass fiber is 3 times lower than carbon fiber.

Keeping this in mind the initial failure moment estimated at 80% of the initial failure of specimen 90-01.

$$M_i = 0,8 * 718 * 10^3 \text{ Nmm} = 574,4 * 10^3 \text{ Nmm}$$

$$F_i = 0,8 * 2.871 \text{ N} \approx 2.300 \text{ N}$$

This results in the following tensile force in the reinforcement

$$F_{re.i.} = \frac{M_i}{84,5 \text{ mm}} = \frac{574.400 \text{ Nmm}}{84,5 \text{ mm}} = 6.800 \text{ N}$$

$$F_{re.i.} = 6.800 \text{ N} > F_{re.u.} = 5.500 \text{ N}$$

The requirement for minimum reinforcement capacity is not reached. The residual load bearing capacity for this girder is estimated on:

$$\frac{F_{re.u.}}{F_{re.i.}} * 100\% = \frac{5.500 \text{ N}}{6.800 \text{ N}} * 100\% = 81\%$$

Ultimate Limit State

The deflection of the girder in the U.L.S. is estimated as follows:

Assuming that the governing factor for ultimate failure is bending moment, the girder is fractured up to the end supports and the maximum tensile force of 5.500N in the reinforcement is reached over the whole length between the supports.

The deflection of the girder will be caused mainly by elongation of the reinforcement:

$$N = E * A * \frac{\Delta l}{l}$$

$$E = 53.000 \text{ N/mm}^2$$

$$A = 0,8 * 6 = 4,8 \text{ mm}^2$$

$$N = 5.500 \text{ N}$$

$$l = 1400 \text{ mm}$$

$$\Delta l = \frac{N * l}{E * A} = \frac{5.500 \text{ N} * 1400 \text{ mm}}{53.000 \frac{\text{N}}{\text{mm}^2} * 4,8 \text{ mm}^2} = 30,3 \text{ mm}$$

A rough estimation for the deflection of the girder in the U.L.S. can be obtained by considering the deformation of the girder presented in *Figure 117*.

$$\frac{u}{500 \text{ mm}} \approx \frac{0,5 * \Delta l}{h}$$

$$u \approx \frac{500 \text{ mm} * 0,5 * 30,3 \text{ mm}}{90 \text{ mm}} = 84 \text{ mm}$$

This method has proven itself to be accurate within 10% for specimens 70-04/06.

